Snow and Wind

A Simulation Approach in Arctic-Built Environments

Fiebig, Jennifer

Publication date:
2023

Document Version
Publisher's PDF, also known as Version of record

Snow and Wind –

A Simulation Approach in Arctic-Built Environments

Jennifer Fiebig

Ph.D. Thesis

Department of Civil and Mechanical Engineering
Technical University of Denmark
Brovej, Building 118
DK-2800 Kongens Lyngby,
Denmark

June 2023

To my daughter Estelle and dedicated to my father.

Abstract

Wind-driven snow and snow deposition can be a major problem for constructions and cities in cold regions and the arctic. A traditional way of studying snow deposition on and around buildings is wind tunnel testing at a reduced scale using substitute material for snow. The accurate replication of snow deposition when modelling snowdrift is a critical issue in wind tunnel testing. Scientists have been unsuccessful to satisfy the similarity requirements when simulating snowdrift with substitution at reduced scale in wind tunnel testing. Very little of the experimental set-up since 1960 until now has changed when simulating snowdrift in reduced scale in boundary-layer wind tunnel testing. Significant scale factors in previous research are flow similarity, geometrical scale, time scale, particle cohesiveness, and saltation length, snowdrift rate and the similarity of the snowdrift formation. Current methods measure the distribution and depths of the substitute snow after the simulation process. Full-scale data from near-ground weather conditions in arctic built environments are rare or often available in poor quality. This study, will start from there and developed an optimised method for simulating snowdrift in Wind Tunnel Testing. The work within this project investigates how present and future architectural designs influence snow accumulation on and around buildings. Systematic observations in full-scale of – a Nuuk Cube Field Experiment - linked with on-site ground measurements of snow heights and weather conditions provide validation data for experimental simulations of snow accumulation at reduced scale in wind tunnel studies. Results confirm that snow accumulation deposit is largely influenced by the flow field around the object. The characteristic variation in wind directions during a snow event is negligible. Predominated northerly and southerly wind directions created ‘eroded areas’ and ‘deposit areas’ in form of a ‘kidney wind scoop’ surrounding the Nuuk Cube. The results from the wind tunnel study provide evidence that critical snow accumulations on and around structures can be located and identified with the developed method. The technique can be applied to generic urban studies testing predominant wind directions for arctic case studies. An approach for an urban study in wind tunnel testing is presented.

Resumé

Vinddrevet sne og sneaflejring kan være et stort problem for bygninger og byer i kolde områder og i Arktis. En traditionel metode til undersøgelse af sneaflejring på og omkring bygninger er vindtunnelforsøg i reduceret skala med erstatningsmateriale for sne. En nøjagtig gengivelse af sneaflejring ved modellering af snedriver er et kritisk spørgsmål i vindtunnelforsøg. Det er ikke lykkedes forskerne at opfylde kravene til lighed ved simulering af snedriver med erstatningsmateriale i reduceret skala i vindtunnelforsøg. Der er kun sket meget få ændringer i forsøgsopstillingen siden 1960, når man simulerer snedrift i reduceret skala i vindtunnelforsøg med grænseflader. De vigtigste skalafaktorer i tidligere forskning er strømningslighed, geometrisk skala, tidsskala, partikelkohærens og saltationslængde, snedriftshastighed og lighed i snedriftsdannelsen. De nuværende metoder måler fordelingen og dybden af erstatningssne efter simuleringsprocessen. Data i fuld skala fra vejrforhold tæt på jorden i arktiske byggede miljøer er sjældne eller ofte tilgængelige i dårlig kvalitet. Denne undersøgelse tager udgangspunkt heri og udvikler en optimeret metode til simulering af snedrift i vindtunnelforsøg. I dette projekt undersøges det, hvordan nuværende og fremtidige arkitektoniske konstruktioner påvirker sneophobningen på og omkring bygninger. Systematiske observationer i fuld skala - et Nuuk Cube Field Experiment - kombineret med målinger på stedet af snehøjder og vejrforhold giver valideringsdata til eksperimentelle simuleringer af sneakkumulering i reduceret skala i vindtunnelundersøgelser. Resultaterne bekræfter, at sneakkumuleringens aflejring i høj grad påvirkes af strømningsfeltet omkring objektet. Den karakteristiske variation i vindretninger under en sne begivenhed er ubetydelig. De fremherskende vindretninger fra nord og syd skabte "eroderede områder" og "aflejringsområder" i form af en "nyreformet vindskovl" omkring Nuuk Cube. Resultaterne fra vindtunnelundersøgelsen viser, at kritiske sneophobninger på og omkring strukturer kan lokaliseres og identificeres med den udviklede metode. Teknikken kan anvendes til generiske byundersøgelser, hvor man afprøver de fremherskende vindretninger i arktiske casestudier. Der præsenteres en fremgangsmåde for en byundersøgelse i vindtunnelforsøg.

Preface

The project “Snow and Wind – a simulation approach for the arctic built environment” was conducted under the supervision of Associate Professor Holger H.Koss and carried out at the Technical University of Denmark (DTU) with Arctic DTU Sisimiut. Experimental work was performed at the Department of Civil Engineering. The Nuuk Cube Field experiment was installed near the premises of the private home of our collaboration partner Peter Barfoed in Nuuk, Greenland. A thank goes to Architect Peter Barfoed, not only could I perform the Nuuk Cube Experiment, but he also was a great host offering me a stay in his house and a cup of tea along with inspiring talks.

A special thank goes to my supervisor Holger H.Koss, he has greatly helped me framing my work and his knowledge in wind tunnel engineering was a great inspiration. Holger has been a close colleague and friend throughout the entire project and over the last 5 years in Copenhagen. In particular, I owe the motivation and drive to start with the doctorate studies to Professor Lisbeth M.Ottosen, head of Section for Materials and Durability at the Technical University of Denmark and former Head of Arctic Engineering and Sustainable Solutions - ARTEK. My research interest started with my master thesis in 2014 about architecture facing the extreme climate in Greenland. Presenting a review of building typologies based on the logic of climate under traditional and cultural aspects. Throughout the research, in my master thesis, I contacted relevant institutes and architects within the field to get further knowledge about Greenland. DTU ARTEK responded to my mail and invited me to apply for the conference ´Artek Event 2014 Urbanization and infrastructure in the Arctic - Challenges from a sustainable perspective` in Sisimiut, Greenland. Here, I met Lisbeth M. Ottosen. Financial support for the research project is partly provided by Laust Løgstrup, Director of Qeqqata Kommunia in Greenland, and fonds from the Technical University of Denmark DTU.

Parts of my study have been presented at the conference on the Artek Event in April 2014. Based on my speech and submitted paper as an architecture student the audience was interested in further ideas and constructive discussions, which motivated me to create a proposal for research work within this field. I’m very grateful for this unique opportunity to see the Arctic and its fascinating environment.

Finally, a grateful thank goes to my friends and family for supporting and encourage me during this exciting time. Their support and kindness for me and my daughter were invaluable to me.

Thank you.

List of publications

Abstract Conference Paper

Fiebig, J., 2016. Snowdrift Simulation in Wind Tunnel Testing as Architectural Design Method for Arctic Buildings, in: ASM2016 Annual Scientific Meeting Arctic Net, Winnipeg, Canada.

Abstract Conference Paper

Fiebig, J., 2016. Snowdift – Visualisation on an Architectural Model in Wind Tunnel Testing, in: International RILEM Conference on Materials, Systems and Structures in Civil Engineering, Conference segment on Cold Region Engineering, Technical University of Denmark, Lyngby, Denmark

Extended Abstract Conference Paper

Fiebig, J., Koss, H.H., 2017. Experimental investigation of snow accumulation, in: 7th EACWE European African Conference on Wind Engineering, Liège, Belgium.

Fiebig, J., Koss, H.H., 2019. Experimental method of snow accumulation in wind tunnel testing, in: The 15th International Conference on Wind Engineering Beijing, China. Beijing, pp. 883–884.

Conference Paper

Fiebig, J., Koss, H.H., 2016. Developing experimental method for investigating snow deposition around buildings using snow substitutes, in: 8th International Conference on Snow Engineering. pp. 41–47.

Journal draft

Fiebig, J., Koss, H., 2021. Nuuk Cube Field Experiment – Part 1: Nuuk Cube Field Experiment - Part 1: Meteorological Observations.

(in preparation for submission to Cold Regions Science and Technology)

Fiebig, J., Koss, H., 2021. Nuuk Cube Field Experiment – Part 2: Snow accumulation monitoring.

(in preparation for submission to Cold Regions Science and Technology)

Fiebig, J., Koss, H.H., 2021. Theoretical and empirical similarity of experimental wind tunnel testing of snowdrift and accumulation

(in preparation)

Paper contribution in Report/Book

Fiebig, J., 2017. Grundsatzüberlegung einer experimentellen Versuchsmethode für das Phänomen der Schneeanhäufung um und an Gebäuden im Windkanal mit Schnee-Ersatzmaterial, in: Koss, H., Ruscheweyh, H. (Eds.), Qualität Im Windingenieurwesen. Windtechnologische Gesellschaft (WTG) e.V., Aachen, p. 165.

Nomenclature

Latin Symbols

Symbol	Unit	Description
D_p	µm	Particle Diameter
K(z)	m/s	Corrected wind velocity
L_m	m/s	Model length
u_*	m/s	Surface friction velocity
U_f	m/s	Fall velocity particle
U_{ref}	m/s	Reference air speed at pitot tube
U_t^*	m/s	Threshold friction velocity
$U_t(z)$	m/s	Observed individual threshold wind speed measured at height z
$U_m(z)$	m/s	Converted wind velocity to specific site height z
U_{Th}	m/s	Threshold velocity speed
$U_{Th_{P1}}$	m/s	Threshold isopleths
$U(z)$	m/s	Normalised mean wind velocity at height z
$\overline{U}_{(z)}$	m/s	Max. daily mean wind velocity at height z
Q_m	g/m	Seeding rate substitute material
T_{air}	°C	Air temperature
T_{int}	min	Intermittence time
z_0	m	roughness length
z_{ref}	cm	Reference height at wind tunnel

Greek Symbols

Symbol	Unit	Description
β		Speed-up Factor
Ω		Velocity Ratio
ρ	g/cm3	Density
ρ_{a_P}	g/cm3	Density prototype
ρ_{a_m}	g/cm3	Density model
θ	°	Angle of repose

Symbol	Description
ABL	Atmospheric Boundary Layer
CCWT	closed-circuit wind tunnel
CoV	coefficient of variation
DMI	Danish Meteorological Institute
FPU	Flow Processing Unit
LSHW	low-speed hot-wire anemometer
IFA	(IFA Institute for Occupational Safety and Health of the German Social Accident Insurance)
ISS	Integrated Sensor Suite
NCE	Nuuk Cube Experiment
RH	Relative Humidity
RPM	Rounds per minute
ROS	Rain-on-snow
SEM	Scanning electron microscope
SSM	Snow substitute material
WD	Wind Direction

Wind driven snowdrift in connection to the local wind climate we refer to the following definitions:

Snowdrift is a product of the process of wind transport of snow. The transport of snow in turbulent air conditions can be described in three processes: In nature, snow transport can appear in the form of creep, saltation, or suspension. In the creep layer, particles stay in contact with the ground and might just move within the layer. Saltation appears in a layer 0.10 m to 1 m above the ground and suspension (aka. turbulent diffusion) from 10 m to 100 m.

Snow-event (precipitation event) is typically described by its duration [min] and intensity [mm/h] to separate one event from another, a length of a separation interval has to be specified to group the single precipitation signals. In this study, precipitation signals are registered with a rain tipping gauge giving a singular signal for every 0.2mm of rainfall. These signals are subsequently grouped to events depending on a maximum allowed interval duration, T_{int}. Separation intervals exceeding T_{int} constitute the beginning of a new snow event. Consequently, the choice of T_{int} influences the number of identified events and the resulting duration distribution and with that the estimation of a typical/characteristic snow event duration.

Table of Content

1. Introduction

1.1 Problem statement

Although the accumulation of wind-blown snow in Arctic regions is a common phenomenon, it still leaves many questions unanswered. The phenomenon of snow drifting in the Arctic as well as other snow-prone regions has been a significant problem for the built environment for centuries, yet the consideration of snow accumulation in wind tunnel studies is still insufficient and challenging. Due to the complexity of the physical process of snow accumulation and distribution in nature, the influence of snow is usually investigated in wind tunnel experiments on a reduced scale with snow substitute material.

Heavy snow accumulations on roofs frequently damage the supporting structure but impose an even larger risk to structural durability and indoor climate due to meltwater penetration. Secondly, large snow accumulations around and between buildings affect basic functions such as accessibility and ventilation. Climate change may further aggravate these issues. The extreme climate is a growing problem caused by climate change in many parts of the world. The need to adapt to the extreme climatic conditions leads to specific traditions of construction forms and development concepts utilizing the available resources. The population of around 56,000 in Greenland (Grønlands Statistik , 2020) and approx 4 million throughout the Arctic may look like a small audience for the wide field of research. But considering the growing problem of rapid climate change in many parts of the world, the research in Arctic regions offers great potential for adaptation for also other extreme climates.

As a consequence, the drifting snow has an impact on building design, structure, and roofs. In case of incorrect design planning such as the shopping mall ´Nuuk Center` in 2012, the snowdrift has a large impact on the structure and causes damages. After one year water was found in the building caused by powerful storms the previous two months. The meltwater has damaged insulation and drywalls in certain parts of the building and also toxic mold was identified.

Figure 1 Masterplan of the Nuuk City Development Plan showing the area outside of Nuuk city with small housing typologies (2018).

Over the next years, Greenland's capital city Nuuk is undergoing a large transformation process. In an ambitious plan, the Greenlandic government has formulated a holistic strategy aiming at establishing a prosperous social and cultural infrastructure and a high level of urban livability as known from other large European cities. In this context, the capital city of Nuuk will radically be transformed to meet the future demands of an urban city. A central role in the transformation is the

densification of urban areas. Old developments in the city center are going to be demolished giving hence space for re-thinking urban structure. The new development, symbolizing Greenland's will for development, shall be sustainable considering the extreme geographic, orographic and climatic boundary conditions and available resources. The 2011 vision of this transformation is described in *"MIDT i VERDEN // MIDT i NUUK"* published by Sermersooq municipality, the world's second-largest commune by area. A new master plan (see Figure 1) from Siorarsiorfik – Nuuk City Development A/S has high ambitions to meet urban livability and sustainability for the future (Siorarsiorfik, 2018). A detailed visualization illustrates the housing type planned for such district, see in Figure 2. In a 12 year plan, Nuuk is extended to new districts, which should ensure 30,000 residents in the future (Siorarsiorfik, 2018). The present urban development in Nuuk is dominated by block-type multiple dwelling units constructed in the 1960s. At the new development site of Nuuk city, several multi-story buildings are dominating the area in an arrangement of rectangular blocks, e.g. area Quinngorput.

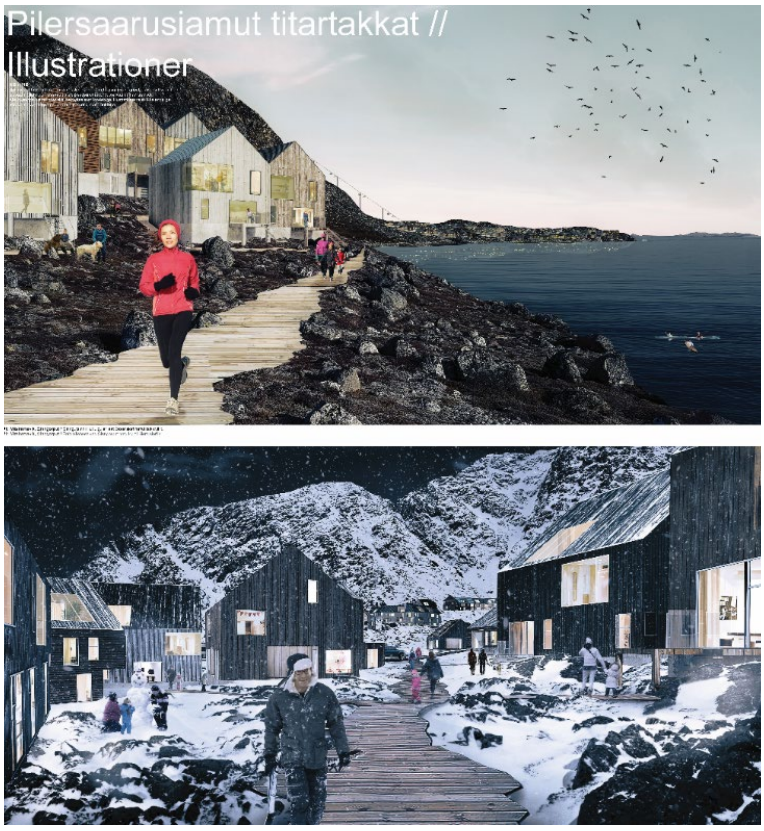

Figure 2 Detailed illustration of the Nuuk City Development Plan (2018).

With the climatic conditions in Greenland the service life of surface treatments is low due to dust, snow and ice particles that hit surfaces such as facades (Møller & Lading, 2020). As a consequence, the drifting snow has an impact on building design, structure, and roofs. In case of incorrect design planning such as the shopping mall ´Nuuk Center` in 2012, the snowdrift has a large impact on the structure and causes damages (see Figure 3). After one year water was found in the building caused by powerful storms the previous two months. The meltwater has damaged insulation and drywalls in certain parts of the building and also toxic mould was identified.

Figure 3 Nuuk Center when snowdrift has a large impact on the structure of the building façade. Snow particles with strong adhesion deposit at metal grid façade. People walking by struggle to pass the high-rise tower at high velocities.

Figure 4 Snowdrifts around a residential building at the outskirts of Nuuk city, Greenland (Photo Peter Barfoed 2015). Snow accumulation needs to get regularly removed from streets and entrances.

Even though snowdrift is a common phenomenon in arctic regions, the accumulation of wind-driven snow still holds many unanswered questions. Proper simulation of the complex process of snow deposition on, around and between structures in a built environment requires reliable and systematic reference data from full-scale observations and measurements. But, only little concrete data on the weather conditions surrounding snow events resulting in accumulation patterns are available from field measurements in Arctic regions. Considering the process of snow formation and redistribution in nature, the impact of snow in built-up areas is usually studied in wind tunnel experiments on scaled models using substitutional material for snow. So far, wind tunnel experiments based on strict theoretical similarity requirements in snowdrift simulations at reduced scale can not be applied without comparison to full-scale.

1.2 Objectives and scope

The research on wind tunnel and near-reality simulations of snow accumulation on and around different group of buildings, are aimed at wind engineers, micro climatologists and specialists from flow mechanics. This work has a clear focus on observing, understanding and simulating snow drift in model and full scale in an arctic environment. Further the scope includes the understanding snow drifts in the built environment from acquiring meteorological data and to understand wind-transported particle dynamics and the use implementation in wind tunnel simulations. Approaches to bridge scaling problems between model tests and full-scale observations are presented.

Even though snowdrift is a common phenomenon in arctic regions, the accumulation of wind-driven snow still holds many unanswered questions. Literature provides some descriptions for practical purposes but a number of them are known to be inaccurate. Proper simulation of the complex process of snow deposition on, around and between structures in a built environment requires reliable and systematic reference data from full-scale observations and measurements. But, only little concrete data on the weather conditions surrounding snow events resulting in accumulation patterns are available from field measurements in Arctic regions. So far, wind tunnel experiments based on strict theoretical similarity requirements in snowdrift simulations at reduced scale can not be applied without comparison to full-scale. There remains a need for improved methods and applications to investigate the impact on housing and urban building design for cold and harsh climates in wind tunnel testing. Identifying and classifying snow events (SNE) for a practical application in experimental snowdrift simulations (e.g. adjustment of wind speed, direction, intensity, and duration for wind tunnel experiments) are needed to improve the simulation method. For this reason a field study, the Nuuk Cube Flied Experiment (NCFE) was initiated to measure ground-near weather conditions during winter period in parallel to observation and documentation of snow accumulation on a nearby 1.2m cube.

The choice to perform wind tunnel experiments instead of numerical simulations was based on the fast availability of the experimental technique and the fact that despite the limited similarity (no real snow and thus no thermodynamic similarity) we are still dealing with physical transport mechanisms of the substitute particles. These physical processes offer a good opportunity to generate validation data for numerical simulations not only despite but rather because of their partial similarity. This was a central aspect in the choice of experimental investigation for this study.

[O.1] The first objective is to study snowdrift in nature by monitoring snow accumulation around a generic object (Nuuk cube) and a weather analysis describing typical, site specific snow events for the arctic region in Nuuk city.

[O.2] Based on the outcome of [O.1], recommendations for simulation-based studies of snow accumulation are formulated for a simulation approach at reduced scale.

How do snow and wind impact the arctic built environment and how can we investigate critical situations? [R.1] Which snow accumulation and drift phenomenon are relevant in arctic built environments? Furthermore, which critical situation can be reflected in wind tunnel testing at a reduced model scale?

[R.2] How can snow events be defined based on weather observations and what is their occurrence characteristic? What is the correlation of wind direction and speed during a snow event. How to describe the weather history of a snow event? What snowdrift pattern will be created during and after a snow event around the Nuuk Cube?

The analysis of data shall identify and classify snow events to define snow simulation conditions for Wind Tunnel Testing (wind speed, direction, intensity and duration).

1.3 Structure of the Thesis

The thesis includes three papers in preparation for submission. Chapters 5 and 6 are coherent chapters with Background information about a field experiment of an object (cube) in Nuuk, Greenland, linking the relation between wind tunnel testing and full-scale.

Chapter 2 Background: Basic definition of snow and wind in Arctic climate. Modelling techniques in wind tunnel testing and the detailed consideration of snowdrift.

Chapter 3 Methodology: Method and Wind tunnel set-up and measuring procedure of model snow.

Chapter 4 Substitute Materials: Classification of snow substitute materials.

Chapter 5 Nuuk Cube Field Experiment – Background of included papers part 1 and 2 to meteorological observations and snow accumulation monitoring.

Chapter 6 Summary of included Papers of the Nuuk Cube Field Experiment.

Chapter 7 Discussion

Chapter 8 Conclusions

2. Background

2.1 Snow transport

Greenland is located in the Arctic and sub-Arctic region but the local climate can vary largely considering the long stretch from north to south of 2600 km, being the world's largest island with 2.2 million square kilometers and 80% of its land is covered by the ice sheet (Cappelen John(ed), 2013). The general characteristics of the arctic region are defined by the warmest month being below +10°C (Nielsen, 2010).

Greenland is divided into seven climate regions (Cappelen John(ed), 2013):

- South
- Southwest
- Northwest
- North
- Northeast
- Southeast
- The Inland Ice Sheet

Generally, the climate is defined as the high Arctic in the North with very cold and dry air with low precipitation where snow conditions are described as tundra (Arctic desert) (Cappelen John(ed), 2013; J. W. W. Pomeroy & Brun, 1990). The region in the middle part of the island is a low Arctic region and can vary in local climate conditions between the cold inland ice and the warm sea. The south of Greenland is located in the sub-Arctic and has larger temperature differences (Cappelen John(ed), 2013). The Arctic weather phenomena are dominated by extremes largely due to its topographic characteristics creating different extreme weather phenomena such as *Tip and barrier Jets, Gap flow and fjord jets, Gap flow and fjord jets, Cold air outbreaks feature strong winds, Downslope wind storms* (Heinemann et al., 2019; Michel et al., 2018)

The cyclonic system over Greenland is associated with a "small scale" cyclonic system, not more than 1000 km (Jung & Rhines, 2007; Michel et al., 2018) also known as Polar mesoscale cyclones (PMCs) and the influence of Greenland's topography on the storm track is large (Jung & Rhines, 2007). This means the mesoscale is more dominant for the climate characteristics in Greenland. Poor data coverage remains a lack of understanding of many of the weather phenomena and errors in weather precision in the Arctic (Spengler, 2020). The project focuses on the mesoscale and

microscale understanding of the phenomenon of snowdrift near the ground. The phenomenon of wind-driven snow is a significant challenge for the built environment in cold climate regions and approaches for its consideration in urban and building design vary considerably. Near the surface, the wind pattern in the lower hundreds meter of the atmosphere is described as the boundary-layer wind profile and is influenced by the earth's surface properties. The wind velocity directly at the surface is practically zero and increases with height.

The shape characteristic of the mean wind profile is dependent on the surface roughness z_0 (Figure 3). Generally, the wind profile is defined by the logarithmic equation:

$$u(z) = \frac{u_*}{k}\, ln\left(\frac{z}{z_0}\right) \qquad (1)$$

where u_* is the friction velocity and z_0 the roughness length of the surface and k the von Karman constant. In a complex terrain like Greenland with mountains and fjords, the wind profile gets distorted at the mountain crests and ridges, as shown in Figure 4 (Föhn, 1980). In full-scale, deviations from the logarithmic profile can occur if complex terrain or katabatic winds and sea-breeze define the conditions (Jaedicke, 2001; Thordarson, 2002). The roughness height z_0 for snow-covered surfaces is varying with friction velocity and is to define as follows:

$$z_0 = c\frac{{u_*}^2}{g} \qquad (2)$$

The value c relates to the different snow types with 0.015 found by Joffre (1982) and 0.018 by Schmidt (1982) for fresh cold snow (Thordarson, 2002). The roughness length varies from flat snow surface with $z_0 = 0.0001$ to a snow covered surface $z_0 = 0.002$ (Jaedicke, 2001; J. W. Pomeroy & Male, 1987; Thordarson, 2002).

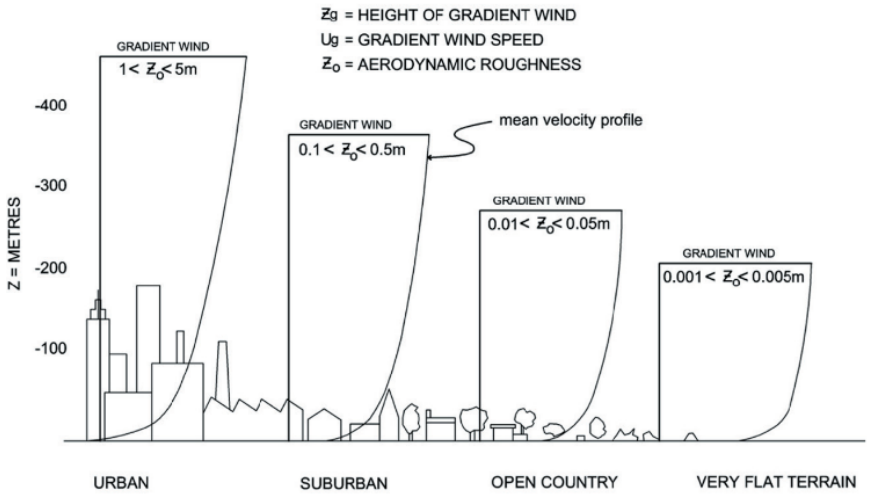

Figure 6 The wind mean velocity profile varying with surface roughness z_0 (Cochran & Derickson, 2005)

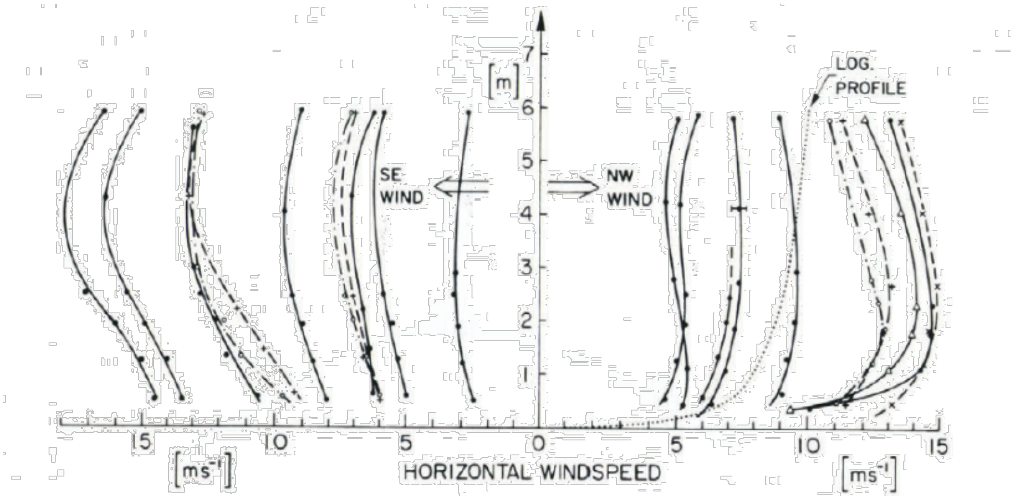

Figure 7 Differences of vertical profiles at mountain ridge crest due to terrain differences (Föhn, 1980).

The snow transport mechanism is described in three modes within the first 100 m over the surface and has been summarized by (Mellor, 1965; R. A. Schmidt, 1982; Tabler et al., 1990). Snow transport can appear in form of creep, saltation, or suspension (turbulent diffusion):

- Creep: when fresh dry snow particles not cohesive start rolling along the surface, but without great significance on accumulation. But the possible impact on the snow surface particles.
- Saltation: Saltation appears in a layer 0.10 m to 1 m above the ground. Drifting begins when the surface shear stress exceeds the threshold value and particles start hopping over the

surface. Field data from literature estimated threshold wind speeds for snow transport for dry snow at 4 to 11 m/s and wet snow at 7 to 14 m/s (Li & Pomeroy, 1997).

- The suspension (aka. turbulent diffusion) occurs from 10 m to 100 m. In this layer, particles travel in the air stream without a contract to the ground. This layer is dominant for polar storms where most of the snow is transported and affecting the wind distribution (Mellor, 1965).

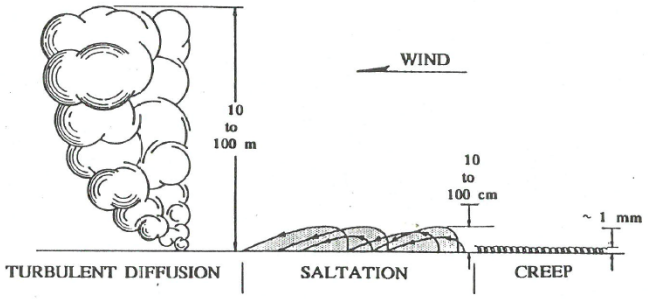

Figure 13 Drawing of three modes of transport for blown snow from (Mellor, 1965)

Promeroy and Brun (1990) describe snow as one of the most complex physical materials on Earth. Its constant change of structure and properties through weather, climate, terrain, or other impacts makes it a fascinating and unique material. A great example of observed snowdrift in turbulent diffusion illustrates Figure 8

Figure 8 Transport of blown snow in Nuuk city (2017). Whiteout causing decreased visibility and can cause safety risk to pedestrians and traffic.

2.2 Snow cover properties

The snow cover on Earth interacts strongly with our global climate, where the polar regions act as large 'mirrors' for solar radiation (Kuipers Munneke, 2009; J. W. W. Pomeroy & Brun, 1990). Snow surface albedo controls the radiation budget of the snow-covered regions. As a result, solar radiation heats our atmosphere and land but due to the spherical geometry of the Earth, the equatorial region heats more than the poles (Kuipers Munneke, 2009). The changes in snow cover on Erath considerably impact the atmospheric transport mechanism. With today's emerging climate change around the world and increasing air temperatures – most notably for the arctic regions, predictions of the climate models show a noticeable increase for most precipitation regimes (McCrystall, M.R., Stroeve, J., Serreze, 2021; N. M. Schmidt et al., 2019). Ultimately higher air temperatures lead to increased transport of moisture in the atmosphere resulting in rain-on-snow (ROS) events that creates high-density snow masses (Abermann et al., 2019; McCrystall, M.R., Stroeve, J., Serreze, 2021; Pall et al., 2019; N. M. Schmidt et al., 2019).

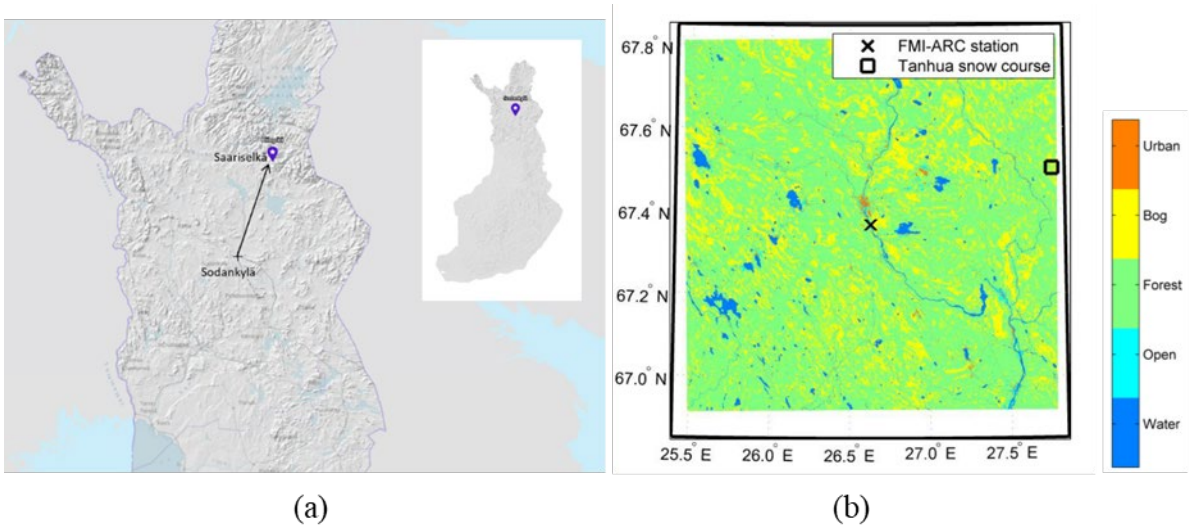

Figure 9 (a) Measuring sites during 3rd Science Snow School, Finland. First site in Sodankylä and second location in Saariselkä. (maps produced by the NLS National Land Survey of Finland). (b) Maps of (a) the 100km×100km area around FMI-ARC station. All the maps are in orthographic projection. The background of the maps is Corine Land Cover 2006 aggregated into five general classes. By Leppänen and et al. (2016).

In situ snow albedo measurements are used to develop and validate methods for remote sensing from satellites to observe the development of large ice sheets around the polar regions. But also, to validate models and predict present and future climates. On February 12-18, 2017, at the 3rd Snow Science Winter School in northern Finland (Lapland), which was organized by the Swiss Snow and

Avalanche Research Institute (SLF) and the Finnish Meteorological Institute (FMI), measurement methods for snow cover properties were studied. The in-situ measurements were obtained at two different locations (see Figure 9). The first location was close to the fields of the Finnish Meteorological Institute (FMI) centre in Sodankylä (67.368° N, 26.633° E). Here, snow cover samples were collected at a forest site and, in contrast, also from a wetland area. In Saariselkä, the second location, additional measurements were collected from a high tundra site in Lapland, Finland.

The traditional way to quantify snow cover properties is the snow stratigraphy. A number of distinctive "stratigraphic" layers in which each of the layers vary vertically in their characteristics is combined the stratigraphy of a snowpack. Quantifying the snow properties helps to understand the transformation of snow from atmospheric precipitation towards a snow deposit as a sediment. In this process it often re-deposits by wind and undergoes close-to the surface metamorphism (change in shape) and recrystallization. In addition to the traditional methods also emerging methods were compared and include snow property observations of snow water equivalent (SWE), temperature, density, stratigraphy, grain size, specific surface area (SSA) and liquid water content (LWC) (Leppänen et al., 2016). Further information about measurement sites as well as the measurement techniques can be found in Leppänen *et al.*, 2015, 2016.

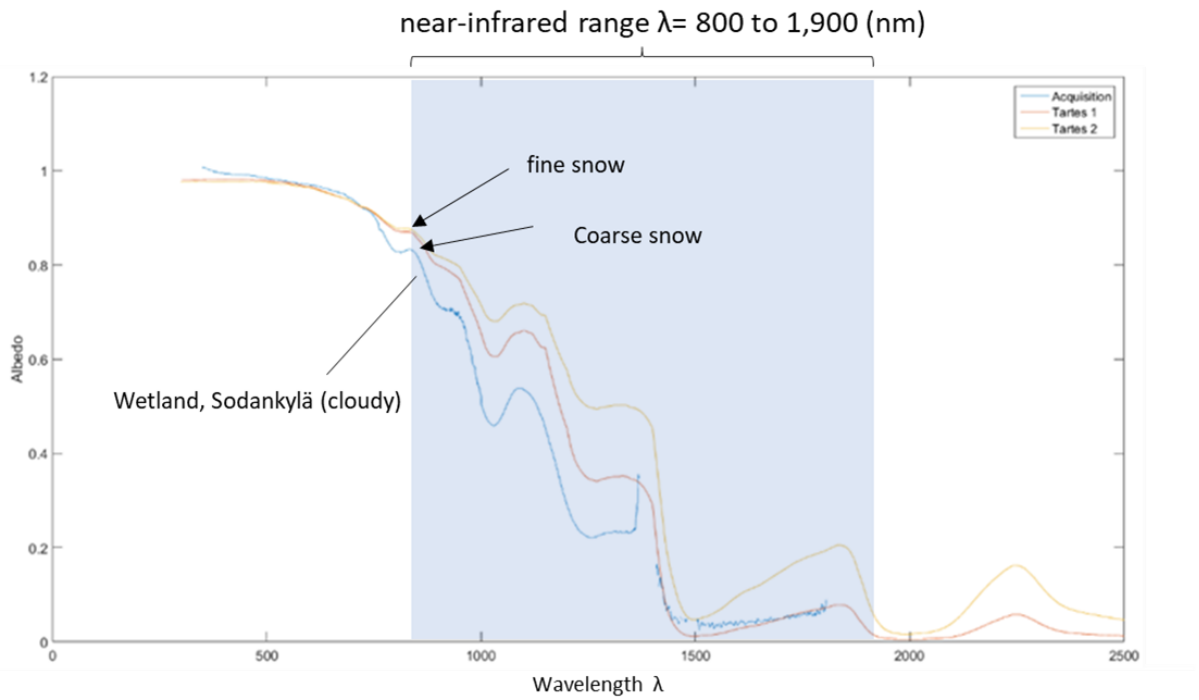

Figure 10 Spectral albedo as a function of wavelength for snow particles with different radius. Measured (blue) and theoretical albedo (orange and yellow) for the wetland area in Sodankylä. The yellow albedo takes into account the fresh snow fall during the day of measurement. TARTES online, 2017.

The Figure 10 shows the spectral reflectance of snow as a function of wavelength for different snow grain sizes. The properties of each layer of the snowpack such as layer thickness, snow density and snow grain optical diameter (or SSA) were specified with the field measurements and used as input values for the online tool 'Snow TARTES'. The specific surface area (SSA) in mm^{-1} (ratio between surface area to mass) were measured by additional instruments, measuring the reflection of the snow in the mid-infrared, more details about the method and instrument are described in Leppänen *et al.*, 2016. Here, we used a spectro-radiometer for the visible and near infrared wavelength to measure the spectral reflectance (albedo) of the snowpack at the wetland site in Sodankylä. With the Snow TARTES tool we compared the measured spectral albedo with theoretical observations from satellites (Figure 9). Snow TARTES is an educational and research purpose web application to compute the reflection (albedo) from multi-layered snowpack. The spectral reflectance of snow differs substantially over the range of wavelengths from λ= 200 to 2,800 nm, here absorption is minimal in the visible range λ= 200 to 800 nm but strongly increases in the near-infrared λ= 800 to 1,900 nm (J. W. W. Pomeroy & Brun, 1990).

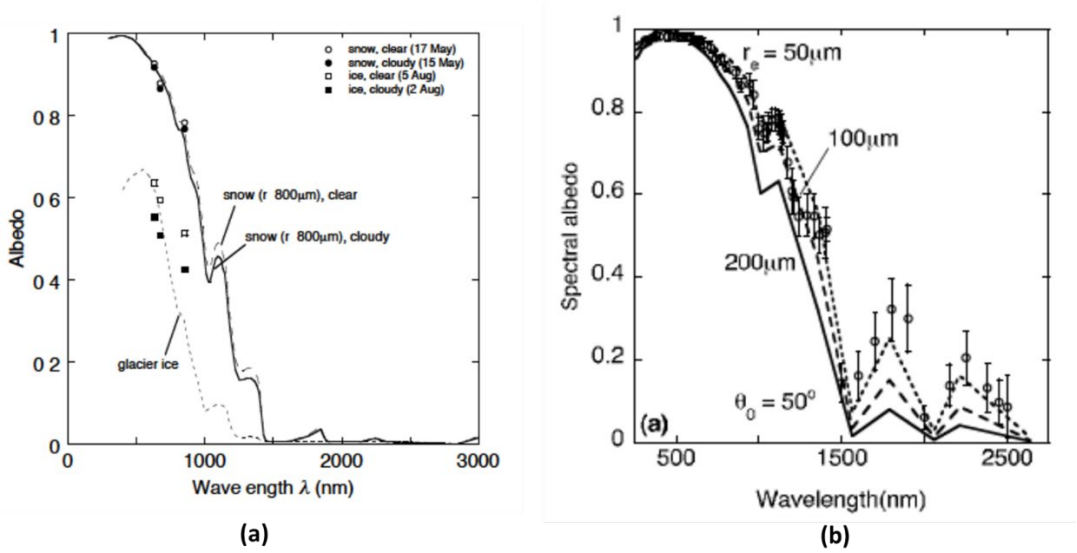

Figure 11 (a) Narrowband albedos on a clear (open symbols) and cloudy day (closed symbols) for a snow radius of r = 800μm (circles) and an ice (squares) surface. The solid and the adjacent dashed lines are theoretical snow albedos for a grain size of 800 μm and the separate dashed line is for glacier ice albedo taken from Zeng et al. [1984], extracted from Munneke (2009).

(b) Spectral albedo as a function of wavelength, for snow particles with different effective radius (r = 50, 100 and 200 μm) of a solar zenith angle of 50°. Circles and corresponding error bars are measurements of spectral albedo reported by Grenfell et al. [1994] for Antarctic snow, reported by Munneke (2009).

In general, grain size, impurities, and thickness of snow layer as well as diffuse and direct radiation (Figure 11 (a)) show an effect on the spectral albedo as reported by Munneke (2009). In Figure 11 (b) the albedo increases with larger snow radius because radiation penetrates deeper into coarser-grained snow and hits more absorbing material before it can backscatter. The reflectance is lower with increased grain size and rounded grain types. The spectral reflectance measured in Figure 9 indicate a coarser-grained snow cover at the wetland site, its snow cover conditions fall into the taiga to alpine class based on Sturm's (1995) classification scheme, see in Figure 12. The site is characterized by low vegetation and high moisture due to the close position of a lake site. Snow layers in Sodankylä vary structurally depending on the characteristics of the environment and weather conditions (Leppänen et al., 2015). To investigate further measurement techniques and the unique physics of snow, additional measurements were obtained with a traditional snow pit at a tundra site in Saariselkä on 18th of February 2017. The second location falls into the subarctic climate regime and snow layer characteristics typically consist of wind induced metamorphism shaping fresh snow particles into "wind slap" particle shapes and recrystallization with rather dominant crystal shapes as "depth hoar" (Sturm & et. al., 1995).

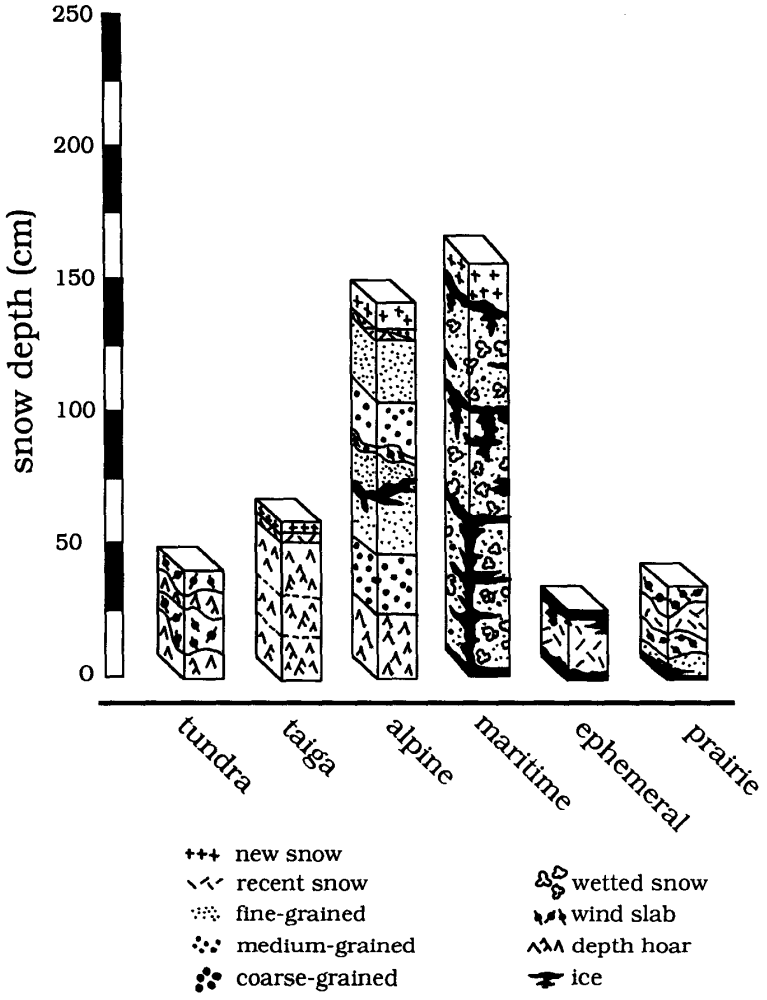

Figure 12 The basic stratigraphy and texture for each snow class in Sturm et al.'s climatic classification, as found in mid-to-late winter (after Sturm et al. (1995)).

The snow pit provides early observation data of the snow properties such as snow crystal types (grain size), the density and temperature of the layer in the snowpack. Basic density cutters were used to obtain the most geometrical property of snow by sampling the volume and optical inspection of the snow layer classification. Snow cover properties depend to a large extent on its surroundings, local climatic conditions, surface type, topography, and altitude above sea level etc. Which means that the distribution of snow and its properties will diverge from each other in different locations. Thus, not only the presence of snow cover will determine the ground energy balance but also the temporal and spatial changes in its properties.

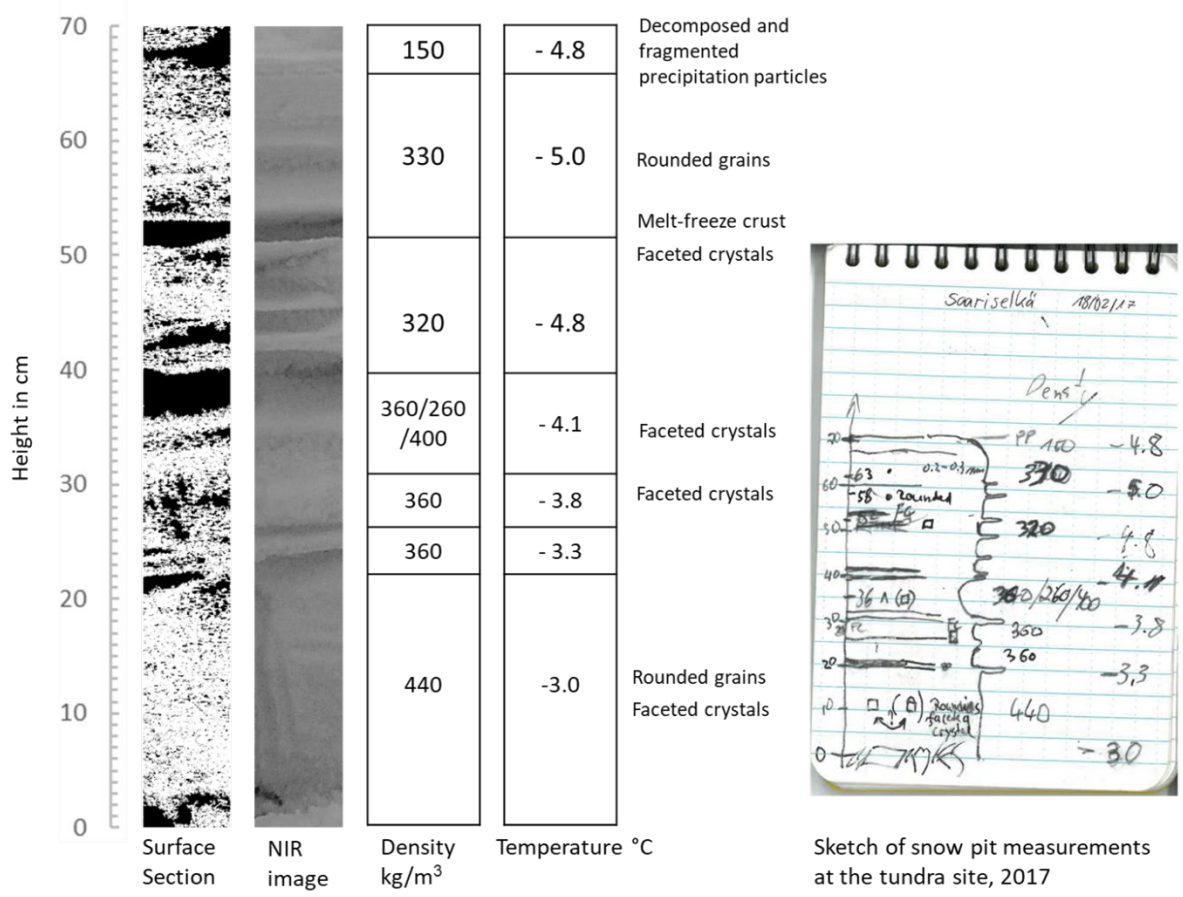

Figure 13 Surface section and NIR image of the tundra site sample and the density [kg/m3], the absolute height of the surface section [cm], temperature [°C] and a sketch of the traditional hand profile.

The surface section of the tundra site and the "stratigraphic" layers with measured density [kg/m3], temperature [°C] and snow crystal types (grain size) are illustrated in Figure 13. According to the climatic classification after Sturm et al. (Figure 11) observations correspond to the alpine or maritime texture with several melt-freeze crusts and rounded and faceted grains. Samples of the density from snow cover were also taken from Nuuk and Sisimiut to compare with the values from Finland. These measurements should be taken with caution as they are a snapshot of the snow properties at the time of measurement and not representative of a typical winter period. The values are listed in Table 4 in Chapter 4.1.3 and compared to other values from literature.

2.3 Theoretical and empirical similarity

When investigating snow accumulation on and around buildings, wind tunnel testing is a well accepted method with models at reduced geometric scale. Research work conducted in the 1990s reached a general consensus that strict similarity requirements for snow are difficult to achieve and have to be replaced with approximations (Kim et al., 1991; Kind, 1986; N.Isyumov & M.Mikitiuk, 1990; Naaim-Bouvet, 1995). The main concern is to match the formation of particles on and around the tested models to full-scale observation (N.Isyumov & M.Mikitiuk, 1990; Naaim-Bouvet, 1995). For the recreation of snow transport and accumulation processes in a wind tunnel experiment substitution materials are widely used, allowing for testing at regular room temperature with less technical and economical effort compared to full-scale studies or tests in special climatic wind tunnels capable of generating real snow crystals at sub-zero temperatures. To determine the scaling parameters, the physical behavior of the considered substitutional material needs to be specified. This specification focuses on one hand on the actual particle with respect to shape, size, density, surface texture, and angle of repose, and on the other hand on their airborne and contact behavior. Only the most relevant similitude requirements were applied and compared to the empirical findings. Common considerations for the level of approximation are condensed in Table 1.

Table 1 Applied similitude parameters from literature. Note: m stands for model and p for the prototype. p refers to the particle.

Selection of similarity parameters in literature	
Geometry	$\left(\frac{D}{L}\right)_m = \left(\frac{D}{L}\right)_\mathrm{p}$
Particle ejection process	$\left(\frac{U^*}{U_t^*}\right)_m = \left(\frac{U^*}{U_t^*}\right)_\mathrm{p}$
Gravity and Fluid Force	$\left(\frac{U_f}{U}\right)_m = \left(\frac{U_f}{U}\right)_\mathrm{p}$
Similarity of particle inertia and gravity forces	$\left(\frac{U^2}{D\ g}\ \frac{\rho_p}{(\rho_p - \rho_a)}\right)_m = \left(\frac{U^2}{D\ g}\ \frac{\rho_p}{(\rho_p - \rho_a)}\right)_\mathrm{p}$
Conventional geometric Froude number similarity	$\left(\frac{U^2}{L_g}\right)_m = \left(\frac{U^2}{L_g}\right)_\mathrm{p}$

Similarity of particle and fluid inertia	$\left(\frac{\rho_p}{\rho_a}\right)_m = \left(\frac{\rho_p}{\rho_a}\right)_{\mathrm{p}}$
Ejection condition	$\frac{\rho_p}{\rho_a} > 600$
Angle of repose	$\theta°_{\mathrm{p}} = \theta°_m$
Time scale	$T_m = \theta°_{m,max}$

Characteristic geometrical modelling such as model, nearby terrain, and particle diameter (3) is suggested to be reduced to the same scale. D is the particle diameter and L the model length scale. Particles small in mean diameter < 30 µm are found not suitable for the erosion process, simply because they show strong particle attachment.

$$\left(\frac{D}{L}\right)_m = \left(\frac{D}{L}\right)_{\mathrm{p}} \tag{3}$$

It is believed that dynamic modeling requires proper scaling of atmospheric boundary-layer (ABL) characteristics with a turbulent flow to initiate saltation and turbulent diffusion (see Figure 63).

Therefore the particle ejection process is important for consideration:

$$\left(\frac{u_*}{U_t^*}\right)_m = \left(\frac{u_*}{U_t^*}\right)_{\mathrm{p}} \tag{4}$$

Once a particle is airborne the similarity parameter Gravity and Fluid Force is achieved when:

$$\left(\frac{U_f}{U}\right)_m = \left(\frac{U_f}{U}\right)_{\mathrm{p}} \tag{5}$$

Froude scaling was found to be not suitable for snowdrift simulations at a reduced scale (Anno, 1985a). Neither the particle Froude number nor the geometric Froude number (Kim et al., 1990) for

surface particle motion was suitable. It was believed that since the particle ratio from model to prototype D_m/D_p is generally larger than the overall building dimensions L_m/L_p, that an alternative approach to the conventional geometric Froude number based on overall dimensions and velocity ratio was more applicable (Kim et al., 1991). As follows, the similarity of Froude including the particle inertia and gravity forces (conventional densimetrical particle Froude number) is achieved when:

$$\left(\frac{U^2}{D\ g}\ \frac{\rho_p}{(\rho_p-\rho_a)}\right)_m = \left(\frac{U^2}{D\ g}\ \frac{\rho_p}{(\rho_p-\rho_a)}\right)_{\mathrm{p}} \tag{6}$$

Varying the model velocity U_m has been proposed to investigate the effects to meet equation (6).

And the alternative conventional geometric Froude number similarity is expressed as follows:

$$\left(\frac{U^2}{L\ g}\right)_m = \left(\frac{U^2}{L\ g}\right)_{\mathrm{p}} \tag{7}$$

Nevertheless, had also this approach shown deficits, but it could be improved by choosing a heavy substitute material according to Kind (1976,1986) ρ_p/ρ_a m > 600 (Kim et al., 1991; N.Isyumov & M.Mikitiuk, 1990). According to Isyumov and Mikitiuk (1990), the similarity of particle inertia and fluid inertia forces seems to be an important parameter for modelling snow removal and deposition on and near buildings and other aerodynamic bluff bodies, meaning particle trajectories in regions of rapidly changing flow. The equation is expressed as follows:

$$\left(\frac{\rho_p}{\rho_a}\right)_m = \left(\frac{\rho_p}{\rho_a}\right)_{\mathrm{p}} \tag{8}$$

Additionally to the consideration of theoretical similarity parameters, Kim et al. in 1991 examined experimental evidence of geometric similarity to full-scale data from Mellor (1965) pointing out the importance for validation through full-scale comparison of snow accumulation shape and volume. Therefore empirical approaches were applied such as drift pattern modelling by the angle of repose and mass rate transport. Additionally to the consideration of theoretical similarity parameters, Kim

et al. in 1991 examined experimental evidence of geometric similarity to full-scale data from Mellor (1965) pointing out the importance for validation through full-scale comparison of snow accumulation shape and volume. Therefore empirical approaches were applied such as drift pattern modelings by the angle of repose and mass rate transport. A crucial requirement to achieve phenomenological similarity when choosing a substitute material is a high cohesion ability. Indication for a strong cohesion is the angle of repose. The angle of repose is believed to be an important parameter to achieve a realistic snowdrift simulation (Anno, 1984) and expressed as follows:

$$(\theta°)_m = (\theta°)_\mathrm{p} \tag{9}$$

Time scaling as an empirical expression was found to match better to nature (Anno, 1984; Kim et al., 1990; Naaim-Bouvet, 1995) by comparing snowdrift rates or the volume of snowdrift. In Anno's and Tomabechi's (1985) experiment, they compared snow cone growth of substitute and natural snow, they found that the height of the cone increases with time. The cone ceased to grow at a specific time and Anno et al. declared an equilibrium state. The duration in this experiment is based on particle accumulation growth comparing the final snow accumulation shape to full-scale measurements.

$$\frac{T_\mathrm{p}}{T_m} \tag{10}$$

Recent publications on this topic reflect a great diversity of possible approaches for snowdrift simulations: from using finely ground glass in water flume tunnels to satisfy saltation length similarity (Irwin, 2016), over the commonly used natron (sodium bicarbonate) powder due to seemingly well-matching behavior in ground-near motion (Kim et al., 1991) or activated (ability to absorb) clay particles (Anno, 1985b; Haehnel et al., 1993), ground styrofoam for modeling snowfall and accumulation (Flaga & Flaga, 2016), to true-to-nature simulations using either artificially generated snow in climatic wind tunnels (Delpech et al., 1998; Thiis et al., 2007) or real snow on outdoor test setups (Beyers & Harms, 2003). Or even outdoor snow-wind tunnel configuration (Liu et al., 2018). Other substances have been considered but deemed impractical due to material costs or hazardous risk with respect to particulate matter pollution or dust explosion. For the replication

of the snow accumulation observed in the Nuuk Cube Field Experiment different substitutional materials have been considered. For this reason, the different substitute materials have been specified and tested regarding their performance within the wind tunnel facility at the Technical University of Denmark (DTU). The most relevant requirements are the empirical similarities e.g. the angle of repose.

3. Methodology

3.1 Method and Definitions

The research field of this study is a research on wind tunnel simulations of snow accumulation with a focus on observing, understanding and simulating snowdrift in model and full scale. The understanding of the natural phenomena of a snowdrift in Arctic and sub-Arctic climate requires measurements from full-scale, here meteorological measurements and monitoring of snow accumulation geometry are necessary. Furthermore, the research study is linking field observations to an experimental simulation method in wind tunnel testing as a design approach in the Arctic built environments. The reconstruction of the full-scale phenomenon of snow deposition around structures is an evidence-oriented method. The research was conducted in collaboration between the sections of Structural Engineering with their experience in wind tunnel testing and Arctic DTU at the Technical University of Denmark with international academic partners experienced in cold climate conditions. The access to full-scale observation sites on DTU premises in Greenland and the availability and development of unique experimental facilities allows performing research on a high international level to provide a platform for future research activities and collaboration beyond the scope of this project. Prior to scale testing in a boundary-layer wind tunnel, the behavior of wind-driven snow in nature will be studied thoroughly.

The project is laid out for three years and consists in essence of two main elements:

A. in situ observation and Nuuk Cube Experiment (NCE)

B. model-scale simulation of snow accumulation

From the first element, we get a better understanding of snow accumulation in urban areas substantiated by measurements of snow distribution on the ground and in height and of the past weather conditions (continuous recording) leading up to the observed and recorded snow accumulation. These data will serve for validation of the simulation technique applied for studying snow accumulation at the model in wind tunnel tests – the second element of the project

3.1.1 In-situ measurements

For the collection of validation data on snowdrift and accumulation for the wind tunnel simulations, a 1.2m cube was installed on a test site in Nuuk, Greenland, as a reference object. Pictures of the snow on and around the cube were taken during the winter periods 2017/2018 and 2018/2019. Simultaneously, ground-near wind speed and direction, air temperature and humidity, barometric pressure, precipitation, sun, and UV radiation were measured with a weather station next to the cube. The combination of observation and measurement of snow accumulation and recording of weather conditions throughout two full arctic winter periods allows the systematic relation of the wind tunnel to full-scale conditions. The relation between wind directions and precipitation has led to different snow accumulations around the reference cube. But, also the thermal effect changed the snow properties over time. Understanding these processes will help to control the wind tunnel tests, hence some substitute materials are more advantageous for simulating specific accumulation phenomena than others. Consequently, the choice of material shall rather be based on the expected dominating accumulation phenomenon, than on a one-material-fits-all-purpose approach.

3.1.2 Experimental Wind Tunnel Testing

For wind tunnel testing a small-scale boundary-layer wind tunnel is available at DTU Civil Engineering, which can be used to conduct fundamental studies regarding the simulation method of snow accumulation and case studies on individual buildings. The wind tunnel was retrofitted for snowdrift studies with substitute materials. The wind tunnel will be used to conduct fundamental studies regarding the simulation method of snow accumulation and case studies on individual buildings. The distribution and magnitude of snow phenomena depend to a large extent on the air motion around buildings. Wind tunnel testing is a proven method for simulating the airflow interaction building structures and provides a suitable platform for investigating snow transportation and deposition. The experiments are evidence-oriented and determine a simulation approach for explorative experiments. The results in this section generate an accurate testing method to reflect new questions for future research.

3.2 Wind Tunnel Set-up

Figure 16 shows the overall layout of the closed-circuit boundary layer wind tunnel at DTU Civil Engineering with the integrated experimental setup for snow studies. The open test section of the closed-circuit boundary-layer wind tunnel at DTU Civil Engineering is at walls and ceiling equipped with spaced wing profiles to be blockage tolerant (Kong & Parkinson, 1997) and with a digital-controlled seeding mechanism. For the generation of the turbulent boundary-layer a combination of Counihan random turbulence generators, wall barrier, and roughness fields have been installed in the flow-processing unit (FPU). Since at times very low airspeeds are applied, the flow velocity is controlled with a standard Pitot tube at the FPU entrance and a low-speed hot-wire probe (LSHW) at the entrance to the test section. To study the role of ground moving and airborne snow on accumulation characteristics, the seeding mechanism allows the controlled and repeatable release of substitute material into the test section (Figure 13). The test section has a cross-flow dimension of 0.48 x 0.48m and a length of 1.5m with blockage-tolerant walls. The wind tunnel air velocity is controlled at a reference height of 150 mm with a low-speed hot-wire anemometer (LSHW) upstream of particle release shown in Figure 13.

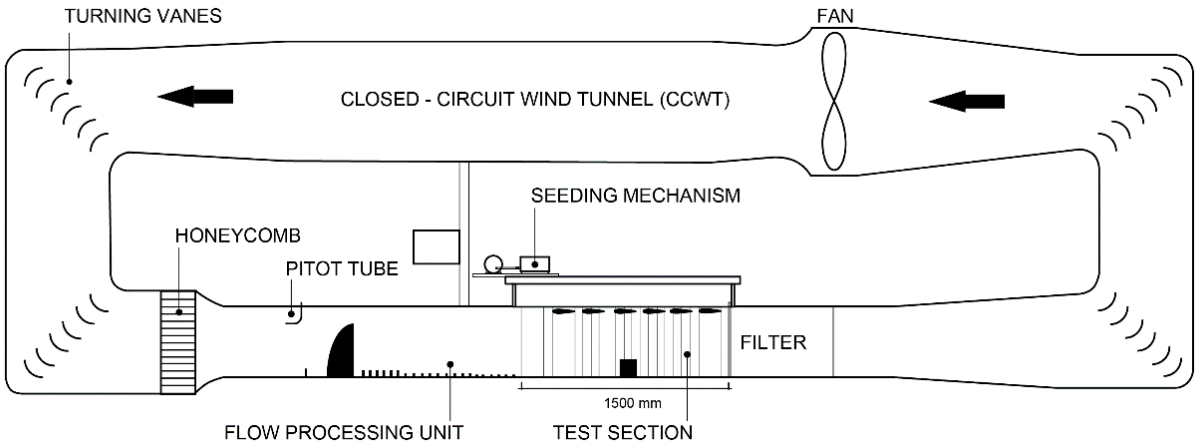

Figure 14 Closed-circuit wind tunnel (CCWT) with a retrofitted configuration for snowdrift simulations.

The normalised measured wind profile K(z) is re-scaled with the LSHW airspeed to control the flow velocity over height (Eq.11):

$$U(z) = U_{ref} * K(z) \tag{11}$$

Based on experience, the rugged terrain around the Nuuk cube was not likely to change its characteristics. The vertical profile of the airspeed distribution in the wind tunnel study was measured without seeding or snow cover to protect the flow speed sensor from airborne particles. With sharp-edged objects in a turbulent flow, the wakes of the object are dominant. Anno (1984) suggested therefore relaxation of the mean wind profile and obtained 10% turbulence intensity level at 1 cm above model snow. A vertically traversed Cobra-probe was used for the wind profile and a stationary Pitot tube at FPU inlet as overall reference speed. Figure 18Figure 65 shows the Measured mean wind speed profile and turbulence intensity in the closed-circuit wind tunnel (CCWT). We obtain a turbulence intensity of 26% at 1 cm model and mantain 14% at 10 cm. With airspeed, the dispersion of the substitute snow on the ground area in the test section indicates the "impact zone" (indicated in Figure 15). Erosion tests for calibration performance of the substitute in the test section determined the airspeeds at which the substitutional materials start to erode over the ground U_{Th} [m/s] threshold velocity. Erosion tests are mostly performed in the literature to simulate the saltation process.

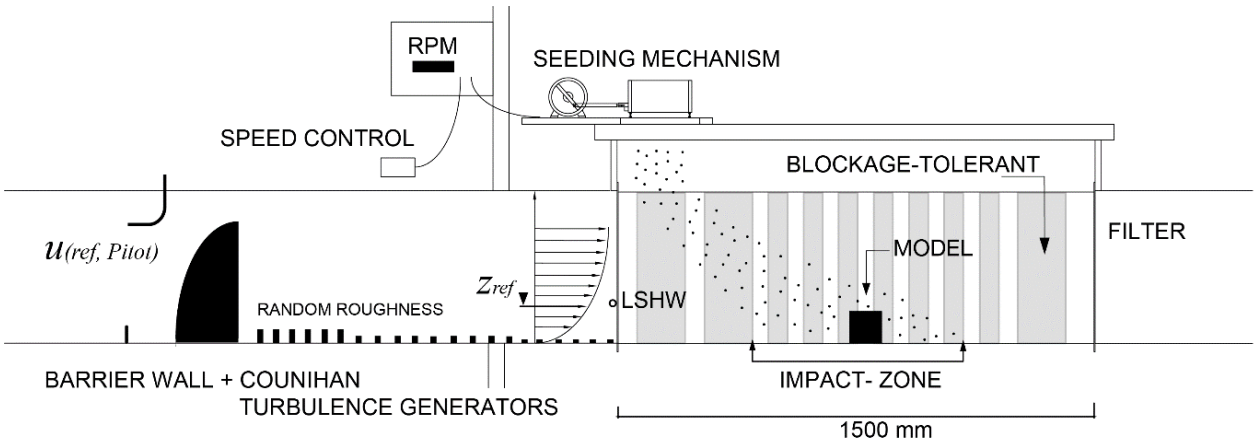

Figure 15 Wind tunnel test section with barrier wall 5 cm height and Counihan turbulence generators 6 cm width. Half-open test section (blockage-tolerant).

ince the snowfall tests have been performed at very low airspeeds, the flow velocity is controlled with a standard Pitot tube at the FPU entrance and a low-speed hot-wire probe (LSHW) at the entrance to the test section. The test section has a cross-flow dimension of 0.48 x 0.48m and a length of 1.5m with blockage-tolerant walls. The wind tunnel air velocity is controlled at a reference height of 150 mm with a low-speed hot-wire anemometer (LSHW) upstream of particle release shown in Figure 15.

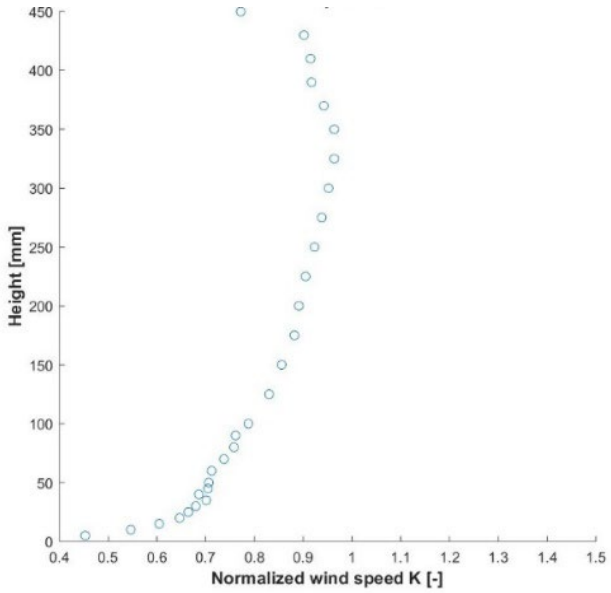

Figure 16 Measured mean wind speed profile in the Closed-circuit wind tunnel (CCWT).

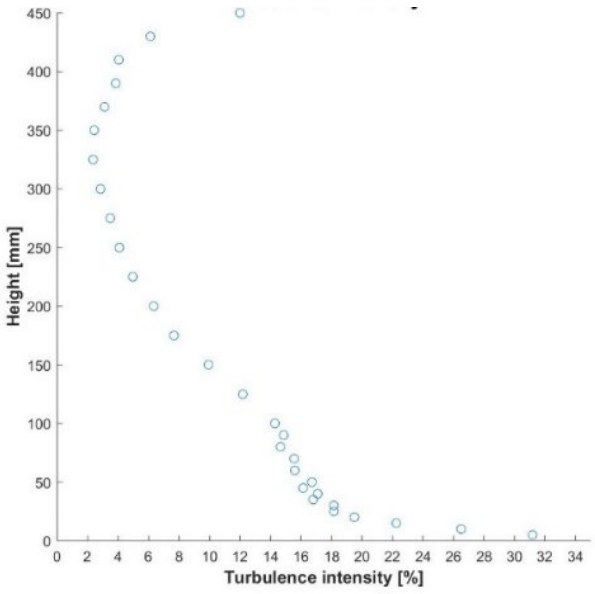

Figure 17 Measrued turbulence intensity in the Closed-circuit wind tunnel (CCWT).

The ABL profile generated in the flow-processing unit fits well for urban model scales in 1:400. The turbulence intensity is underrepresented from 10 cm model height. Simultaneously, the ABL setup was applied to the Nuuk Cube experiment. The expression of the logarithmic profile is not defined below z_0 in the Eurocode (see Figure 18). Therefore a comparison to the Eurocode terrain categories is not effective. Important is the turbulence intensity and the flow field of the model in the wind tunnel simulation (Figure 19).

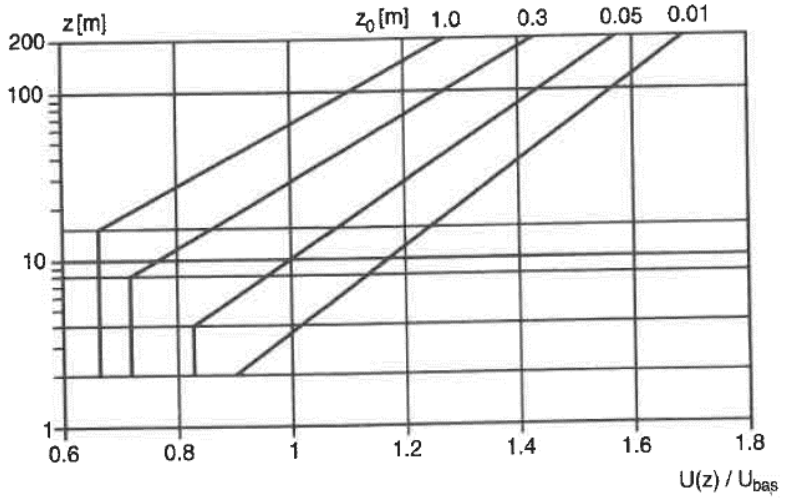

Figure 18 Variation of mean wind velocity with height according to Eurocode 1.

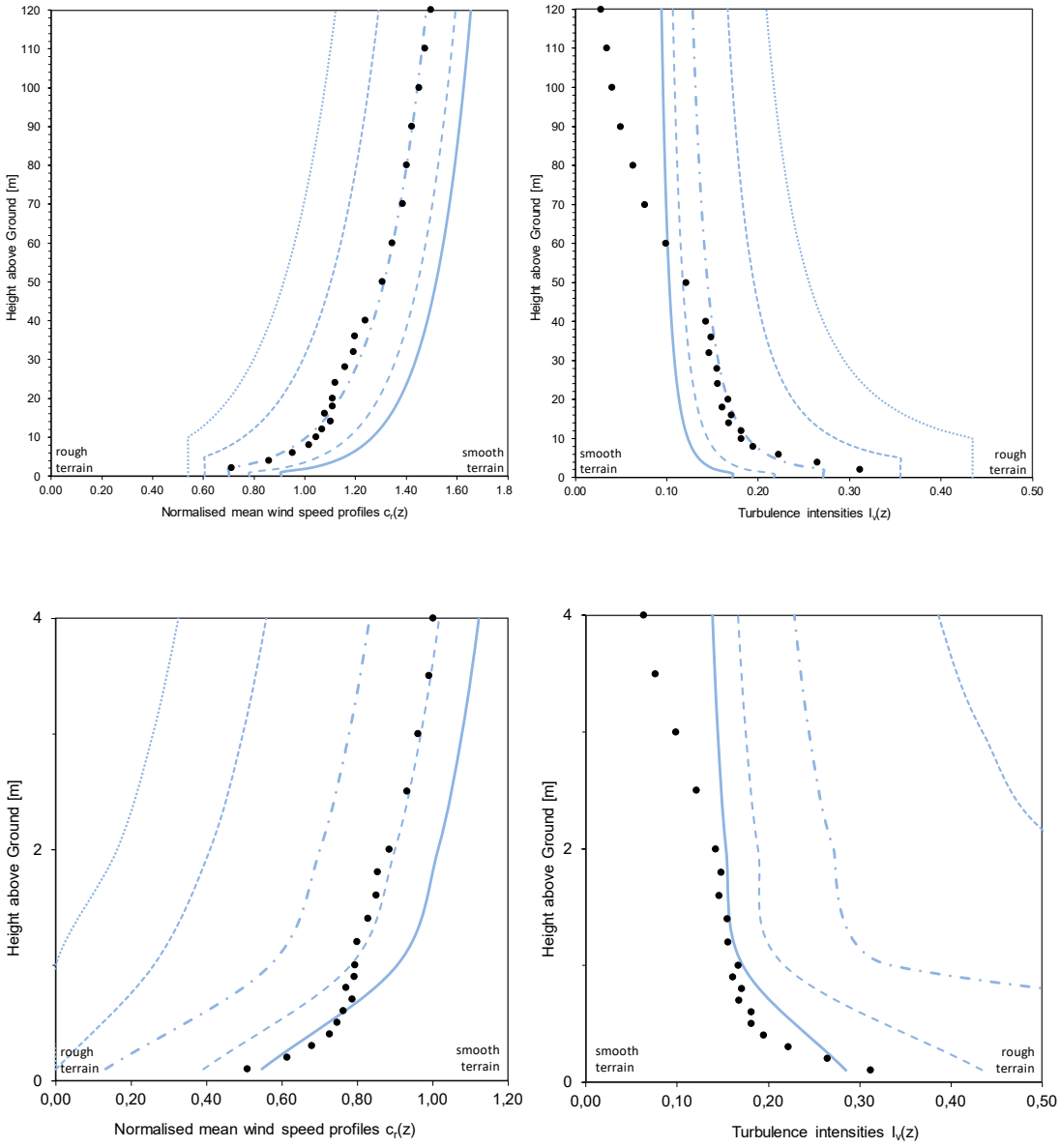

Cat. No.	Index	z_0 [m]	Description of Terrain Category
0		0,003	Sea or coastal area exposed to the open sea
I		0,01	Lakes or flat and horizontal area with negligible vegetationand without obstacles
II		0,05	Area with low vegetation such as grass and isolated obstacles (trees, buildings) with separations of at least 20 obstacle heights
III		0,3	Area with regular cover of vegetation or buildings or with isolated obstacles with separation of maximum 20 obstacle heights
IV		1	Area in which at least 15% of the surface is covered with buildings and their average height exceeds 15m

Figure 19 Measured mean wind speed profile and turbulence intensity fitted with Eurocode at a scale of 1:400 and a scale of 1:20. The model was extrapolated to z_0

3.2.1 Measuring procedure of model snow and set-up

After all snowdrift test procedures at the wind tunnel facility, each test result of the accumulation shape was captured with a 3D-scanner method to measure the depth of the accumulated substitute material on and around the test model. The structured 3D light scanner from HP was used to create contour images and depth of three-dimensional distribution. For each test, the test model was scanned once without particles supplied and again after the snowdrift testing. Which allowed measuring the thickness of the cover and its distribution on the model. The enhanced structured 3D light scanner consists of a projector, two cameras, and a calibration plate and was positioned near the model test section (Figure 20). According to the manufacturer, the physical dimensions of an object can be captured with accuracy up to 0.05 mm. Prior to scanning, the scanner was calibrated with a calibration scale to the model object size and the distance to the scanner. The calibration scale consists of patterns of different sizes (Figure 20). The scanner technology casts light patterns onto the object and produces a digital representation of the object by fusing single dimension scans that are captured at multiple angles. If the distance between the object and the scanner has changed, the scanner needs a re-calibration. Black curtains are used as background, to avoid scanning any parts of the wall or wind tunnel facility and to have the projected light pattern visible on the test model. To calibrate the object, both cameras have to be adjusted until both can see the object in the viewport of the HP 3D scan software (Figure 20). The HD Camera detects the patterns beamed out by the projector to generate a digital model of the physical object. The red lines in the viewport indicate if areas are overexposed. The projected pattern is adjusted to the panel calibration plate to perform the scan. For best results at least 16 scans for a 360 degrees scan of complex building shapes were performed.

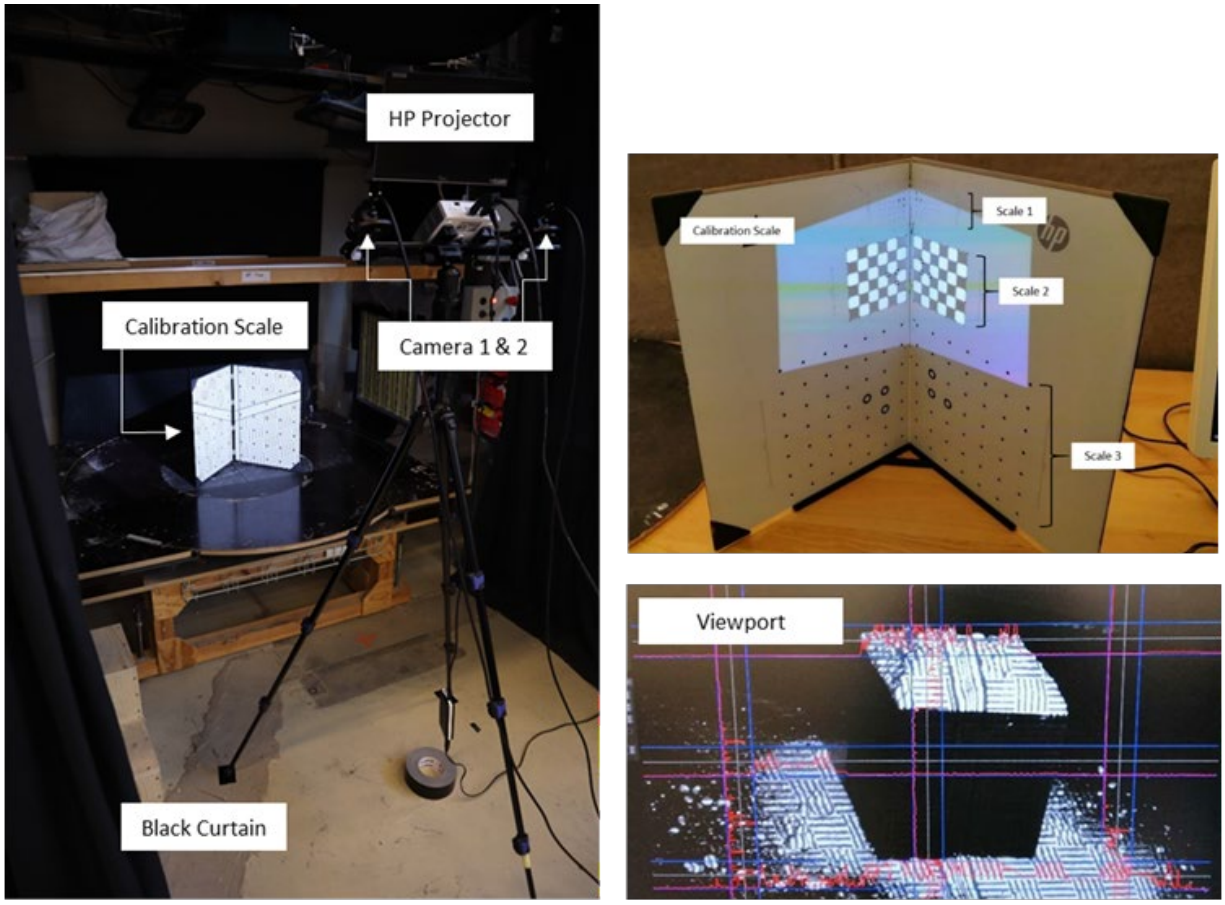

Figure 20 *Left*: Scanning Test Set-up at Wind Tunnel Section. *Top*: Calibration Scale and configurations to scan cube model objects with max. 60 mm. *Below*: Vieport of HP 3D Scan software for brightness and contrast configuration of HD Cameras

Prior to the test procedure, a sensitivity study was performed to test high-contrast and sharp-edged objects with the structured 3D light scanner. In order to test the performance of the structured 3D light scanner, a high contrast such as black and white cube objects were scanned. Since the substitute materials have bright colours and textures, the brightness settings and lighting was tested to differentiate the material from the model cube. A black cube of 5 cm, 7 cm and a white 7 cm cube object was scanned with the structured light scanner. As a comparison, the object's volume was measured by python and the HP 3D Scan software against the original object size.

Table 2 Scanned volumes for different cube sizes, contrast and texture according to calibration scale:

Cube	Calibration scale	Volume Python [cm^3]	Volume HP [cm^3]	Volume [cm^3]
5 cm black	60	128	120	125
7 cm black	120	335	317	343
7 cm white	120	343	344	343

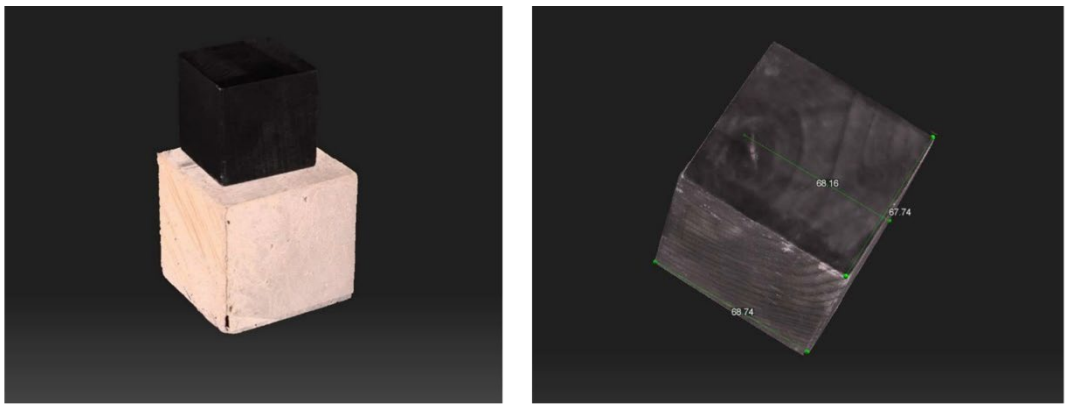

(a) (b)

Figure 21 Demonstration of model scan with the HP 3D Scan software. Testing contrast on a small black cube against a white cube and accuracy of generated mesh model of a 5 and 7 cm cube. (a) Scanned model object of a 5 cm black cube and 7 cm white cube of high contrast. (b) Dimensions measured by HP 3D Scan of a 7 cm cube.

Generally, for clear scan results, the test facility of the laboratory should be darkened to allow the projected light to be visible onto the object. The first test scans of a 5 and 7 cm black cube were performed with a dimmed ambient light. The measuring accuracy increased significantly when avoiding any flickering light sources in the last scan of the white 7 cm cube (Figure 21). Both, white and black model cubes could be captured entirely by the structured light scanner. Although, the black

cube needed higher brightness settings in the scanning phase to differentiate the object from the background. Therefore, when scanning objects with a high contrast (texture white balance) it is recommended to scan them separately.

3.2.2 Seeding control

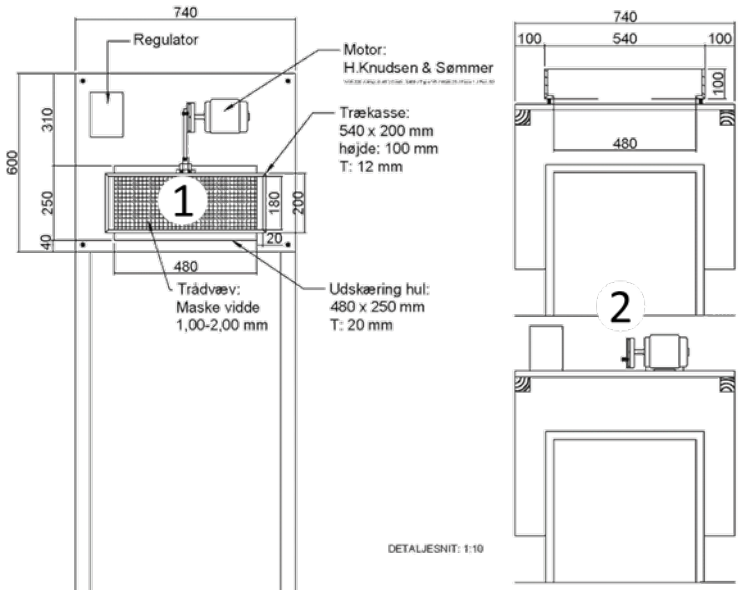

Figure 22 Drawing of the seeding control mechanism (1) above the test section at the Closed-circuit wind tunnel (CCWT) (2). And seeding antistatic mesh.

According to IFA (IFA Institute for Occupational Safety and Health of the German Social Accident Insurance, 2016), organic powders such as potato flour and wheat flour can be a dust explosion hazard. To this end, an anti-static mesh ((1) in Figure 22) was built into the seeding box and an industrial vacuum cleaner with anti-static material was used when clearing the test facility. In literature, organic substitutes have been discussed regarding their explosive properties. Kim el. 1991 used nonexplosive sodium bicarbonate (in Europe Natron) which is also an ingredient of baking powder to prevent an explosion danger also mentioning Anno's simulation method (Anno, 1984) with activated clay of discharged particles. Furthermore, economy and availability play an important role in the selection of a substitution material. All presented substitute materials in our specification tests are available in supermarkets or industrial suppliers.

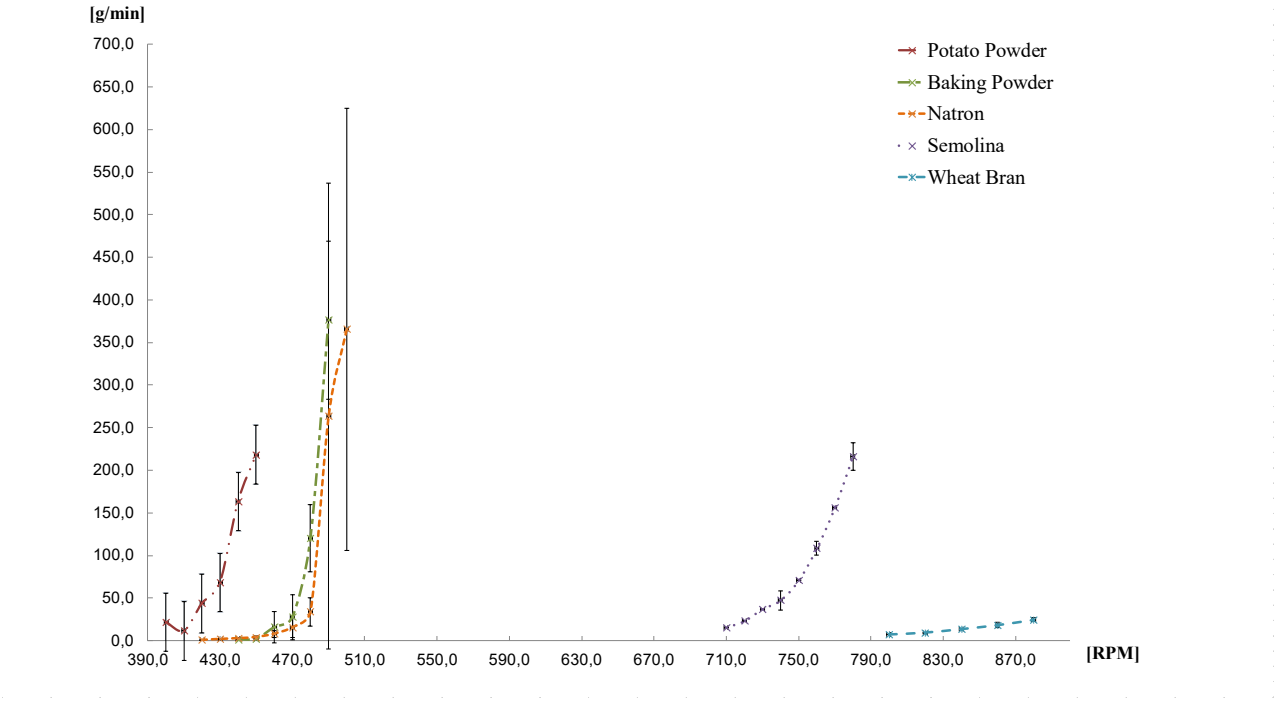

Figure 23 Particle seeding rate after particle release in the seeding machine in Q [g/min]. Fine grained materials: Natron, Baking powder and Potato starch. Coarse grains: Semolina and Wheat Bran.

The amount of released substitute at the test section with different speed ranges was measured at zero airspeed. Snowfall rate data from nature can then be adapted to the experiment if neccessary. Figure 23 shows the different amounts of seeding rates as a function of the frequency (here in revolutions per minute, (RPM)) of the actual amount released by the sieve.

4. Substitute Materials

4.1 Specification tests

Prior to the investigation of drifting snow in wind tunnel testing at reduced scale multiple specification tests of common snow substitute materials were conducted to study the physical properties and the performance while air-bone. The tests serve to calibrate and classify the snow modelling procedure.

4.1.1 Particle properties

In general, the substitute materials can be categorized into two groups: fine grain and coarse grain. Figure 24 shows the microstructure of the substitutional material under a scanning electron microscope (SEM) at various magnifications. Particle morphology and surface texture are the primary factors for inter-particle adhesion and to other objects.

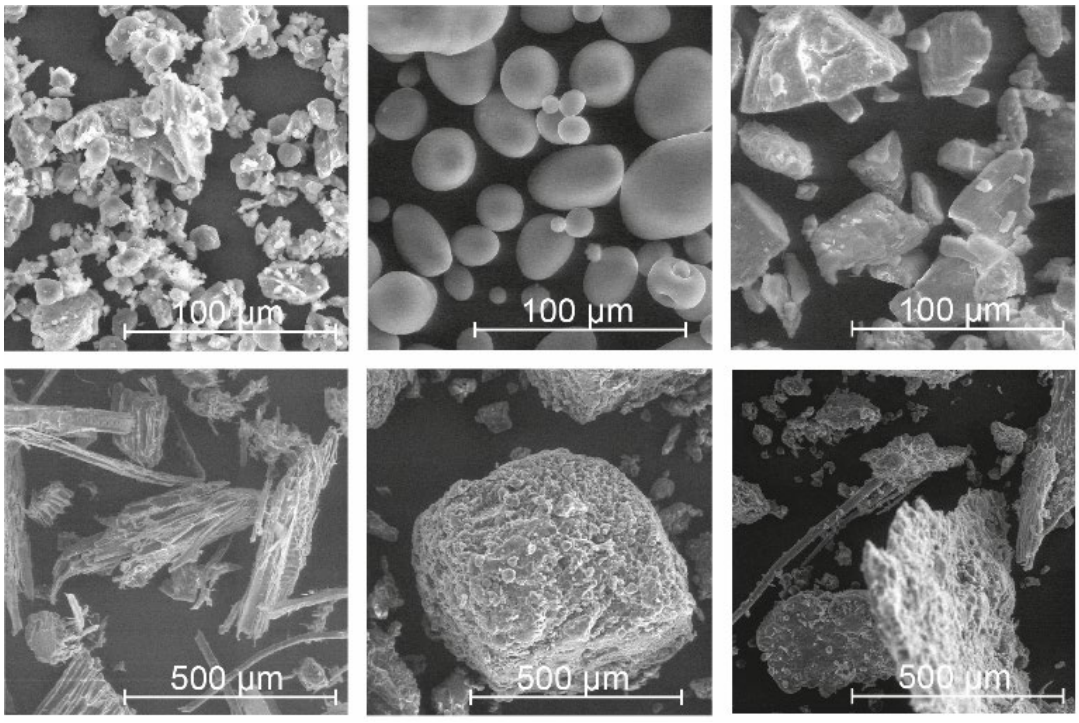

Figure 24 Snow substitutes under a scanning electron microscope (SEM). **A:** Baking powder (500 x); **B:** Potato starch (500 x); **C:** Natron (500 x); **D:** Saw dust (100 x); **E:** Semolina (100 x); **F:** Wheat bran (100 x)

Grain sizes and distribution were measured with a Laser Diffraction Size Analyser and the density was determined by using pycnometers. The fine-grained materials such as e.g. baking powder and natron (sodium bicarbonate) are more difficult to control in their flow due to the wide particle size distribution (see in Figure 25).

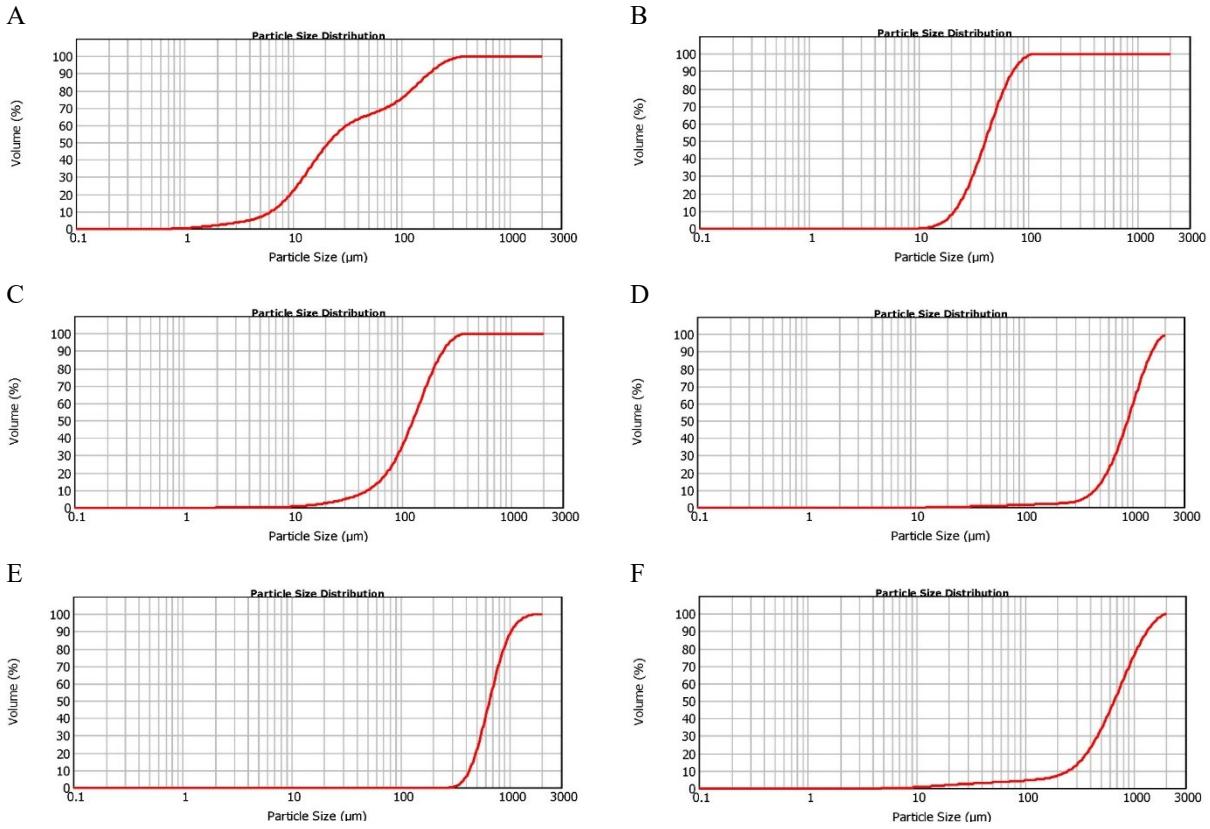

Figure 25 Particle size distribution of substitute materials: **A:** Baking powder; **B:** Potato starch; **C:** Natron ; **D:** Saw dust; **E:** Semolina; **F:** Wheat bran

The angle of repose indicates how cohesive the material is (see Figure 26). In literature, this method was used to compare the properties of snow when different climatic parameters have changed, see in Figure 27 (KUROIWA et al., 1967). An angle of repose of natural snow can vary from 45 degrees up to 90 degrees due to increasing temperature measured by D. Kuroiwa, Y. Mizuno, and M. Takeuchi in 1967 (Equation (12). Here particles are dropped gently through a nozzle and pile up to a cone shape on a disk. When the cone reaches the end of the disk the height of the cone becomes constant. The following equation has been applied:

$$\theta = tan^{-1}\left(\frac{h}{R}\right) \tag{12}$$

Here h is the total height of the cone pile. R is the radius of the disk where the applied material accumulates, here the radius was 5 cm. As a recommendation for similarity the angle of repose of the substitutional material shall approximate the angle of real snow as close as possible. For similarity requirements, the terminal fall velocity of substitutional materials was compared in snowdrift simulation with the prototype snow. In Greenland, the snow types are varying largely in size and shape. In this method, a range of substitutes was measured to cover a possible variety in comparison to natural snow. The determination for geometrical similarity can not be transferred accurately as the model decreases in scale.

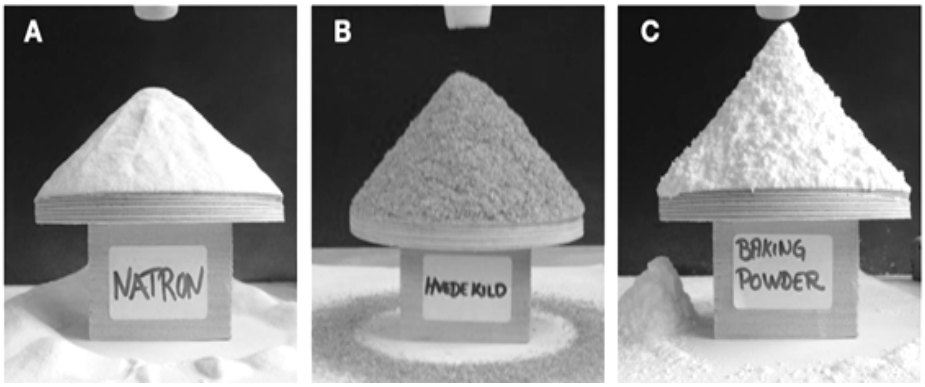

Figure 26 Measured Angle of repose of substitute snow. **A**: 39°, **B**: 43°, **C:** 52

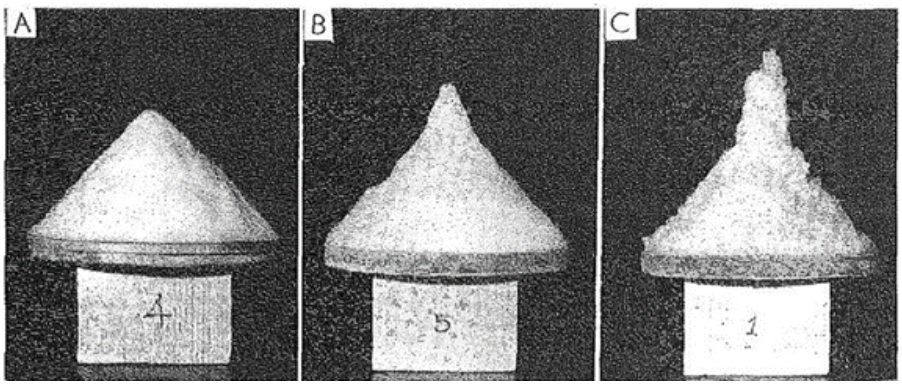

Figure 27 Angle of repose of natural snow in literature by Kuroiwa et al. 1967. **A**: ~ 47°, **B**: ~55°, **C:** ~ 90°

4.1.2 Performance tests of snow substitute

The performance of the substitutional material in the wind tunnel setup is important for validation of natural snowdrift and to show the limitations when testing snowdrift at a reduced scale. Kim el.(1991) mentioned that the first tests have been failed because the sodium bicarbonate could not erode with low velocities. In their second approach, they supplied the material into the flow and tested it with lower wind velocities. The threshold velocity U_{Th} [m/s] at which different snow substitutional materials start to erode over the ground, are mostly performed in the literature to simulate the saltation process. Therefore, we tested all selected substitute materials to determine the threshold speeds.

Figure 28 shows all tested substitute particles on the surface ground in the wind tunnel section with their ejection abilities when applying wind velocity:

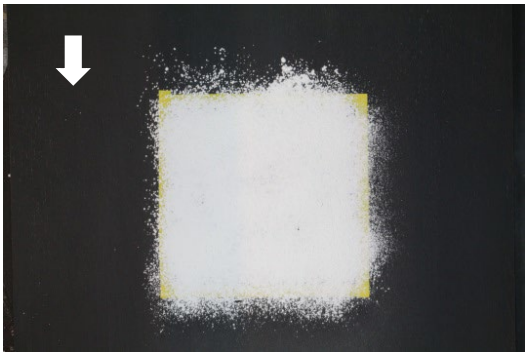

1.Baking powder $U_{Th,Pitot}$ = 10,26 [m/s]

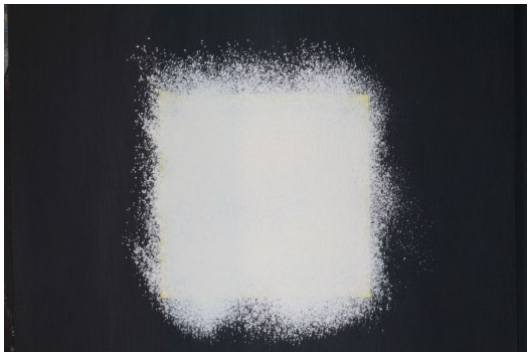

2. Flour (Wheat) $U_{Th,Pitot}$= 10,34 [m/s]

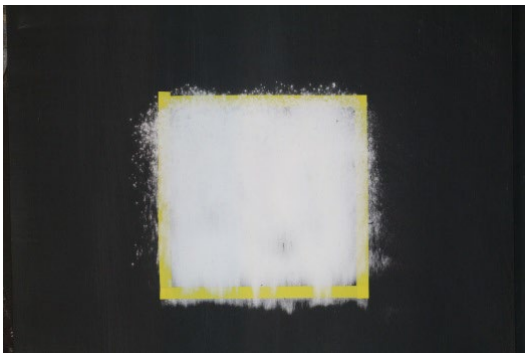

3.Potato Powder $U_{Th,Pitot}$ = 10,34 [m/s] 4.Wheat Bran $U_{Th,Pitot}$ = 4,96 [m/s]

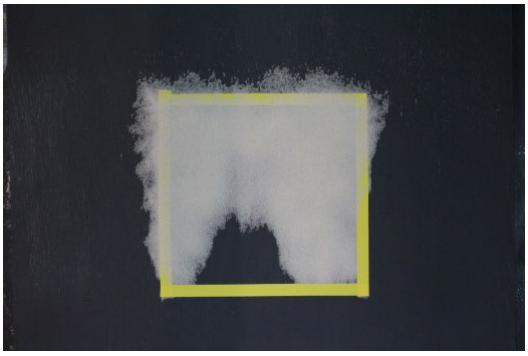

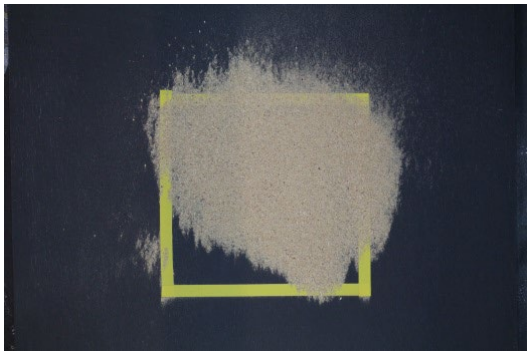

5.Sand $U_{Th,Pitot}$ = 7,37 [m/s] 6.Sawdust $U_{Th,Pitot}$ = 4,62 [m/s]

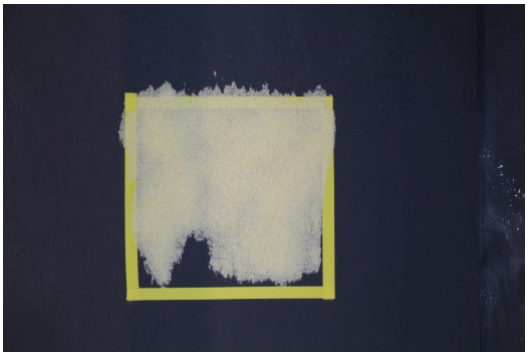

7.Semolina $U_{Th,Pitot}$ = 7,9 [m/s] 8.Sodium Bicarbonate (Natron) $U_{Th,Pitot}$= 5,3 [m/s]

Figure 28 Threshold speeds of substitutes at $U_{Th,Pitot}$ in wind tunnel test section. Flow direction from Top.

With airspeed, the dispersion through the seeding mechanism of the substitute snow (e.g. Natron) on the ground area indicates the “impact zone” (Figure 29) at the test section. The estimation of change in snow density distribution and rate over the covered area is used to determine where models should be placed within the test section.

U_{ref} 1 m/s dispersion over WT- section area

U_{ref}1,5 m/s dispersion over WT- section area

U_{ref}2 m/s dispersion over WT- section area

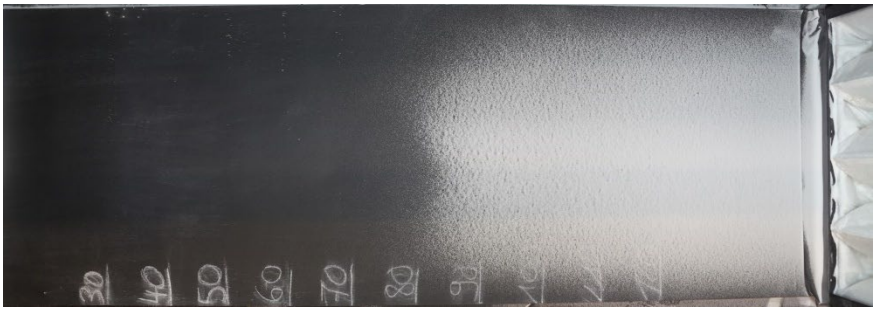

U_{ref} 2,5 m/s dispersion over WT- section area

Figure 29 Distributions of Natron at different reference wind speeds $\boldsymbol{U_{ref,LSHW}}$. Flow direction from left.

To that end, a variety of different model cubes sizes were tested for calibration of the modelling. Based on the prior specification tests and the test set-up, the test conditions have been defined until phenomenological similarity was obtained. The model cubes have sizes of 5 cm, 7 cm, and 10 cm. All cubes have been tested with the same configurations to compare the scaling effect. The tested materials reflect the scouring effect in the horseshoe vortex for cubes larger > 5 cm (see also Figure 30). Here, semolina and sand showed the strongest response to scour or erosion phenomena, but could not deposit on the model roof.

A: *5 cm* ***B:*** *7 cm* ***C:*** *10 cm*

Figure 30 Reference cube in 80 cm test section with Natron: Camera 1/30sec; $\boldsymbol{U_{ref,LSHW} = 2}$ m/s; $\boldsymbol{Q}$ = 60 g/m. Flow direction from left.

All material specifications and performance tests of the substitute materials serve as configuration settings of all presented wind tunnel experiments in this work.

4.1.3 Results substitute specifications

Natron could accumulate well on a model due to its adhesion ability (angle of repose) and at the same time being able to perform erosion. Other fine-grained materials had a higher angle of repose but showed pure erosion properties due to the attachment phenomenon by small particles (D < 30 µm). Also The particle size for snow can very largely, in our wind tunnel experiments we assumed Dp = 500 µm for blowing snow according to (Mellor, 1965)) they tend to be smaller in size than particles on the ground.

A list of the measured material properties used in the specification tests are reported in Table 3.

Table 3 Measured material properties: density ρ [g/cm3], angle of repose Θ [°], mean particle size D_p [µm] (determined by particle distribution). Size at 50% volume. Erosion and U_{Th} [m/s] threshold velocity at $U_{ref,Pitot}$. Fall velocity U_f of substitute without airflow (free fall), with photographic analysis through laser visualization of particles.

Material	ρ [g/cm^3]	D_p [µm]	Θ [°]	$U_{Th,Pitot}$ [m/s]	U_f [m/s]
Baking powder	2,07	22	52	Low/ no erosion	0,98
Potato starch	1,49	41	42	Low/ no erosion	0,76
Wheat flour	1,46	82	51	Low/ no erosion	0,72
Natron	2,24	127	39	5,3	0,44[1]
Saw dust	1,35	902	52	4,6	0,33
Semolina	1,31	658	27	7,9	1,28
Wheat bran	1,32	663	43	4,9	0,75
Sand	2,63	250	24	7,4	No data

[1] calculated value with U_f = 2,6 U_t^* (Kim et al., 1991)

Table 4 Selected studies with measured properties of natural snow in field studies. Snow properties: density ρ [g/cm3], mean particle size D_p [µm], angle of repose Θ [°] and fall velocity U_f (free fall).

Natural Snow	ρ [g/cm^3]	D_p [µm]	Θ [°]	U_f [m/s]
Mitsuhashi (1982)	0,50-0,90	100-150		
Kim et al. (1991)		70-4000		0,3-2,0
Kuroiwa et al. (1967)			45,63,90	
Liu et al. (2018)	0,22-0,28	2000-4000	60	0,5
Author of this work (sample: Finland 2017)	0,15-0,44			
Author of this work (sample: Sisimiut /Nuuk, Greenland 2016)	0,44-0,60	500-3000		

Natural snow properties from full-scale are summarized in Table 4 and selected studies from Kim et al.(1991), Kuroiwa et al.(1967), Liu et al. (2018) and Mitsuhashi (1982). The measured values of snow density in chapter 2.2 of the samples in Finland had a snow density of $\rho = 0{,}15$ to 0,44 g/cm^3 with an alpine texture and rounded and faceted grains, while the measured densities in Greenland had much higher values with even up to $\rho = 0{,}60$ g/cm^3. The sample in Sisimiut was taken from a low angle roof of a single house at the premises of the Technical University of Denmark. Similar snow density values were measured at the Nuuk Cube Field Experiment (NCFE) location. The Antarctic snow densities at the field study of Mitsuhashi (1982) are even higher than the measured values from Greenland.

It should, however, be noted that the substitute snow particles differ in their mass and size compared to real snow properties. Additionally, natural snow particles vary in their properties to a large extent depending on the region and climatic conditions while a substitute e.g. baking powder does not change its properties. It is difficult to simulate the snowdrift phenomenon at reduced scale when substitutes compared to the natural particle does not have similar properties.

5. Nuuk Cube Field Study

5.1 Meteorological observations

This chapter gives a brief overview of the Nuuk Cube Field observation as the appended paper and background to the statistical treatment of the meteorological observations to identify snow events and their characteristics. A weather station next to the object cube recorded weather data continuously throughout three years. In retrospect, the weather history has been reviewed to get insights into the climatic conditions which had led to the snow formation of the object cube. Concerning the general understanding of possible snow events forming characteristic accumulation shapes around the cube a statistic about possible correlated weather variables to describe or identify such snow events needed to be tested. For a definition of the snow events following variables are tested:

a) *The precipitation as a function of temperature over time. Is there a certain temperature range for snowfall? And what is the duration of snow events?*

b) *Classification of NCFE snow events with respect to registration interval of 'tipping' mechanism of the weather station.*

c) *Testing the correlation between precipitation and wind direction? Is there a variability of wind direction and speed during a snow event? And is there a dominating snowfall direction?*

The winter season in this analysis is from October to April. A detailed description of the data set and quality is presented in the appended paper *Nuuk Cube Field Experiment - Meteorological observations*.

The idea for the set-up for a Nuuk Cube came when traveling first to Sisimiut. Originally an observation of a building or building site on premises of the Sisimiut campus of the Technical University of Denmark DTU was planned. No suitable site was found to ensure easy access and data acquisition computer with stable internet and the weather in Nuuk is more unstable and extreme compared to Sisimiut. Architect Peter Barfoed offered his premises in Nuuk for this experiment. The experiment was a great opportunity to get measurements near-surface ground and with a generic object for an optimal validation case. The Ph.D. economics did not allow installing an automatic

professional weather station used by meteorological institutions. To relate observed show accumulation patterns to past weather history, a Vantage Pro2 Plus weather station by Davis Instruments was installed on a tripod. The cube was made of plywood and coated with a dark grey colour. The Nuuk Cube set-up has three set-up campaigns.

The first arrival at the site was at the end of the winter period 2017 in March. The snow had already accumulated over the winter and covered the area with a deep snowpack. The cube was therefore betted into the snowpack (see in Figure 31). To level the cube a pallet as foundation was mounted under the backside of the cube. After the cube has been placed the snowpack has been lifted evenly to the base of the cube at 0.00 m. The base of the cube was covered in snow, this allowed no entering of wind flow and prevented the object to be lifted by wind force. In phase one the data of the weather station was conducted from March to April 2017.

Figure 31 Installation and assembly of the Nuuk Cube Field Experiment on the outskirts of Nuuk City in March 2017.

The definition for a precipitation-event in climatology is not a new invention. A precipitation event is defined as a period of continuous precipitation with intervals of no precipitation (Isyumov & Mikitiuk, 1977). In order to separate one event from another, a length of a separation interval is often specified to group the single precipitation signals. A separation interval of a snowfall-event refers to the number of dry hours (intermittence time) where no precipitation is recorded for a certain time

and determining where a new event starts. The Davis weather station defines a rain-event as a period of time upon which one rain-event is considered separate from another rain-event when time exceeds roughly 15 minutes without a “rain” signal. It is not clear if this definition is also applicable to snowfall-events. In a search for an appropriate separation interval, Robinson and Walsh (1895)studied the impact of separation choice compared when using 1 hr up to 5 hr. The smallest separation was 1 hr, hence the observation resolution was set to one hour data records. Therefore, no shorter intervals could have been tested. The result was that a 2 hr interval was chosen arbitrarily, hence no clear indication was given by any natural or climatologically determined value. Event durations according to Robinson and Walsh *“[…] may be 50 hr long, but the vast majority have a duration of less than 10 hr”* (Robinson & Walsh, 1895) but not longer than 20hr at a separation interval of 2 hr. One hour separation was defined by Brown et al., (1985). Here a precipitation-event is a period of one or more consecutive hours of precipitation followed by one or more hours of no precipitation. In other words, is the interval longer than 1 hr or more than it is a separate event, and if it is close to 1 hr between 2 “wet” hours its considered to be the same event. Like the previous study, the recorded observations have only a 1 hr resolution. Much larger separations to identify precipitation-events with a 12 hr period were chosen by Jennifer Luppens Mahoney (1991). She specifically analysed the climatology for snowfall-events and their characteristics. Her study had two steps, first, the snowfall amounts were separated into events, herafter the event characteristic has been analysed. The starting and stopping time and predominant wind direction are discussed for individual events. It was not explained why a 12 hr separation was chosen to be appropriated. But it was mentioned that forecasters deal with individual events daily and an event-climatology was found to be appropriated. Another study with large separation intervals (Isyumov & Mikitiuk, 1977) found an application to roof snow-load specifications with data obtained from 28 Canadian stations and a record length of 30 years. Isyumov and Mikitiuk defined statistical variables of individual snowfall amounts with wind speed, wind direction and air temperatures only by readily available 24 hr totals. They mention snowfall durations on average range between 12 and 18 hours but daily totals should be representative for snowfall quantities associated with individual snowfall events. The intermittence time here is simply a snow day or no snow day with snowfall depth over 2.54mm. But hence they have only 24h totals, they cant choose a smaller interval. They assumed daily snowfalls are independent events. Figure 32 is a summary of the separation intervals found in literature.

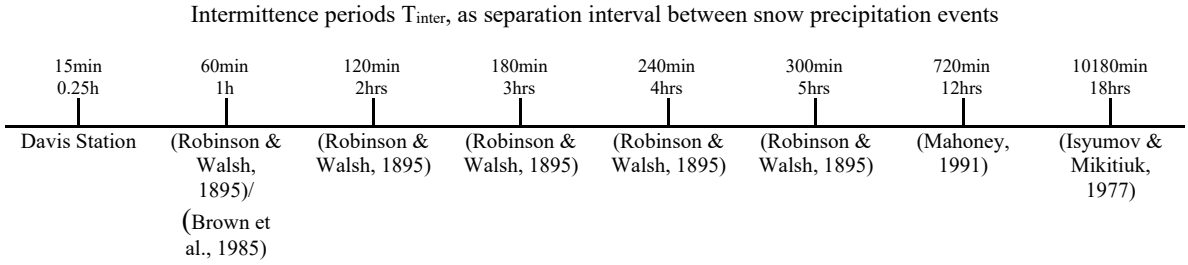

Figure 32 Intermittence periods in the literature to separate individual events from each other.

Nevertheless, no general rule for separation intervals was found to be most applicable. So far nothing indicates by any climatologically phenomenon or in literature the choice of a separation interval. Due to the missing registration of precipitation at the Davis Station, especially snowfall events, does not allow to work with the time interval between registrations as an indicator for snow event durations. A suggestion for the investigation of the snowfall events at the Nuuk Cube is further described in the appended paper.

5.2 Snow Accumulation Observations

The wind speed and direction directly measured at the cube should be used and average wind speed over uneven terrain surrounding the NCE applies primarily to this particular location for all data and derived conclusions (Figure 34). No significant influence, on the measured average wind speeds in the turbulent near-surface layer over the changing snow cover height, was assumed. A study recording data near-surface snow particle dynamics was measuring wind speeds at surface heights of 40 cm and 200 cm (Aksamit & Pomeroy, 2016). The study showed that difference of the wind speeds over the two heights are negligible as can be seen from Figure Figure 33. The small differences of a few centimetres in the height of the changing snow cover does not affect our statement about the wind measurements at the Nuuk Cube.

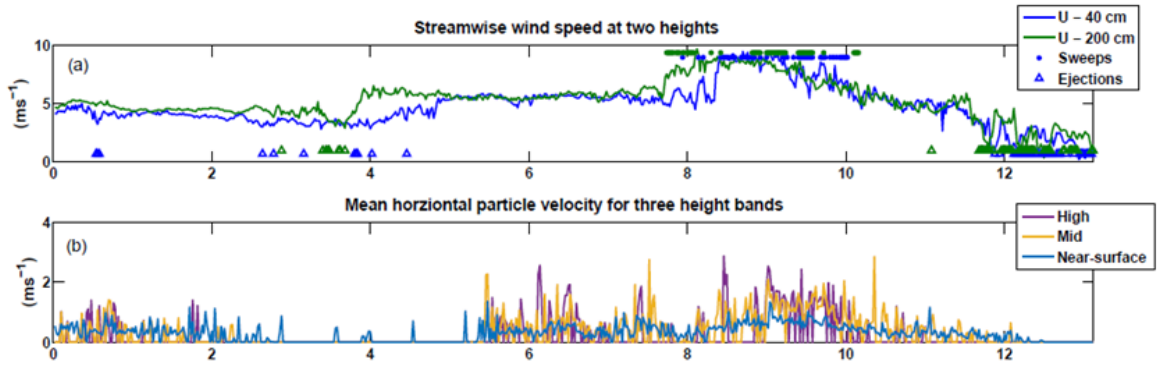

Figure 33 Wind speed near snow surface cover extracted from (Aksamit & Pomeroy, 2016), original figure 9: Recording no. 3 time series for 23 March: (a) 50 Hz streamwise wind speed at 40 and 200 cm above snow surface; (b) 50 Hz snow particle velocities obtained by binning particle vectors in three height bands ($1 < z < 4$ mm, near-surface; $4 < z < 8$ mm, middle;$8 < z < 30$ mm, high), then temporally averaged over 25 frames

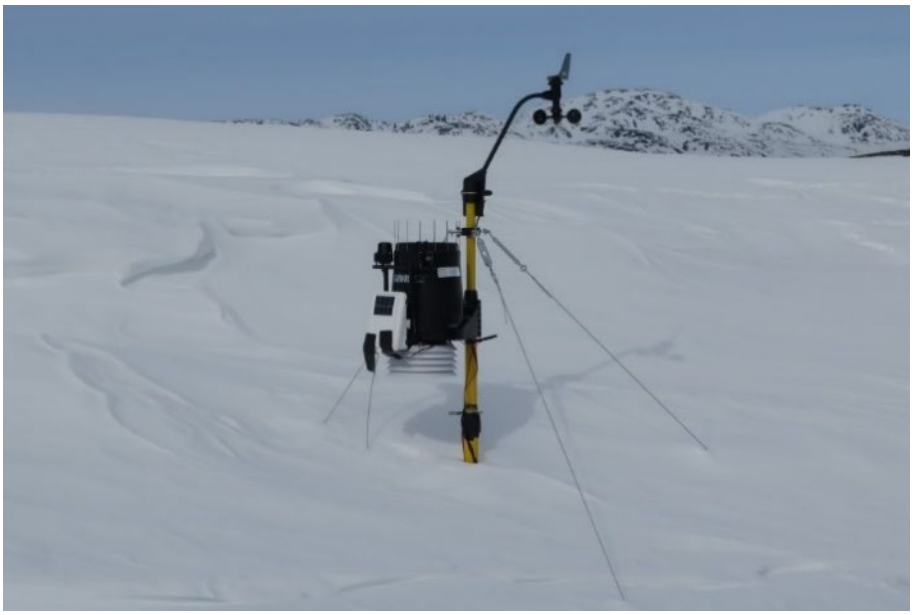

Figure 34 Vantage Pro2 Plus weather station by Davis Instruments was installed on a tripod with storm guys in 3m distance from the cube weather station with wireless data transfer to receiver and logging computer. he outdoor sensor unit (Integrated Sensor Suite – ISS) was equipped with a heating element to keep the rain gauge and collector operable at temperatures below freezing point.

5.3 Measurement of Nuuk Cube

A full-scale measurement of the Nuuk Cube object was carried out with a Photogrammetry method to replicate a small scale 3D model of the cube for a snowdrift wind tunnel performance. The advantage of using this method is the accurate typography representation in the model design. This would be difficult to achieve with a hand built foam model. To compare the full-scale dimensions with the actual generated model construction a random sample of the photometry model dimensions at the cube top edge was measured and measured again in the 3D scan model with the HP software and Rhino (Table 5). Here, two corner edges dimensions have been compared, first length A and second B.

Table 5 Full-scale Measurement of Nuuk Cube with shooting distance of 3 m compared to Photometry measurement and Nuuk Cube model in 1:20.

Nube Wall	Full-scale [m]	Photometry [m]	Model Scan 1:20 (HP) [mm]	Model Scan 1:20 (Rhino) [mm]
A	1,46	1,41	67,5	68,5
B	1,25	1,23	60,16	61,5

In order to scale the photometry model to the correct dimensions, the reference marks at the full-scale cube object helped to find the correct scaling to generate the 3D mesh surface.

6. Included Papers

6.1 Nuuk Cube Field Experiment – Part 1: Meteorological Observations

The motivation for the Nuuk Cube Experiment was to collect full-scale data near ground on the weather conditions to correlate those with snow accumulation observations on a generic object cube and finally to draw recommendations for simulations of snowdrift and accumulation processes. The explorative analysis classified snow events in this study with respect to registration intervals (tipping signal rain gauge). Typical wind speeds during snow events are separated between precipitation falling at ambient air temperatures below -2°C for *dry snow* events and precipitation between -2°C and +1°C as *wet snow* events According to Li and Pomeroy (1997), "*dry snow is snow that has not received temperatures of 0℃ or above, or wet precipitation since the last snow event*". The variability of wind direction during snow events was found to be negliable and wind speeds are below threshold speeds for snowdrift. The wind tunnel facilicty at the Department of Civil Engineering has been retrofitted to perform such phenomenon of low wind speed snowfall combined with erosion for wet snow accumulation pattern.

The anemometer of the weather station was placed at 1.4m above terrain to be at a height approximately corresponding to the top of the 1.2m cube, which in turn is mounted on a small platform to compensate for the uneven terrain. Main aspect of measuring the wind speed at that height is to get an exact reading of the wind speed responsible for the snowdrift and deposition mechanism hence allowing for a better control of the key boundary conditions. The distance between test object and wind measurement point varies amongst full-scale snowdrift studies and the estimation of the ground wind speed becomes naturally more accurate, the closer these locations are. In this study, the "at corresponding height" measurement was preferred over the standard 10 m height to obtain the best possible consistency between observed snow accumulation patterns and the corresponding wind flow data. For the purpose of comparison, the ground-near wind speed can be extrapolated to the standard 10 m above ground within the accuracy of the boundary-layer

description. For snowdrift simulations however, the wind speed and direction directly measured at the cube should be used.

6.2 Nuuk Cube Field Experiment – Part 2: Snow Accumulation Observations

This paper is linking the various meteorological conditions with the observed accumulation behaviour. The Nuuk Cube Field Experiment (NCFE) revealed in the first paper valuable information regarding the characteristics of arctic snow events in Nuuk area. *But how does this compare to other single event observations in the field of research?* Observations in the NCE have shown that the accumulation pattern is influenced by the flow around the cube. While isolated single events are satisfactory to predict the effect of accumulation on wind tunnel model tests, multiple-events obtain a more critical situation of snow deposit compared to a single event. We considered here no isolated event but rather a situation that reflects a snow deposit seen with housing objects in cities. Are single event consideration for a city study even feasible? Here, the accumulations of multiple events may well be similar to the single events.

Unlike single event observations, the cumulative accumulation deposit surrounding the object to a larger extent than single mono-directional events. This means that multiple-events are more relevant for issues related to functionality of buildings or arrangement of buildings. The single events with higher wind speed observations are to a large extend, free from deposit around the object. Single storm events with high wind speeds lead to a higher peak accumulation at cube object wall but large erosion areas keep the object free from snow to settle.

6.3 Nuuk Cube Experiment – Part 3: Wind tunnel experiment of snow accumulation

In the second paper we established the design event from the Nuuk Cube observation to develop a practical approach in wind tunnel testing. For modelling the wind flow and airborne particle motion standard similarity rules in wind tunnel testing can be applied. Modelling the adhesive behaviour, however, is limited due to inadequate reflection of thermodynamic effects and transformation of snowflakes in nature. This deficiency is usually compensated by approximating the appearance of snow accumulation in nature through the right choice of substitutional material in the scaled experiment. Consequently, simulations using simplified particle models for snowdrift and accumulation studies rely substantially on a phenomenological similarity to observations in full-scale. This applies equally for both, experimental and numerical simulations. The wind tunnel validation test of the Nuuk Cube Experiment (NCE) suggest an experimental procedure used to investigate snow accumulation around buildings. The physical properties of snow are complex and can only be simplified for modelling approaches. But how can city layouts at reduced scale compare to the simulations of the scaled Nuuk Cube? In the initial tests no attempt was made in different scale testing due to lack of available time. All tests should be repeated with emphasis to the quantitative accumulation in a wider range of model scales to optimise and calibrate the simulation for different use of substitute materials.

7. Discussion

In reviewing the literature, accurate replication of the characteristic snowdrift mechanism remains a difficult task and model-specific disadvantages and limitations can only be overcome through phenomenological "tunning". The main question in this study sought to determine *how snow and wind impact the arctic built environment and how to investigate critical situations e.g. in wind tunnel testing.* In order to thoroughly investigate snowdrift modelling, unique observation data are necessary to gain considerable insights of current snow drift and accumulation in the low-Arctic region. An initial objective of the Nuuk Cube Field Experiment was to expand the current knowledge of snow drifting and accumulation in Arctic settlements to enable reliable consideration of climatic impacts in urban planning for environmentally friendly Arctic development.

With respect to the first research question [R 1] *which snow accumulation and drift phenomenon are relevant*, this study found that snow accumulations are flow-field-oriented for the specific site at the Nuuk area. The most obvious observation to emerge from the *snow accumulation observations* (NCFE Part 2) is that the cube was at no time during the observation period covered with snow or even significantly immersed even though the surrounding snow surface came up to 30% of the cube's height. Simultaneously, the limited or small amount of snow on the flat roof can be observed on flat roofs of low-rise residential buildings in the wider Nuuk area and therefore seem to be less of concern with the current roof design. Exceptions to this are stepped roofs or complex architectural elements that create a lee zone and can therefore be problematic for snow loads.

One other explanation for this result is that the black-painted surface of the cube led to higher surface temperatures on the roof due to solar radiation. This might differ from building roofs depending of the constructed material. To this end, no further attempt was made to measure or systematically investigate the effect and needs to be considered speculative. But a clear distinction between dry and wet snow events showed that wet snow events seem to occur at significant higher wind speeds (see also Figure 11, NCFE Part 1). In case of dry snow events, the mean event wind speed does not exceed the mean threshold by more than 4% (NCFE Part 1). Hence, it can be concluded that dry snow event occur practically without ground particle transport. The accumulation of snow is in this case dominated by the flow field around the cube or buildings in general (streamline deposition). For the simulation of wet snow accumulation, the streamline deposition is to a certain degree altered by ground transport, i.e. erosion, with 20-30% of gusts exceeding the transport mean threshold value.

Given the noted phenomenon of snow accumulation and drifting in the current low Arctic region of Nuuk, another question must be asked. [R 1] *Which critical situation can be reflected in wind tunnel testing at a reduced model scale?* Prior tests have clearly shown that the choice of material shall rather be based on the correct accumulation shape than on a one-material-fits-all-purpose approach. Models are a simplification of the natural phenomenon and the results of the specification tests as well as the Nuuk Cube model experiments (NCFE, Part 3) have shown that a calibration based on observations is sufficient. Comparison of the results with those of other studies confirms that it is still difficult to meet the explicit similarity requirements and that ensuring adequate similarity to nature is based on both physical scaling laws and phenomenological calibration. The initial investigations of the classification of different materials showed that only a few particle properties fulfilled the similarity laws. Therefore, it is important, and even crucial, to apply both phenomenological and adapted scaling laws equally.

The size of the model cubes is associated with model-specific disadvantages and limitations. As the model sizes become smaller, but the particle diameters remain the same, details become less accurate. It was found that Model sizes L_m < 5 cm are not recommended to simulate the particle accumulation and the distribution on the model roof. Most particle did not accumulate (due to e.g. saltation length). The snow accumulation shape depends to a large extent on the flow regime around sharp-edged bodies. Important for the snowdrift performance in the wind tunnel simulation is that the model design reflects the surface roughness (material roughness and terrain) close to nature. The established accurate testing method allows reflecting characteristic snow accumulation features around buildings. The parameter of air humidity could be of additional interest since it may influence adhesion behavior (Anno, 1985b). Anno (1985) for example added water to the clay before the initiation into the wind tunnel and air humidity was particularly varied.

It seems paradox to pick one substitute to reflect a wide range of possible snow particle characteristic for different model scale. It is recommended to classify a range of spespecifications aboute differnt substitute materials and their performance in air-bone as a benchmark for modelling approaches in Computational Fluid Dynamics. Due to the unchanged physical properties, it is assumed that they can be better controlled in CFD. However, as with wind tunnel simulations, it is inevitable to validate with observations from nature.

The outcome of the specification for the different material shall provide the necessary information for this decision and shall lay the ground for future development of substitute materials with a wider similarity range.

The second research question on [R 2] *how snow events are defined based on weather observations and their occurrence characteristic*, this study found that short events with 20 to 20 minutes occurs for both, dry and wet snow events, with a slight dominance for the dry snow events. And longer events from 1 to 4 hours are found more pronounced for wet snow events with higher occurrence frequencies between 1 and 1.5. The signals were subsequently grouped to events depending on a maximum allowed interval duration T_{int} for 10 min interval and 30 min interval yielding in rare occasions to snow event durations of almost 10 hours (596 minutes). Increasing T_{int} further would add longer durations but obscure distribution characteristics of shorter events. Typical durations as found in literature with 12 and 18 hours as found by Isyumov and Mikitiuk (1977) are not reflected in the NCFE data and could indicate a main frame for relevant durations as a sub-structure (local microclimate) of a larger meso-scale structure.

The study also found *what the correlation of wind direction and speed during a snow event is.* The most important result was that the variability of wind direction during snow events was negligible and wind speeds are below threshold speeds for snowdrifts from literature (. Typically, dry snowfall events are characterised by low wind speeds, and wet snow is coming with stronger wind speeds.

The wind sensor was located in close proximity and approximately at the same height as the top side (roof) of the cube. This position was specifically chosen to record the wind velocity directly relating to the wind field around the cube. In most field studies (Table 1), the measurement height for wind is 10m above terrain and all observations relate to this reference speed such as the threshold for ground transportation of snow. Wind velocities at other heights can be calculated with the logarithmic equation of the mean wind speed profile defined by shear velocity u* as indication for terrain roughness. In case of the NCE, the ground-near location of the anemometer allows a more direct measurement of the wind speed driving the transport and accumulation process. Due to the uneven terrain surface at the cube location an extrapolation from a 10m reference position would require a more accurately calibrated mean wind speed profile. The snow cover during winter season will affect the wind speed at anemometer height and the wind field around the cube at the same time. Hence, with the low anemometer height the influence on the driving force of snow transportation will be more accurately recorded compared to a reference wind speed at 10m above terrain surface. Conversion factors of the

mean wind speed to 10m range between 1.2 (snow cover) and 1.3 (no or little snow cover) as derived in Fiebig and Koss (2023).

The graph in the NCFE Part 1 at the bottom left of Figure 16 in Fiebig and Koss (2023) indicates two levels of turbulence. This approach seems plausible when assumed different levels of roughness with and without snow cover. However, closer examination of the occurrence of the corresponding data points as a function of time or wind direction does not reveal any systematics and the plausible idea cannot be substantiated, at least on the basis of the data. This experiment did not detect any evidence for the non-existence of such a connection, thus inconclusive. It should therefore be avoided to infer transmission errors, e.g. from Norway to Greenland.

Valuable insights of *what snowdrift pattern are created during and after a snow event around the Nuuk Cube to define snow simulation conditions for Wind Tunnel Testing (wind speed, direction, intensity and duration)* were found and descriptions and specific data and further discussions can be found in the included papers.

8. Conclusions

The aspect for all simulated investigations of snow drift formation, whether experimental or numerical, is to achieve a sufficient similarity to the observation of the phenomenon in the regional area. The information obtained from the "Nuuk Cube Field Experiment" and observations of snow accumulation around different buildings within moderately dense developed settlements in Greenland like Nuuk allow to specify the particular snow drift and accumulation phenomenology for this region. The difference to expected snow accumulation as observed for example in the Alpes reinforces the notion of a regional distinguishable snow drift and accumulation characteristic. For the area of interest in this study, the low-Arctic region of southwest Greenland, the built-up of a snow layer on building roofs is in general significantly smaller than for example in Central Europe. There are however exceptions where the roof geometry creates recirculating airflows enhancing the snow deposition process.

A reason for such regionalism in snow accumulation processes are differences in the weather parameters defining the boundary condition of snow events. According to the Köppen climate classification, the Alpine region is for example situated in the humid continental climate zone. Moisture in this climate regime is characterized by heavy snowfall in wintertime and snow cover is often deep. Houses are covered with snow and struggle with snow load exceedance. Here, the airborne snow precipitation is more dominated by gravity than by the wind or more specifically of the flow field around the roof or the building as such. The accumulation characteristic observed in Greenland is by comparison more wind flow-field-oriented for both airborne snow flakes and surface-near snow particles. These differences need to be considered in the investigation, i.e. in the simulation or modelling approach.

The following conclusions were drawn:

1. Considerable insight has been gained with regard to the current understanding of snow drift and accumulation for the low-Arctic region. The variability of wind direction during snow events was negligible and wind speeds below threshold speeds for snowdrifts. Typically, dry snowfall events are characterised by low wind speeds, and wet snow is coming with stronger wind speeds. This insight leads us to recommendations for a simplified modelling procedure consisting of a two-step

approach scenario with a low-speed induced seeding mechanism followed by an erosion test.

2. Similarity of the accumulation around the Nuuk Cube could be established in the wind tunnel experiment using substitutional material for the snow. Here, a specific combination of airflow deposition and subsequent erosion showed the best results. It should be made clear that apart from explicit scaling laws, the result of the accumulation pattern is in all cases - also those reported in the literature - "tuned" to full-scale observation through the testing procedure. This constitutes a hybrid approach (?) to achieve similarity, which is partially based on explicit scaling laws and phenomenological tuning. This applies in principle to all simulations using substitutional material (experiment) or an idealised thermodynamical snow model (numeric). These approaches have an intrinsic deficiency to nature, which can only be overcome by phenomenological tuning. And ultimate validation derives from the similarity of snow drift formation (phenomenological similarity) in model and full-scale. However, accurate replication of the characteristic snow drift remains a challenging task, and one can solve this through the procedure of snowfall and erosion.

The developed experimental simulation approach needs further investigation to optimise and calibrate the simulation for different use of substitute materials. All tests should be repeated with emphasis to the quantitative accumulation in a wider range of model scales. In the initial test of different building layouts no further attempt was made in different scale testing with the generated ABL profile used in all tests.

Experimental testing with substitute materials in a circuit boundary-layer wind tunnel required constant cleaning of the facility and the filter used to collect fine particles, avoiding explosion risk when recirculated into the wind tunnel. The use of a different type of wind tunnel facility with no circulation should be considered when testing with fine grain particles. Further more, it is uncertain at this point how the built in filter, after the test section, changes the properties along the test section also during snowfall procedure while testing and what effect it has on the resulting snow accumulation deposit. Due to the fine grained particles sensitive measuring tool would be harmed. Uncertainties remain also in the chosen method to measure the snow accumulation in full-scale.

Some measurements at site would be helpful to compare errors of the measured accumulation height to the generated 3D mesh.

This thesis is a complete framework for understanding snow drift problems in built environments with a clear focus on observing, understanding and simulating snowdrift in model and full scale. Due to the interdisciplinary work of climatology, wind engineering and fluid dynamics are following limits addressed:

1. The focus of the work is certainly on snow and wind in arctic built environments and the initial tests of urban building pattern does not consider other climatic aspects than snow accumulation around buildings. This is mentioned as a limitation in the analysis of solely snowdrift related design challenges. Further studies regarding the influence on other climatic aspects such as pedestrian comfort should be considered.

2. The wind tunnel facility limits the exploration of various scale testing due to its dimensions of a relative small test section of 1,5 m and cross-flow dimension of 0.48 x 0.48m. This makes it difficult to test large model objects when also including topography.

Thank you/Qujanaq/Tak/Danke

9. References

Abermann, J., Eckerstorfer, M., Malnes, E., & Hansen, B. U. (2019). A large wet snow avalanche cycle in West Greenland quantified using remote sensing and in situ observations. *Natural Hazards*, *97*(2), 517–534. https://doi.org/10.1007/s11069-019-03655-8

Aksamit, N. O., & Pomeroy, J. W. (2016). Near-surface snow particle dynamics from particle tracking velocimetry and turbulence measurements during alpine blowing snow storms. *The Cryosphere*, *10*, 3043–3062. https://doi.org/10.5194/tc-10-3043-2016

Anno, Y. (1984). REQUIREMENTS FOR MODELING OF A SNOWDRIFT. *Cold Regions Science and Technology*, *8*, 241–252.

Anno, Y. (1985a). Froude number paradoxes in the modeling of a snowdrift. *Cold Regions Science and Technology*, *10*(2), 191–192. https://doi.org/10.1016/0165-232X(85)90030-8

Anno, Y. (1985b). Modelling a snowdrift by means of activated clay particles. *Annals Of Glaciology*, *6*, 48–52.

Anno, Y., & Tomabechi, T. (1985). DEVELOPMENT OF A SNOWDRIFT WIND TUNNEL. *Cold Regions Science and Technology*, *10*, 153–161.

Beyers, J. H. M., & Harms, T. M. (2003). Outdoors modelling of snowdrift at SANAE IV Research Station, Antarctica. *Journal of Wind Engineering and Industrial Aerodynamics*, *91*(4), 551–569. https://doi.org/10.1016/S0167-6105(02)00409-9

Børve, A. B. (1987). *Hus og husgrupper i klimautsatte, kalde strøk. Utforming og virkemåte.* Oslo School of Architecture.

Børve, A. B. (1988). Settlement and housing design with special regard to local climatic conditions in cold and polar regions - examples from Northern Norway. *Energy and Buildings*, *11*(1–3), 33–39. https://doi.org/10.1016/0378-7788(88)90021-7

Brown, B. G., Katz, R. W., & Murphy, A. H. (1985). Exploratory Analysis of Precipitation Events with Implications for Stochastic Modeling. *Journal of Climate and Applied Meteorology*, *24*(1), 57–67.

Cappelen John(ed). (2013). *Technical Report 13-04 Greenland - DMI Historical Climate Data Collection -with Danish Abstracts*. http://www.dmi.dk/fileadmin/Rapporter/TR/tr14-04

Cochran, L., & Derickson, R. (2005). Low-rise buildings and architectural aerodynamics. *Architectural Science Review*, *48*(3), 265–276. https://doi.org/10.3763/asre.2005.4833

Delpech, P., Palier, P., & Gandemer, J. (1998). Snowdrifting simulation around Antarctic buildings. *Journal of Wind Engineering and Industrial Aerodynamics*, *74–76*, 567–576. https://doi.org/10.1016/S0167-6105(98)00051-8

Fiebig, J. (2023). *Snow and Wind - A Simulation Approach in Arctic Built Environments* (Issue June). Technical University of Denmark.

Fiebig, J., & Koss, H. H. H. (2023a). Nuuk Cube Field Experiment – Part 1 : Meteorological Observations. *Manuscript in Preparation*.

Fiebig, J., & Koss, H. H. H. (2023b). Nuuk Cube Field Experiment – Part 2 : Snow Accumulation Observations. *Manuscript in Preparation*.

Flaga, A., & Flaga, Ł. (2016). Wind tunnel tests and analysis of snow load distribution on three different large size stadium roofs. *8th International Conference on Snow Engineering Wind*, 232–239.

Föhn, P. M. B. (1980). Snow transport over mountain crests. *Journal of Glaciology*, *26*(94), 469–480.

Haehnel, R. B., Wilkinson, J. H., & Lever, J. H. (1993). Snowdrift Modeling in the CRREL Wind Tunnel. *61st Western Snow Conference*, 139–147.

Heinemann, G., Claud, C., & Spengler, T. (2019). Polar low workshop. *Bulletin of the American Meteorological Society*, *100*(2), ES89–ES92. https://doi.org/10.1175/BAMS-D-18-0103.1

IFA Institute for Occupational Safety and Health of the German Social Accident Insurance. (2016). *GESTIS - DUST-EX*. Database. https://staubex.ifa.dguv.de/

Irwin, P. A. (2016). Prediction of snow loads: past, present and future. *8th International Conference on Snow Engineering*, 200–207. http://www.snoweng2016.org/preliminary-proceeding

Isyumov, N., & Mikitiuk, M. (1977). Climatology of Snowfall and Related Meteorological Variables With Application To Roof Snow Load Specifications. *Canadian Journal of Civil Engineering*, *4*(2), 240–256. https://doi.org/10.1139/l77-028

Jaedicke, C. (2001). *Drifting snow and snow accumulation in complex arctic terrain - Field experiments and numerical modelling*. University of Bergen.

Jung, T., & Rhines, P. B. (2007). Greenland's pressure drag and the Atlantic storm track. *Journal of the Atmospheric Sciences*, *64*(11), 4004–4030. https://doi.org/10.1175/2007JAS2216.1

K.C.S. Kwok, D. J. Smedley, D. H. K. (1993). Snowdrift Around Antarctic Buildings - Effects of Corner Geometry and Wind Incidence. *International Journal of Offshore and Polar Engineering*, *3*(I), 61–65.

Kim, D. H., Kwok, K. C. S., & Rohde, H. F. (1990). Wind loads on and snowdrift around Antarctic buildings. *Proceedings of the First Pacific/Asia Offshore Mechanics Symposium*, *1962*, 45–50.

Kim, D. H., Kwok, K. C. S., & Rohde, H. F. (1991). *Similitude Requirements of Snowdrift Modelling for Antarctic Environment*.

Kind, R. J. (1986). Snowdrifting: A review of modelling methods. *Cold Regions Science and Technology*, *12*(Cold regions science and technology, 12), 217–228. https://doi.org/10.1016/0165-232X(86)90036-4

Kong, L., & Parkinson, G. V. (1997). A 3-D tolerant wind tunnel for general wind engineering tests. *Journal of Wind Engineering and Industrial Aerodynamics*, *69–71*(71), 975–985. https://doi.org/10.1016/S0167-6105(97)00221-3

Kuipers Munneke, P. (2009). *Snow, ice and solar radiation*. 142.

KUROIWA, D., MIZUNO, Y., & TAKEUCHI, M. (1967). Micromeritical Properties of Snow. *Physics of Snow and Ice : Proceedings = 雪氷の物理学: 論文集*, *1*(2), 751–772.

Leppänen, L., Kontu, A., Hannula, H., Sjöblom, H., & Pulliainen, J. (2016). *Sodankylä manual snow survey program*. 163–179. https://doi.org/10.5194/gi-5-163-2016

Leppänen, L., Kontu, A., Vehviläinen, J., Lemmetyinen, J., & Pulliainen, J. (2015). *Comparison of*

traditional and optical grain-size field measurements with SNOWPACK simulations in a taiga snowpack. *61*(225), 151–162. https://doi.org/10.3189/2015JoG14J026

Li, L., & Pomeroy, J. W. (1997). Estimates of Threshold Wind Speeds for Snow Transport Using Meteorological Data. *Journal of Applied Meteorology*, *36*(3), 205–213. https://doi.org/10.1175/1520-0450(1997)036<0205:EOTWSF>2.0.CO;2

Liu, M., Zhang, Q., Fan, F., & Shen, S. (2018). Experiments on natural snow distribution around simplified building models based on open air snow-wind combined experimental facility. *Journal of Wind Engineering and Industrial Aerodynamics*, *173*(December 2017), 1–13. https://doi.org/10.1016/j.jweia.2017.12.010

Mahoney, J. L. (1991). *Climatology of snowfall-event characteristics at Denver*. 57–66. https://doi.org/ISSN: 01610589

McCrystall, M.R., Stroeve, J., Serreze, M. et al. (2021). New climate models reveal faster and larger increases in Arctic precipitation than previously projected. *Nat Commun*, *12*, *6765*(2021), 1–12. https://doi.org/10.1038/s41467-021-27031-y

Mellor, M. (1965). Blowing Snow. In *Cold Regions Science and Engineering, Part III, Section A3c* (Issue November).

Michel, C., Terpstra, A., & Spengler, T. (2018). Polar mesoscale cyclone climatology for the Nordic seas based on ERA-interim. *Journal of Climate*, *31*(6), 2511–2532. https://doi.org/10.1175/JCLI-D-16-0890.1

Mitsuhashi, H. (1982). Measurements of snowdrifts and wind profiles around the huts of Showa Station in Antarctica. In *Antarctic Record* (Vol. 75, pp. 37–56).

Møller, E. B., & Lading, T. (2020). Current building strategies in Greenland. *E3S Web of Conferences*, *172*, 1–8. https://doi.org/10.1051/e3sconf/202017219004

N.Isyumov, & M.Mikitiuk. (1990). Wind Tunnel Tests of Snow Drifting on a Two-Level Flat Roof. *Journal of Wind Engineering and Industrial Aerodynamics*, *36*, 893–904.

Naaim-Bouvet, F. (1995). Comparison of Requirements for Modeling Snowdrift. *Surveys in Geophysics*, *16*, 711–727.

Nielsen, A. B. (2010). *Present conditions in Greenland and the Kangerlussuaq area. Working Report 2010-07*. 70. http://www.posiva.fi/files/1244/WR_2010-07web.pdf

Pall, P., Tallaksen, L. M., & Stordal, F. (2019). A climatology of rain-on-snow events for Norway. *Journal of Climate*, *32*(20), 6995–7016. https://doi.org/10.1175/JCLI-D-18-0529.1

Pomeroy, J. W., & Male, D. H. (1987). Wind Transport of Seasonal Snowcovers. In H.G. Jones W.J. Orville Thomas (Ed.), *Seasonal Snowcovers: Physics, Chemistry, Hydrology* (pp. 119–140). Springer Netherlands. https://doi.org/10.1007/978-94-009-3947-9_7

Pomeroy, J. W. W., & Brun, E. (1990). Physical Properties of Snow. *Snow Ecology: An Interdisciplinary Examination of Snow-Covered Ecosystems*, *97*, 45–126.

Robinson, P. J., & Walsh, S. J. (1895). Precipitation Regime Changes associated with Climatic Changes. In *Oxford University: Vol. XXX*.

Schmidt, N. M., Reneerkens, J., Christensen, J. H., Olesen, M., & Roslin, T. (2019). An ecosystem-wide reproductive failure with more snow in the Arctic. *PLoS Biology*, *17*(10), 1–8. https://doi.org/10.1371/journal.pbio.3000392

Schmidt, R. A. (1982). Properties of blowing snow. *Reviews of Geophysics and Space Physics*, *20*(1), 39–44. https://doi.org/10.1029/RG020i001p00039

Spengler, T. (2020). *Arctic weather phenomena and extremes*. Association of Polar Early Career Scientists (APECS). ww.vimeo.com/390980914

Sturm, M., & et. al. (1995). A Seasonal Snow Cover Classification System for Local to Global Applications. *Journal of Climate*, *8*(5). https://doi.org/10.1175/1520-0442(1995)008%3C1261:ASSCCS%3E2.0.CO;2

Tabler, R. D., Pomeroy, J. W., Santana, B. W., & ASCE, M. (1990). Drifting snow. *Cold Regions Hydrology and Hydraulics*, *0*.

Thiis, T. K., Barfoed, P., Delpech, P., Gustavsen, A., Hofseth, V., Uvsløkk, S., & Dufresne de Virel, M. (2007). Penetration of snow into roof constructions-Wind tunnel testing of different eave cover designs. *Journal of Wind Engineering and Industrial Aerodynamics*, *95*(9–11). https://doi.org/10.1016/j.jweia.2007.02.017

Thordarson, S. (2002). *Wind Flow Studies for Drifting Snow on Roads*. Norwegian University of Science and Technology NTNU.

10. Appendix

A Nuuk Cube Field Experiment – Part 1: Meteorological Observations

Nuuk Cube Field Experiment – Part 1: Meteorological Observations

Jennifer Fiebig, H. Holger H. Koss
Technical University of Denmark; Department of Civil Engineering, Section of Structures and Safety
jenfi@byg.dtu.dk; hko@byg.dtu.dk

Abstract: Built-in areas as well as individual building in arctic regions are exposed to extreme environmental conditions. Snow accumulation on and around buildings reduce the functionality of buildings and affect structural durability. For proper investigations of snow accumulation the applied simulation methods need to be validated. Even though similarity laws have been suggested in the past, only little concrete data on the weather conditions surrounding a snow event and resulting accumulation patterns are available from field measurements. For this reason a field study, the Nuuk Cube Experiment (NCE) was initiated to measure ground-near weather conditions during winter period in parallel to observation and documentation of snow accumulation on a nearby 1.2m cube. This paper focuses on the analysis of the weather data, recorded over four winter periods between 2017 and 2020. The analysis focuses in particular on simulation-relevant information such as the characteristic duration of snow events, the variability of wind direction during the events, distribution of wind direction for different types of snow, and the correlation of wind speed to precipitation type and ground transportation. Based on the outcome, recommendations for simulation-based studies of snow accumulation are formulated.

Keywords: Field study; Nuuk; Greenland; Precipitation; Snow Events; Ground-near wind characteristic; Simulation recommendations

1 Introduction

1.1Background

For the simulation of ground-near snow drift and accumulation on and between buildings, a variety of methods are available. In wind tunnel testing, usually substitutional materials are used reflecting to a certain degree the behaviour of snow in nature (Brooks et al., 2016; Flaga and Flaga, 2016). In some climatic wind tunnels water spray is used to generate snow artificially. Even though true-to-nature in its physical making, artificial snow covers only a certain range of snow types as they appear in nature. Numerical simulations allow replicating a wider range of boundary conditions and behaviour properties of the airborne snowflakes and particles in ground contact but need, as well as experimental simulations do, validation data to calibrate and verify the testing method. To obtain information about snow events, prevailing climatic boundary conditions and their influence on the processes of ground-near transport and accumulation a 1.2m cube was installed near the premises of the private home of a collaboration partner in Nuuk, Greenland, for surveillance of snowdrift and

accumulation and continuous climate measurement during four winter seasons. This monitoring campaign is in the following referred to as the “Nuuk Cube Experiment – NCE”. Nuuk was chosen for being an arctic city with considerable snow precipitation (Cappelen et al., 2001), making it hence as an ideal spot for field studies of snow accumulation on and around buildings. This paper focuses on the analysis of the weather observations to understand the characteristic of snow events and to determine the variability of weather conditions before, during and after an event.

1.2 Location of Cube and Weather Station

Fig. 1 to Fig. *3* illustrate the location of the cube in the northern part of the developed area of Nuuk. The choice of the location is a compromise between a relatively open area with wind flow and snow drift and accumulation sufficiently undisturbed by nearby buildings and terrain objects, the possibility of data receiver installation with a stable internet connection for remote data download, the possibility of manual snow accumulation observation and photometric documentation and financial restrains, which could otherwise allow for a more remote and automated setup.

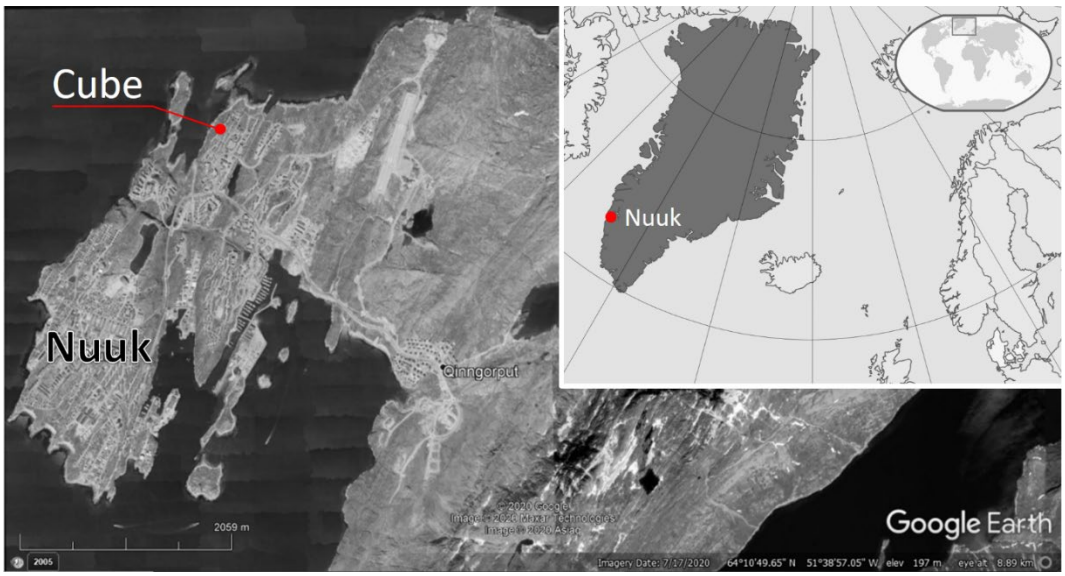

Fig. 1. Location of the cube in the northern part of Nuuk, Greenland, about 1500m west of Nuuk Airport and 350m south of the nearest shoreline (Google Earth, accessed on October 9, 2020).

Fig. 2. The cube has been installed on an open stretch 13m west of the nearest building (observation base, housing of data acquisition computer). The surface topography is moderately uneven but still flat enough to allow representative snowdrift and accumulation. The footprint of the cube is rotated 45° to north south direction to face the most frequent direction for snow events based on experience (Google Earth, accessed on October 9, 2020). Geographic reference of cube position 64°11'37.3"N 51°42'121.2"W (64.1936, -51.7030), elevation 36.7m above sea level (position and elevation provided by land registry office for Nuuk).

Fig. 3. Cube and nearby weather station with wireless data transfer to receiver and logging computer. The distance between cube and station is 3m.

The distance between the cube and the nearest building is 13m. The actual placement was based on experience of local residents regarding a patch of seemingly undisturbed and even snow cover during past winter seasons. This assumption was confirmed in retrospect by the observations during

the field experiment. More relevant for the snow transport is the terrain morphology as such and presence of singular objects, described and discussed in detail in Fiebig and Koss (2021).

1.3 Weather Station and Data Acquisition

To relate observed show accumulation patterns to past weather history, a Vantage Pro2 Plus weather station by Davis Instruments was installed on a tripod with storm guys in 3m distance from the cube (Figure 3). The outdoor sensor unit (Integrated Sensor Suite – ISS) was equipped with a heating element to keep the rain gauge and collector operable at temperatures below freezing point. Eight weather parameters are measured directly at the station and transmitted wireless 13m to the receiver and acquisition computer in the nearest building. The measurement specification of the recorded parameters are given in Table 1.

The measured data are updated every 2.5 seconds and transmitted to the receiver. However, the shortest data storage interval provided by the inbuilt acquisition software is one minute corresponding to a sampling frequency of 0.0167Hz. This is low with respect to turbulence measurements but fast enough to get weather records for sufficient statistical description prevailing weather conditions and correlation to snowdrift and accumulation around building structures.

The wind sensor is installed at 1.4m above the terrain surface. During winter season, snow covers the ground around the weather station with varying thickness. For the analysis, an average snow cover of 20 to 30cm is assumed, which mainly affects calculations of 10m wind values to sensor height. At no instant during the study, the snow reached up to the anemometer or the main unit of the ISS below the anemometer (Fig. 3). The ground-near location of the anemometer allows a more direct measurement of the wind speed driving the transport and accumulation process. Due to the uneven terrain surface at the cube location an extrapolation from a 10m reference position would require a more accurately calibrated mean wind speed profile. The snow cover during winter season will affect the wind speed at anemometer height and the wind field around the cube at the same time. Hence, the influence on the driving force of snow transportation will be more accurately recorded compared to a reference wind speed at 10m above the uneven terrain surface.

Table 1. Measured weather parameters and manufacturer specifications for Vantage Pro2 Plus by Davis Instruments (Davis, 2017).

Parameter	Unit	Sensor	Specification
Wind speed	[m/s]	3-cup anemometer	Resolution 0.4m/s. Sensor installed at 1.40m above terrain surface.
Wind direction	[°]	Separated vane	16 directional (22.5°) sectors
Air temperature	[°C]	Radiation shielded sensor	Range -40° to +65°C with 0.1°C resolution and ±0.3°C sensor accuracy
Air humidity	[%]	Radiation shielded sensor	Range 1 to 100% with a resolution of 1% and 2% sensor accuracy.
Precipitation	[mm]	Tipping spoon (heated at temperatures below freezing point)	Increments of 0.2mm. Accuracy for rain rates up to 250mm/hr is about ±3% of total or ± one tip (whichever is greater).
Barometric pressure	[hPa]	Integrated sensor	Range between 540 to 110hPa with a resolution of 0.1hPa
Sun radiation	[W/m^2]	Individual sensor	Range 0 to 1800W/m2 with a sensor accuracy of ±5% of full range
UV index	[W/m^2]	Individual sensor	Readings are equal to EAS-weighted irradiance [W/m2] where an index of 10 equals 0.25W/m^2. Index ranges between 1 and 15.

2 Data Screening and Snow Event Identification

2.1 Data Sets

Climatic data were recorded during 27 months in total and are organised in four periods, where the measurements were conducted continuously (Table 2). Not all monthly records are complete due to unsuccessful data transfer between the ISS and the receiver (Fig. 4). However, all received data are used, since the study is predominantly based on a conditional analysis, i.e. focused on weather situations at and surrounding a registered precipitation.

Table 2. Months of weather measurements in the NCE, organised into four continuous observation periods.

Period	Years/Months
1	2017 (MAR ; APR)
2	2017 (DEC) / 2018 (JAN ; FEB ; MAR ; APR)
3	2018 (OCT ; NOV ; DEC) / 2019 (JAN ; FEB ; MAR ; APR ; MAY)
4	2019 (JUL ; AUG ; SEP ; OCT ; NOV ; DEC) / 2020 (JAN ; FEB ; MAR ; APR ; MAY ; JUN)

Apart from gaps in data transfer, measurements might be affected by temperature and elevation of the ISS over terrain surface. Following considerations have been made in this respect for the analysis:

Temperature: Since installed about 260km south of the Arctic Circle ($Lat_{AC} \approx 66°33' N$), extreme low temperatures can be expected during winter season potentially rendering the rain gauge of the ISS inoperable. The installed heating element will largely prevent freezing of the gauge and tipping spoon, but some malfunction can be expected. In Fig. 4, the monthly collected precipitation from the ISS is compared to Data from weather archive of the Danish Meteorological Institute (DMI, 2021). Apart from September 2019 (rel. diff. 1.6%), all months show a noticeable difference with the ISS-data always falling short of the DMI records, in some cases significantly (rel. diff. > 90%) like for January 2020, where the data transfer success is 100%. There is a certain tendency that the relative difference increases with falling monthly average temperature, but 33.6% of all precepitation registrations with the ISS have been made at air temperatures below 0°C, 8.7% at temperatures below -5°C and 1.3% at below -10°C (Fig. 5). This does at least proof that low air temperatures do not prevent preceipitation measurements in general.

Elevation: The rain collector (Fig. 3, right) is about 1m above terrain surface where the streamlines of the ground-near wind can be assumed being nearly horizontal. This might lead to a signifficant undercatch even for lower wind speeds since the rain drop/snow flake trajectories resemble a pattern at the collector more typical for strong wind events. In this respect, the ISS is more exposed compared to standard requirements for rainfall measurements (Snow and Harley, 1988). However, Fig. 6 illustrates a dense rain registration rate for December 2018 at high ground-

near wind speeds in excess of 10m/s. This, again, suggests the conclusion that low air temperature is most likely the main reason for deficits in precipitation measurements, or more precisely, the reason for missing out on snowfall events.

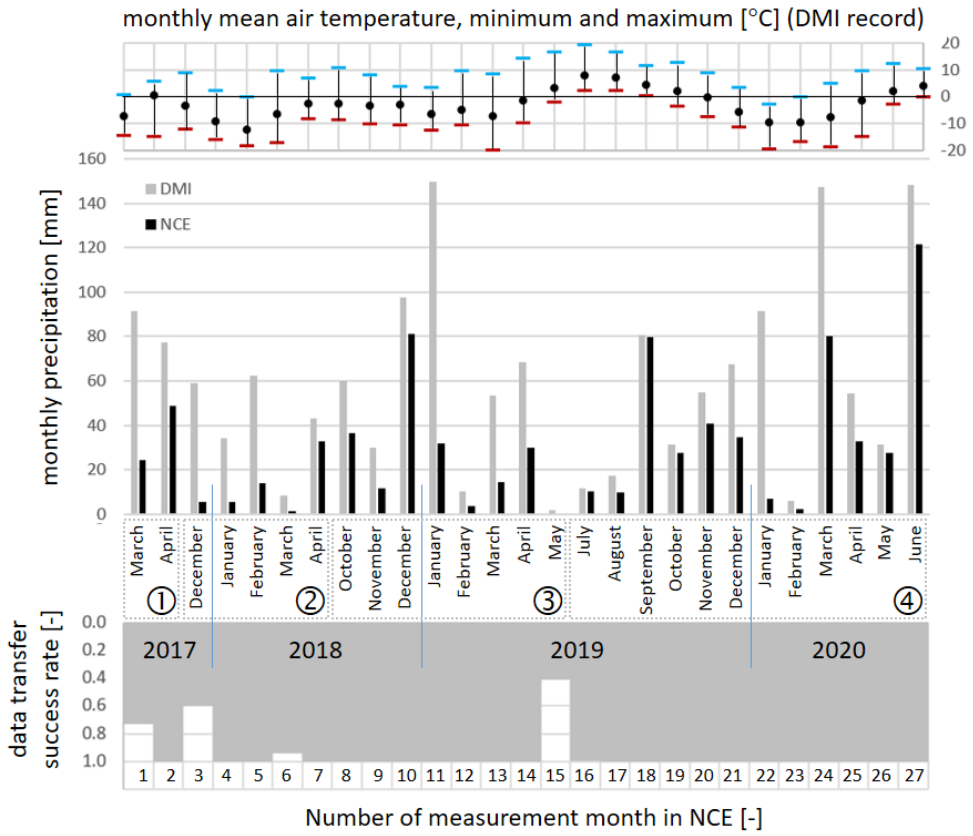

Fig. 4. Comparison of registered precipitation with the weather station at the cube (Nuuk Cube Experiment – NCE) to the official data from the Danish Meteorological Institute (DMI). Additional information on the monthly data set completeness (transfer success) and on the prevailing monthly air temperature.

The missing registration of precipitation, especially snowfall events, does not allow to work with intermittency between registrations as an indicator for snow event durations. However, assuming that a rain gauge release always occurs with precipitation (no 'ghost' events), those events can be used to study the climatic condition surrounding them. All-in-all 4082 basic precepitation events (= rain gauge releases) have been been registered and are shown in Fig. 5 as histogram distribution over prevailing airtemperature upon gauge release. Fig. 6 shows an example of the time records for the main weather parameters during December 2018.

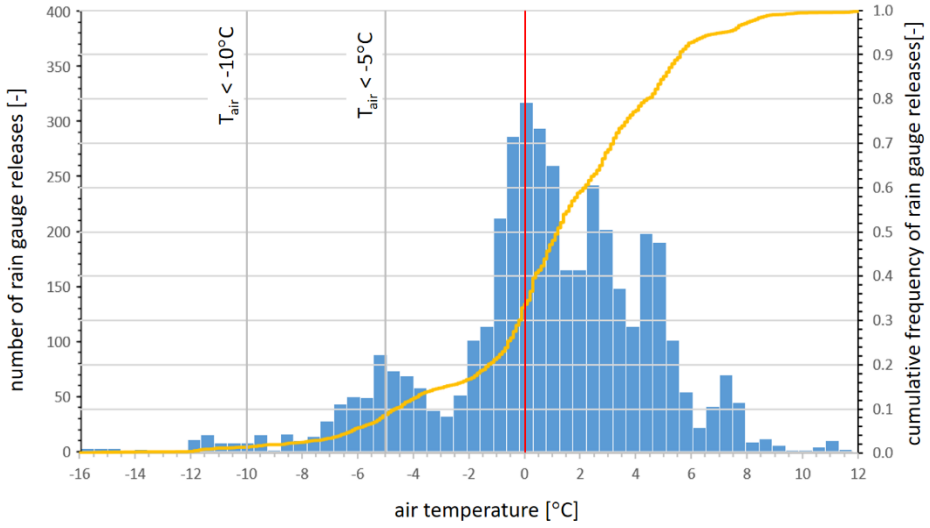

Fig. 5. Distribution of rain gauge releases over instantaneous air temperature upon release.

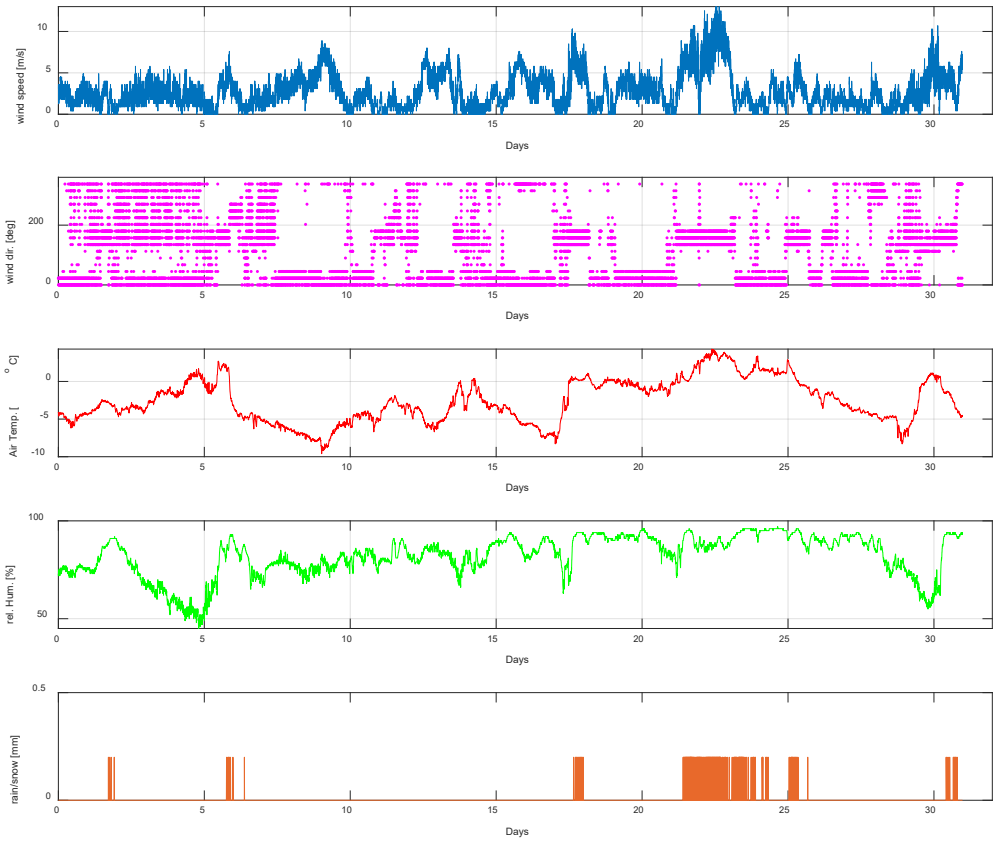

Fig. 6. Time history of main weather parameters measured in December 2018, with a relatively high monthly precipitation (405 gauge releases), a data transfer success rate of 100% and low relative difference to DMI records of 17%.

2.2 Snow or Rain?

According to Fig. 5, about 33% of the precipitation registrations happened at air temperatures below freezing point. The likelyhood for precipitation occurs as snow is primarily a function of air temperature and secondarily depending on atmospheric pressure. Fig. 7 combines two approaches from literature indicating the precipitation type as a function of temperature and barometric pressure. Where Schemenauer et al. (1981) indicate based on previous work from Fulkes (1935) a transition range between -6 and 0°C, within which both forms, rain and snow, may appear, Dai (2008) gives a more detailed distribution of likelyhood for precipitation to appear as snow. The data range from the Nuuk Cube Exepriment (NCE) is indicated on both graphs as well as their overlap.

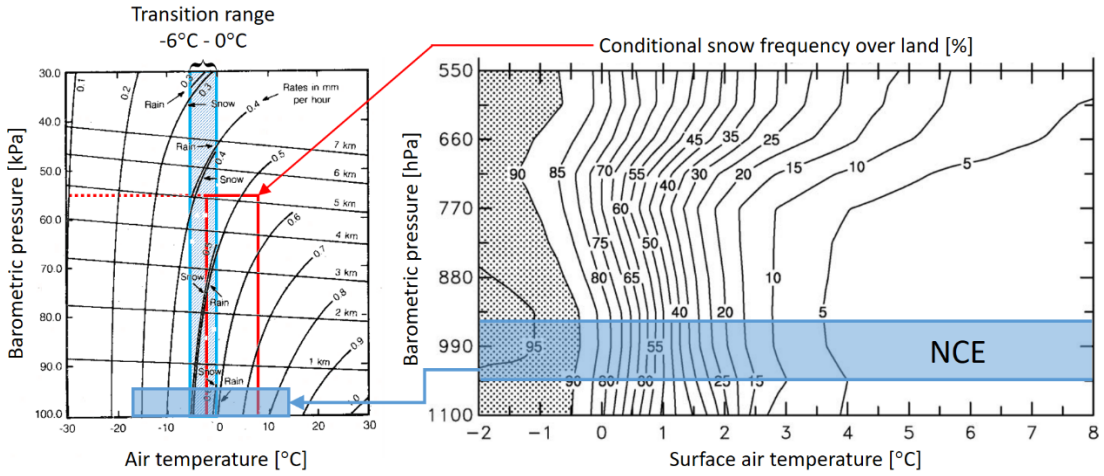

Fig. 7. Transition between precipitation occurring as rain or snow as function of air temperature and barometric pressure. *Left:* indication of precipitation form after Schemenauer et al. (1981) referring to Fulkes (1935) with an overlapping transition range between -6 and 0°C. *Right:* curves of conditional probability for precipitation occurring as snow after Dai (2008).

The NCE-data range indicates according to Dai (2008) that the probability for the occurrence of precipitation as snow is largely independent of barometric pressure. A representative probability distribution curve extracted from this graph is compared to the scatter chart of the NCE data to the left in Fig. 8. To the right, this distribution is compared to data from Dai (2008) for confirmation of consistency with other sources. The primary data selection to identify a snow event is based on a

probability level of 98%, corresponding to a temperature threshold of -2°C. This leads to a sample space 684 registrations or 16.8% of all NCE precipitation registrations.

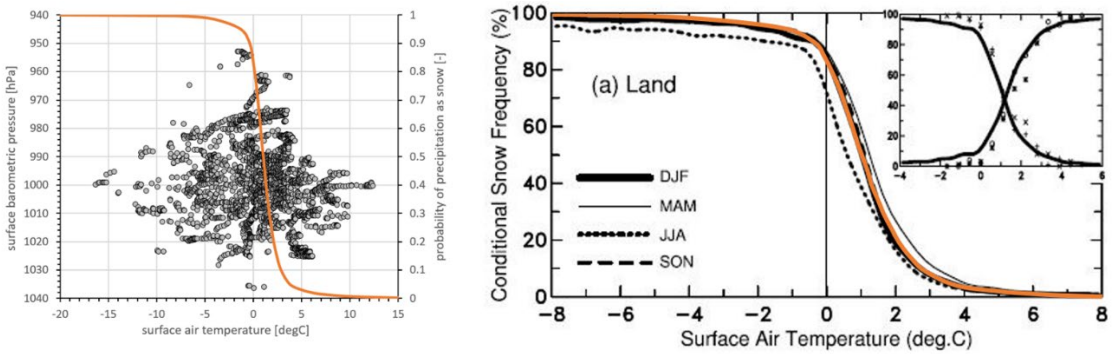

Fig. 8. *Left:* probability distribution for precipitation occurring as snow as extracted for and applied on the NCE-data based on Dai (2008). *Right:* comparison of extracted probability function with conditional snow frequency over land from different stations, reported in Dai (2009).

3 Snow Event Analysis

3.1 Snow Event Length

A precipitation event is typically described by its duration [min] and intensity [mm/h]. For snow accumulation studies wind speed and direction play an important role, since they relate to the flow field around an object (building) and the airborne and ground transport of snow flakes and particles. In this field study, precipitation is registered with a rain tipping gauge giving a singular signal for every 0.2mm of rainfall. These signals are subsequently grouped to events depending on a maximum allowed interval duration, T_{int}. Separation intervals exceeding T_{int} constitute the beginning of a new snow event. Consequently, the choice of T_{int} influences the number of identified events and the resulting duration distribution and with that the estimation of a typical/characteristic snow event duration.

For the NCE data, two separation intervals have been considered: T_{int} = 10 minutes, as standard duration for stationary meteorological observations, and T_{int} = 30 minutes as reasonable upper limit, yielding in rare occasions to snow event durations of almost 10 hours (596 minutes). Increasing T_{int} further would add longer durations but obscure distribution characteristics of shorter events.

Since the registration of rain gauge signals indicate popper operation of the tipping mechanism, the measured precipitation events are considered to reflect the true event sufficiently.

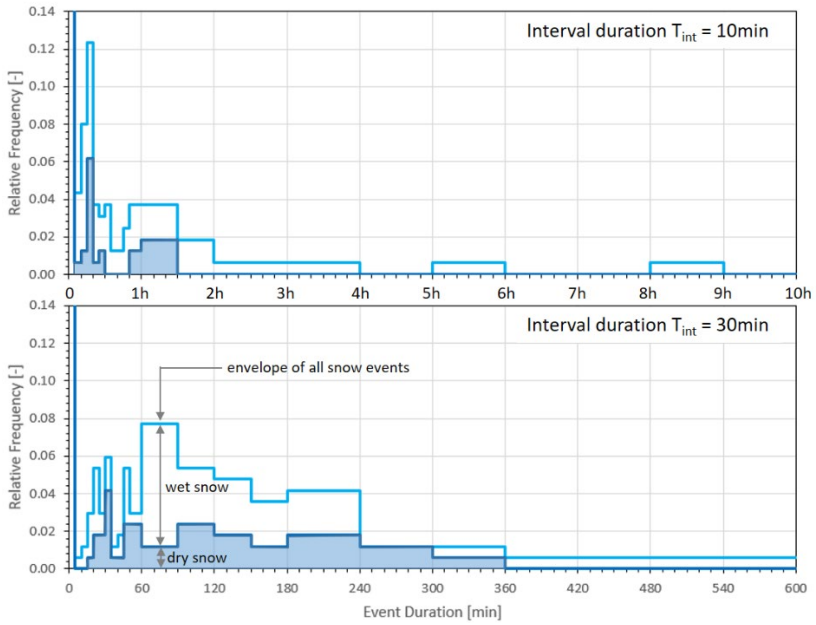

Fig. 9. Distribution of estimated snow events based on two interval durations.
For the distinction between dry and wet snow see chapter 3.3.

In Fig. 9, the distributions of identified event durations are shown for the two interval durations of 10 and 30 minutes, differentiated for dry and wet snow (discussed in chapter 3.3). The discrete distributions are calculated with varying resolution for the duration, namely 5 minutes for up to one hour, 30 minutes between one and 3 hours, and one-hour resolution for event durations longer than 3 hours.

The left end of the duration distributions is dominated by a high frequency of ultra-short events formed by just two immediate consecutive gauge release signals (1-minute events), which for the overall evaluation of duration lengths are omitted. For T_{int}=10min the most frequent duration is around 20 minutes for both, dry and wet snow. Then second group, again for both snow types, is between 1 and 1.5h, where wet snow events extend the duration to two hours. Events up to 9 hours occur but as rare events. For T_{int}=30min the most frequent duration for dry snow events is around ½ hour, whereas for wet snow events between one and 1.5h are most frequent but a further significant number of events last up to 4 hours. Hereafter the probability of longer events is low but on rare occasions (wet) snow events up to 10 hours have been observed. This allows defining two main event duration ranges:

1. Short events: 20 to 30 minutes

   Occurring for both, dry and wet snow events, with a slight dominance of dry snow events.

2. Longer events: 1 to 4 hours
   Higher occurrence frequencies between 1 and 1.5 hours for both snow types but duration range is generally more pronounced for wet snow events.

Isyumov and Mikitiuk (1977) state that snowfall durations on average range between 12 and 18 hours. These duration are based on an intermittency of a significant number of days without a measurable snowfall (below 0.2in or 2.54mm) separating periods with random discrete precipitation events. Kao and Ganguly (2011) focus on describing extreme precipitation events with durations ranging between 6 and 240 hours. The 6 hours duration is associated with an annual extreme of convective rainfall, which is generally considered to be the predominant generative mechanism of precipitation extremes, especially for shorter subdaily duration. This duration is weakly reflected in the NCE data and could indicate the main frame for relevant event durations with an occurrence probability sub-structure leaning towards shorter events of 1 to 4 hours.

3.2 Ground Snow Transport and Snow Types

For the simulation of snow accumulation, the ground transport of snow during precipitation plays a significant role. Here, the wind speed indicates the combination of direct (streamline) deposition of flow field controlled (airborne) snowflakes and erosion-driven scour and accumulation of snow particles on the ground. Li and Pomeroy (1997) give threshold values of wind-driven snow transport, summarised in Fig. 10. The information is used to assess the deposition process during a snow event.

To correlate the threshold values to the NCE data, the 10m wind speeds are converted to 1.2m by applying the logarithmic profile equation after Eurocode 1 (2007):

$$U_m(z) = 0.19 \cdot ln\left(\frac{z}{z_0}\right) \cdot U_{10} \qquad (1)$$

The data entering the threshold estimation in Li and Pomery (1997) have been measured at meteorological stations in Canada during 6 winter periods between 1970 and 1976. The roughness length z_0 of surrounding terrains varied between 0.0005m and 0.001m based on assessments for snow-covered terrain according to Oke (1978). This yields to reduction factors between 0.83 and 0.77 (decreasing with increasing roughness) applied on the observed mean value and the 95%

confidence lower and upper limit. The corresponding 10m curves (shown in Fig. 10) are calculated with following equation given in Li and Pomeroy (1997):

$$U_t(10) = \mathrm{a} + \mathrm{b} \cdot T + c \cdot T^2 \qquad (2)$$

Where $U_t(10)$ [m/s] is the observed individual threshold wind speed measured at 10m height, T [°C] is the ambient air temperature at 2m height, and a, b, and c are parameters: a = 9.43m/s, b = 0.18m/(s·°C), and c = 0.0033m/(s·°C^2). The confidence interval limits are 4.0-13.0 for a, 0.05-0.19 for b, and 0.0015-0.003 for c.

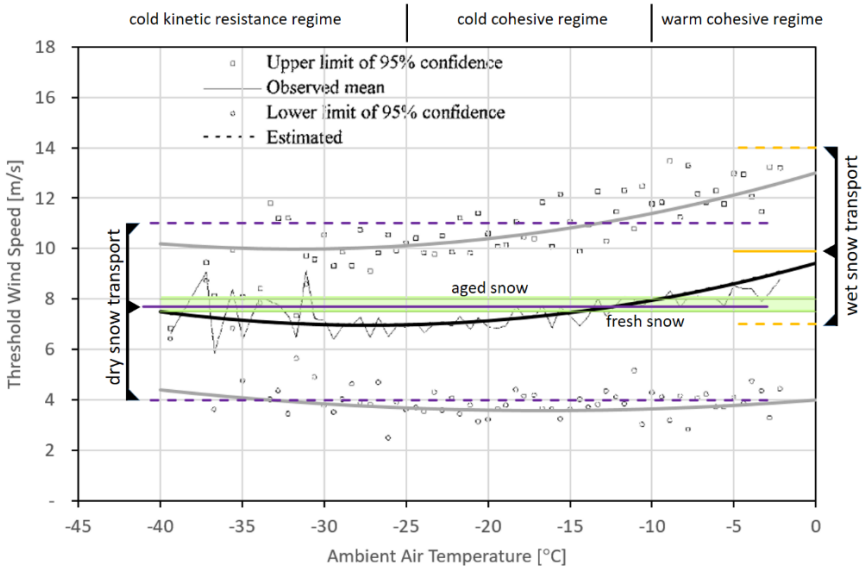

Fig. 10. Estimated threshold wind speed and observed mean threshold wind speed as function of ambient air temperature. Summarised data from Li and Pomeroy (1997). The wind speed values are defined at 10m above terrain.

The graph in Fig. 10 distinguishes between dry and wet snow transport. According to Li and Pomeroy (1997), "dry snow is snow that has not received temperatures of 0° C or above, or wet precipitation since the last snow event". To include wet snow precipitation, the temperature range is extended to +1°C, where the probability of precipitation occurs as snow is still 50% according to Schemenauer et al. (1981) and Dai (2008), shown in Fig. 8. For simplicity, precipitation falling at ambient air temperatures below -2°C are considered as DRY SNOW events and precipitation between -2°C and +1°C as (increasingly) WET SNOW events.

3.3 Wind Speeds and Ground Transport during NCE-events

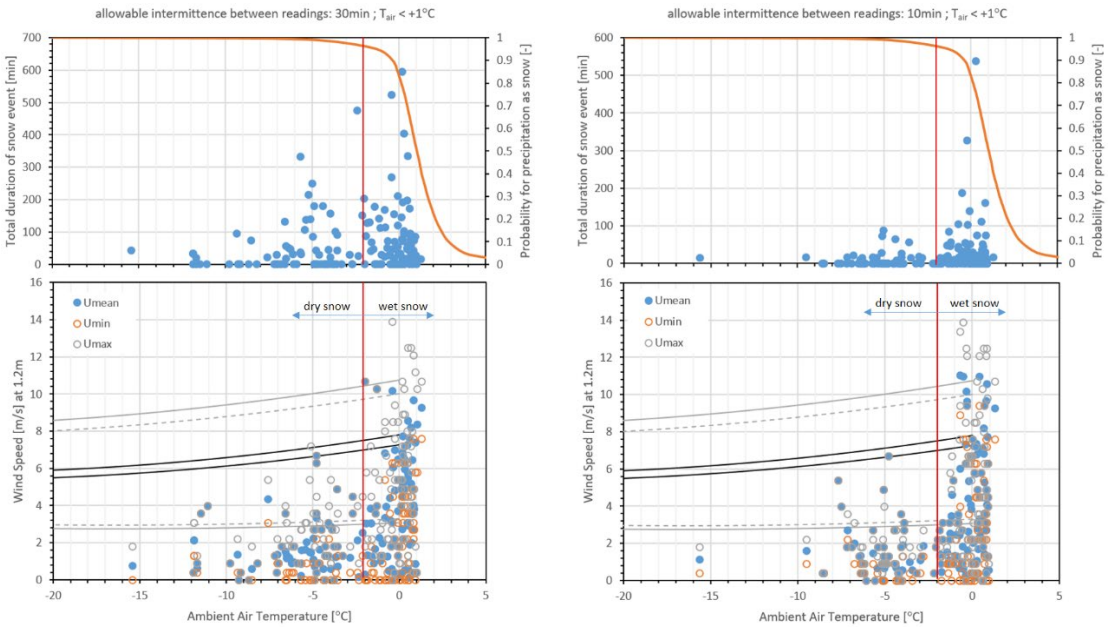

Fig. 11. *Upper row:* Duration of identified snow events over ambient air temperature for interval duration of T_{int} = 10min (left column graphs) and T_{int} = 30min (right column graphs). *Lower row:* comparison of snow event wind speeds (min, mean, max) to ground transport threshold values. The double lines for threshold speeds indicate the variation due to the considered range of roughness length z_0.

Fig. 11 shows that wet snow events seem to occur at significantly higher wind speeds compared to dry snow events. Table 3 lists the probabilities for ground transport for all identified snow events and Table 4 and Table **5** for dry and wet events, respectively. The threshold values have been calculated for different terrain roughness (z_0) and the calculation of the exceedance probability of observed events in the NCE-study refers to the respective lowest threshold of mean value, lower and upper 95% confidence limit. Based on all observations (dry and wet snow), the mean threshold value for ground transport is exceeded by 10% of the event mean wind speeds and by 16% of the maximum event wind speeds. For dry snow events, these values range between 2 and 4% and for wet snow events between 15 and 26%.

Table 3. Exceedance probability of the mean and maximum wind speed of a snow event exceeding threshold values for snow ground transport. Consideration of ALL SNOW events calculated for maximum interval durations of 10 and 30 minutes, respectively.

Threshold for snow	T_{int} = 10min		T_{int} = 30min	
transport on ground	U_{mean}	U_{max}	U_{mean}	U_{max}
Lower 95% confidence	36%	43%	40%	55%
Mean value	10%	14%	8%	16%
Upper 95% confidence	3%	7%	2%	7%

Table 4. Exceedance probability of the mean and maximum wind speed of a snow event exceeding threshold values for snow ground transport. Consideration of DRY SNOW events only (below -2°C), calculated for maximum interval durations of 10 and 30 minutes, respectively.

Threshold for snow	T_{int} = 10min		T_{int} = 30min	
transport on ground	U_{mean}	U_{max}	U_{mean}	U_{max}
Lower 95% confidence	10%	15%	18%	37%
Mean value	2%	2%	3%	4%
Upper 95% confidence	0%	0%	1%	1%

Table 5. Exceedance probability of the mean and maximum wind speed of a snow event exceeding threshold values for snow ground transport. Consideration of WET SNOW events only (above -2°C but below +1°C), calculated for maximum interval durations of 10 and 30 minutes, respectively.

Threshold for snow	T_{int} = 10min		T_{int} = 30min	
transport on ground	U_{mean}	U_{max}	U_{mean}	U_{max}
Lower 95% confidence	50%	59%	59%	70%
Mean value	15%	21%	12%	26%
Upper 95% confidence	5%	11%	2%	11%

There is a clear distinction between dry and wet snow events. For dry snow events, the mean event wind speed does not exceed the mean threshold by more than 4%. Even the maximum wind

speeds reach only up to 37% over the lowest threshold limit. Hence, it can be concluded that dry snow event occur practically without ground particle transport. The accumulation of snow is in this case dominated by the flow field around the cube or buildings in general (streamline deposition). For the simulation of wet snow accumulation, the streamline deposition is to a certain degree altered by ground transport, i.e. erosion, with 20-30% of gusts exceeding the transport mean threshold value.

3.4 Wind Directions and Variation during NCE-events

Snow accumulation processes depend on wind direction during a snow event and the corresponding variability. The first determines in relation to an exposed object or building the overall flow field driving the streamline deposit of airborne flakes and erosion transport of ground particles yielding to the characteristic accumulation pattern. The latter introduces a blur to the accumulation pattern.

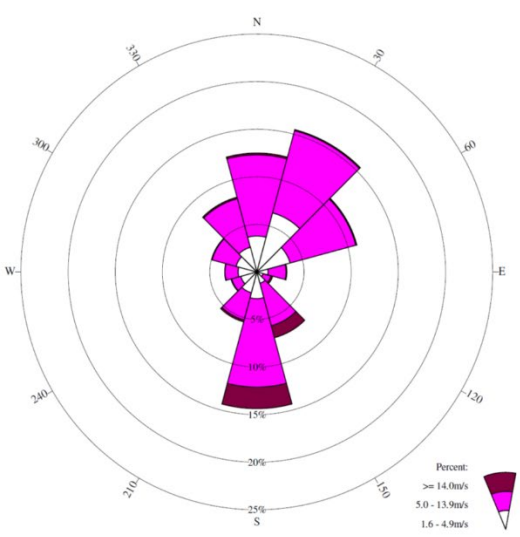

DMI data for Nuuk (station 04250). Annual statistic from observations between 1963 and 1999.

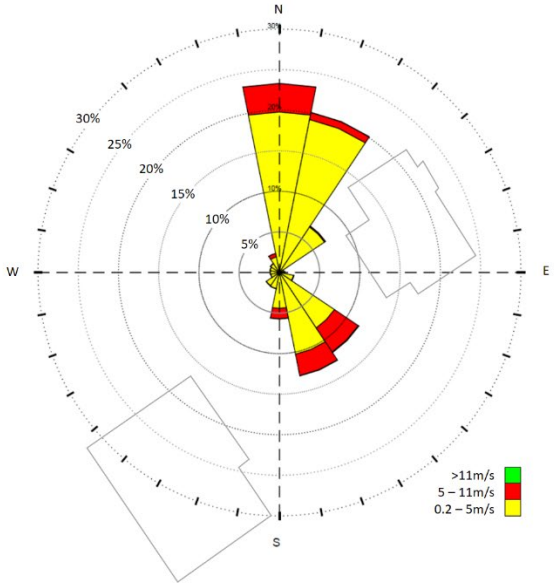

NCE data for December 2018. The position of the nearby buildings are indicated relative to the weather station.

Fig. 12. Comparison of wind statistic measured at Nuuk Airport (annual) and derived from Nuuk Cube Experiment (NCE).

The distribution of wind directions for Nuuk is characterised by dominating directions from south and from north to northeast as shown in Fig. 12 to the left as annual statistic for station 4250 from the Danish Meteorological Institute indicating north as the most frequent direction (21-29%) during winter season (Cappelen et al., 2001). The NCE data reflect the same directional structure. However,

nearby low-rise one storey residential buildings affect the directional reading at the ISS. The ground plan of these buildings relative to the ISS is shown to the right in Fig. 12 with the directional distribution for December 2018. In spite of their proximity, the influence on these buildings on the recorded data is deemed being low or even negligible, since wind occurring in these "blind zones" are rare events compare to unobstructed directions and secondly, these events would still be registered according to their direction and speed with minor alteration due to the building's low height.

Fig. 13 shows the distributions of mean wind directions averaged over the duration of the identified events for both, T_{int} = 10 and 30 minutes. The distributions indicate the share between dry and wet snow events. Even though according to Cappelen et al. (2001) north and northeast are the most frequent wind directions throughout the colder period of the year (October to April) and southern directions are dominant from May to September, snow events occur during winter predominantly from southern directions. Most prominent are directions between 150° to 180° (24 to 31% for T_{int} = 10 and 30 minutes, respectively) and about 50% of all snow events occur between 120° and 210°. Events from northeast accumulate between 14 to 17 (T_{int} = 30 and 10 minutes, respectively).

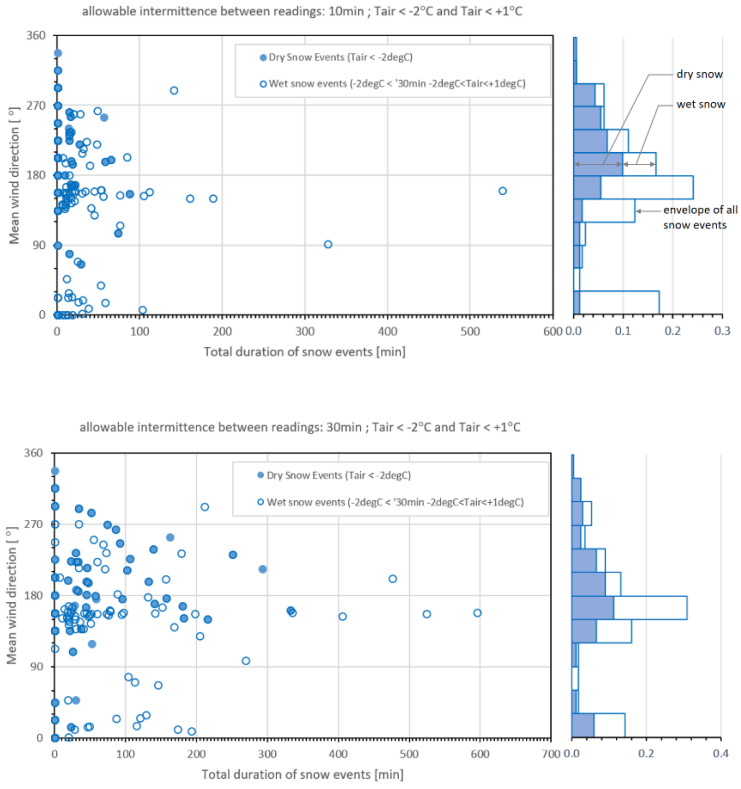

Fig. 13. Mean wind direction during snow events.

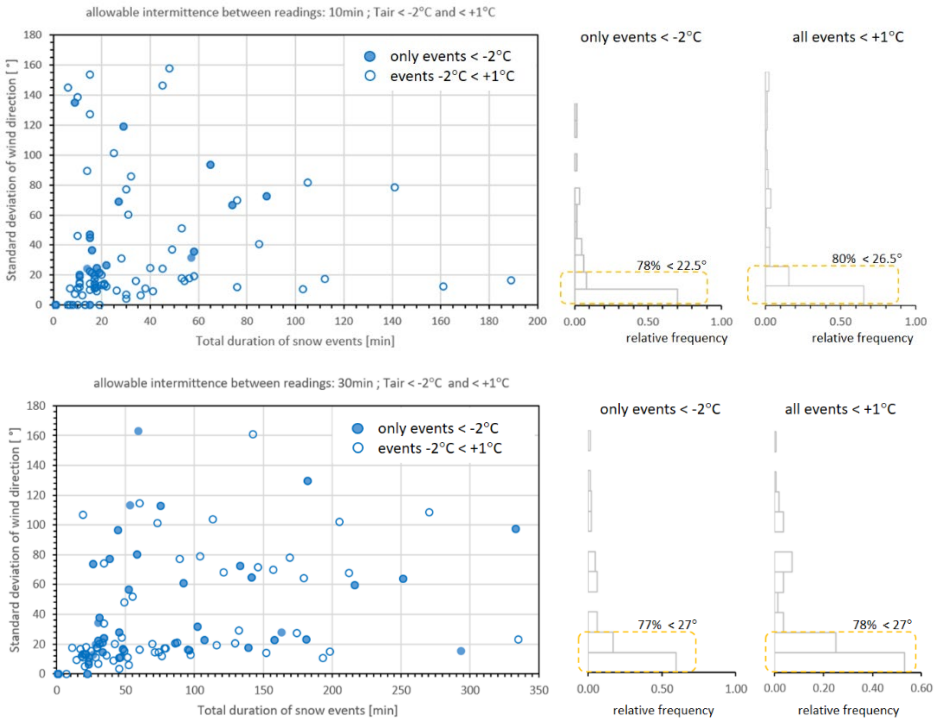

Fig. 14. Standard deviation of wind direction for snow events distributed over event duration. The events are distinguished according to the interval duration T_{int} for and snow type. Upper graph T_{int} = 30min, lower graph T_{int} = 10min.

The variability of the wind direction is indicated by the standard deviation for each snow event as a bulk measure (Fig. 14). The variability concentrates in a relative narrow range below 27° for about 80% of all events and below 14° for 50 to 60% of all events. This concentration applies to both, dry and wet snow events and independent of their length. A variation range of ±27° equals a direction sector of 54° and for ±14° an inner sector of 28°. The latter might have a limited influence on the sharpness of snow accumulation, whereas a direction sector of 54° will quite likely blur an otherwise mono-directional snow accumulation pattern. For studies, a single direction simulation will as a standard approach cover most situations. Blurring through directional variation will be more true-to-nature, but might on the other hand smear critical accumulation patterns out. A decision for including directional variability depends hence on the purpose of the study.

3.5 Correlation between Snow Event Parameters

Fig. 15 shows the correlation between the snow event mean wind speed (at 1.2m above ground), the corresponding mean wind direction, and mean air temperature during an event. The correlations are shown for intermittence times of 10 minutes (left) and 30 minutes (right) between precipitations

as basic definition for a continuous snow event. The general directional distribution reflects the overall wind statistic (Fig. 12) with dominating sectors between 0° and 30° sectors and 130° to 180° both mainly for wet snow events (T_{air} > -2°C). Dry snow events (T_{air} < -2°C) seem to occur more from southern to westerly directions (160° to 300°). This observation is also indicated in Fig. 13. Section 3.3 discusses the probability of exceeding the threshold wind speed for ground transportation. Fig. 15 confines these occurrences to wet snow events approaching predominantly from southern directions between 130° and 180°.

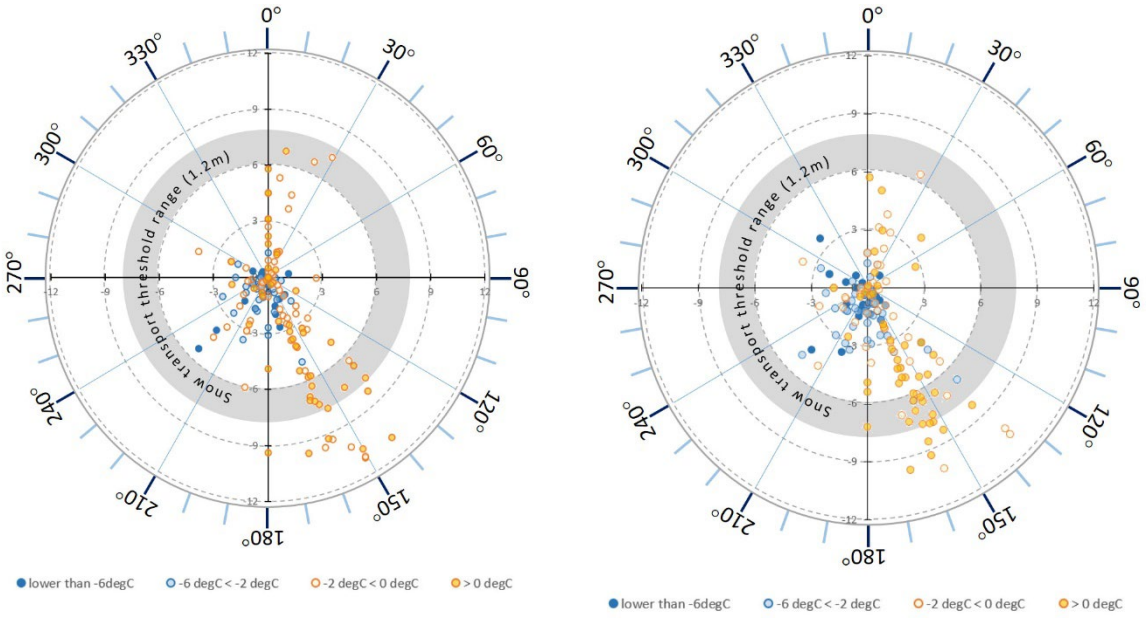

Precipitation intermittence time T_{int} = 10 minutes.

Precipitation intermittence time T_{int} = 30 minutes.

Fig. 15. Correlation between snow event mean wind speed, mean wind direction and mean air temperature. The blue-coloured data points refer to dry snow (T_{air} < -2°C) and the orange-coloured points to wet snow events (T_{air} ≥ -2°C).

3.6 Correlations to Wind Speed Variability

Li and Pomeroy (1997) base their threshold wind speed on an hourly mean value and point out that the observations of ground transportation of snow are subjected to a high variability. This variability or uncertainty results from the properties of both falling and surface snow particles, the negligence of the wind turbulence intensity in meteorological records, difference between air and snow surface temperature, time and geographical variation of snow surface roughness length, and from the visual determination of "drifting" snow by the observer. For application in snow

accumulation studied, the threshold value should be considered more like a transition range of increasing likelihood for ground transportation, maybe even broader than indicated in Fig. 15.

With respect to the data from the NCE, the variability of the wind speed during an event is expressed by the coefficient of variation (CoV) calculated as the ratio of standard deviation of wind speeds recorded within an event to the corresponding mean value. Due to the recording frequency of one minute, the CoV does not equal the turbulence intensity but gives still a good indication of the overall wind speed variability. Fig. 16 shows the correlation between snow event duration and the corresponding wind speed variability (CoV) including as well mean air temperature ranges during the event and an indication of the overall mean wind direction.

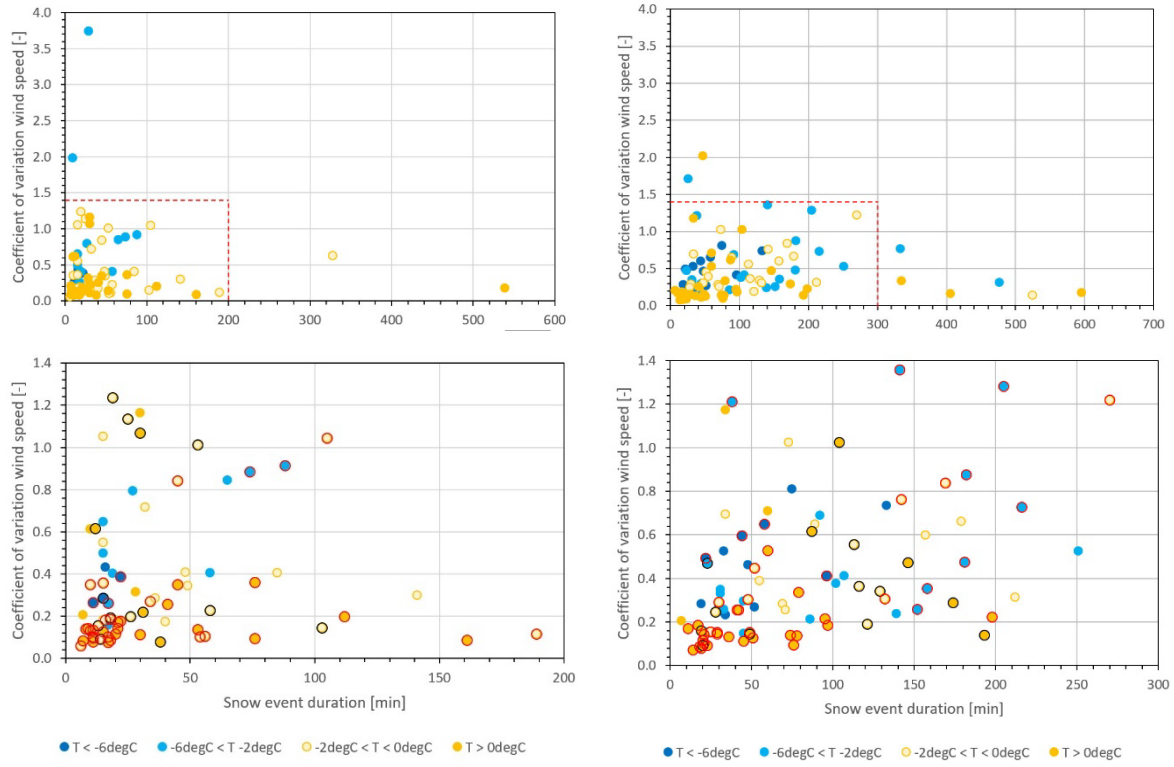

Precipitation intermittence time T_{int} = 10 minutes. Precipitation intermittence time T_{int} = 30 minutes.

Fig. 16. Correlation between snow event duration and the coefficient of variation of the wind speed during the event. *Upper row:* all results, *lower row:* zoom in on main result area. Further differentiation of event mean air temperature by colour code and wind direction by additional circling of data points. Black-circled data points refer to the directional sector of 0° to 90° and red-circled data points to the sector between 90° and 180°.

For both event definitions (intermittence time of 10 and 30 minutes) the wind speed CoV lies for the majority of all events below 1.4. For T_{int} = 10 minutes (lower left in Fig. 16) there seem to be two apparent CoV ranges: one from 0 to 0.4 and the second from 0.7 to 1.3. This could indicate an influence of terrain roughness for different wind directions or at different times like at the start or

end of snow seasons with no or little snow cover on the terrain. Even though plausible, the NCE data set does not provide conclusive evidence regarding a directional and only a weak indication for seasonal dependency. The data for T_{int} = 30 minutes do not show any apparent CoV ranges. In both cases however, the bottom CoV range between 0 and 0.2 is dominated by wet now events.

This observation is substantiated when plotting the relation between mean event wind speed and the corresponding CoV in Fig. 17. Disregarding on how a snow event is defined by T_{int}, the higher the mean wind speed U_m the lower the CoV. This dependency can be described by a power-law decay function, eq.(3), where *c* is the scaling factor and *k* the decay exponent.

$$CoV(U_m) = c \cdot {U_m}^{-k} \tag{3}$$

Dry snow events seem to occur with lower mean wind speeds whereas wet snow events occur over the entire velocity range. As already indicated in Fig. 15, only wet snow events seem to exceed the threshold range for snow ground transportation and if this occurs, the CoV is, with few exceptions, below 0.25. Even though not directly comparable, the CoV matches a turbulence intensity of 20 to 25%, which is expectable near the ground in smooth snow covered but uneven terrain.

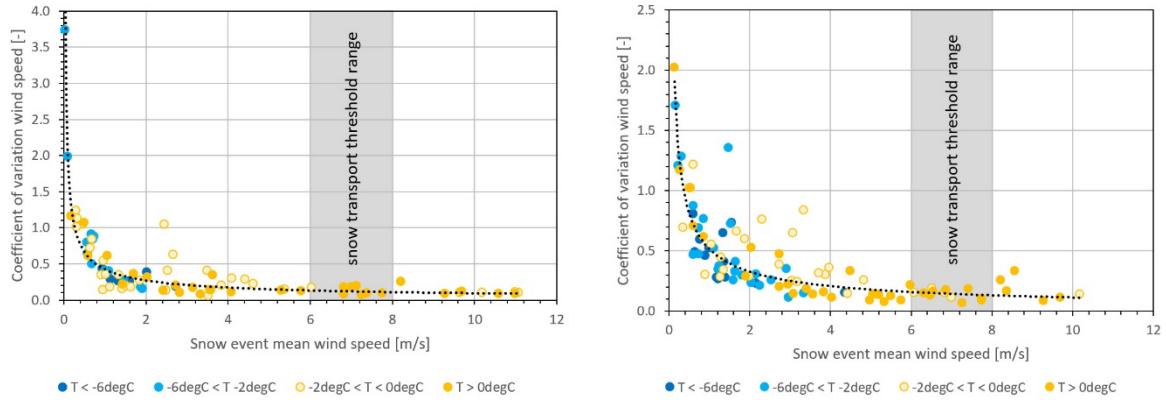

Precipitation intermittence time T_{int} = 10 minutes.
Scaling factor c = 0.423, decay exponent k = 0.65

Precipitation intermittence time T_{int} = 30 minutes.
Scaling factor c = 0.515, decay exponent k = 0.65

Fig. 17. Relation between the CoV of the wind speed recorded during a snow event to the corresponding mean value. The wind speed was measured between 1.0m and 1.4m over terrain, depending on the snow cover thickness. The grey area indicates the threshold range for snow transportation at the ground.

3.7 Precipitation Intensity

The precipitation intensity is calculated as the accumulation of precipitation signals occurring randomly within a snow event related to its duration. Fig. 18 shows the precipitation intensity for dry and wet snow events derived with T_{int} = 30 minutes. For long durations, the mean values for dry and wet snow intensities converge to 1.25mm/h (standard deviation 0.5mm/h). For shorter event durations (< 200min), the intensity increases significantly for wet snow events, but remains almost constant for dry snow events.

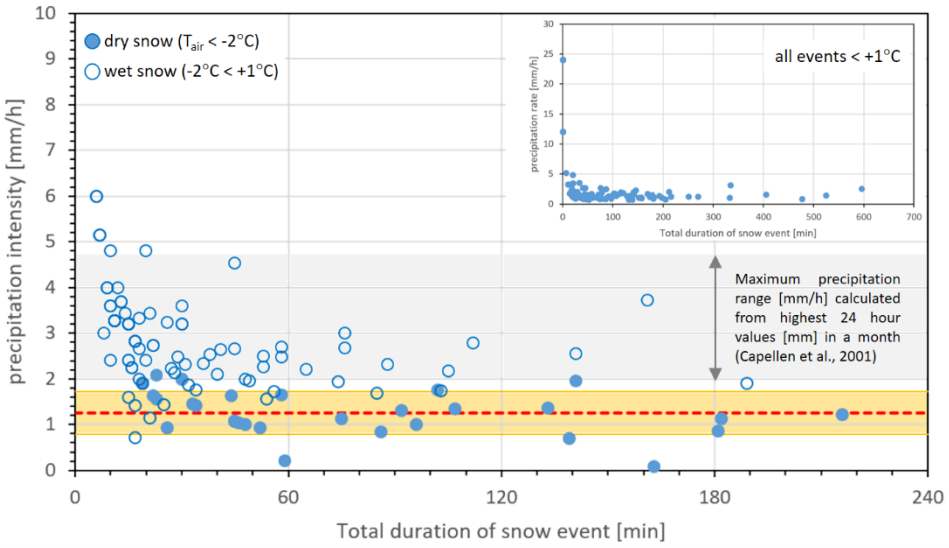

Fig. 18. Precipitation intensity for dry and wet snow events defined by T_{int} = 30min. Mean value and standard deviation ratio refer to dry snow events (T_{air} < -2°C)

This tendency is not observable for events based on T_{int} = 10min, where both snow types have a common mean value of 2.8mm/h (standard deviation 1.0mm/h) but the scatter increases as well with decreasing event durations. The difference in the calculated mean precipitation intensity results from the definition of an event based on different interval durations (T_{int}). Apart from very short events (<20min), the extreme calculated intensities match the range of reported highest precipitations (Cappelen et al., 2001), ranging from 1.96 to 4.75mm/h. The latter being observed in March. These maximum precipitations can be taken as a basis for simulation of extreme scenarios

Conclusions

Weather data have been recorded over four winter periods between 2017 and 2020 close to terrain surface (1.4m sensor height) as reference data for observations/measurements of snow accumulations at and around a 1.2m cube in 3m distance to the weather station – the Nuuk Cube Experiment (NCE). Due to the low sensor height and the unevenness of the terrain surrounding the NCE, all data and derived conclusions apply primarily to this particular location. However, even though influenced by terrain and nearby low-rise residential buildings, the results reveal valuable information regarding the characteristics of arctic snow events in Nuuk area. The essence of these findings and the derived recommendations have been used in validation tests of the NCE (Fiebig and Koss, 2021) and simulation-based snow accumulation studies on generic arctic built-in environments.

Event duration: In this study, the duration of a precipitation event depends solely on the accepted maximum interval time between rain gauge signals. As a reasonable estimate for this interval, two maximum time gap limits have been applied: 10 and 30 minutes. With these assumptions, two significant ranges for snow events could be identified. Shorter periods between 20-30 minutes mainly represented by dry snow events, and a longer period between 1 and 4 hours which is statistically more pronounced for wet snow events. The event duration forms the basis for organising and statistical analysis of records for air temperature, wind speed, wind direction, and precipitation.

Deposition process: With respect to simulating snow accumulation processes one can distinguish between dry snow events, where ground-near wind speeds practically do not exceed the threshold for transportation (erosion), and wet snow events, where gust wind speed exceed the mean transport threshold at about 20 to 30%.

Variation of wind direction: For the majority of snow events (nearly 80%) the wind direction does vary predominantly between ±27° and 50 to 60% of all events vary predominantly between ±14°. This suggests mainly mono-directional wind conditions for accumulation processes during a snow event. In some cases, depending on the object geometry or arrangement of objects, small variations of wind direction might still be relevant for the accumulation process and should to be taken under consideration.

For larger validity of the findings, comparative field measurements at more exposed but unobstructed locations should be conducted and the operation stability of the weather station under arctic conditions should monitored continuously. Stress tests of the equipment in climatic chambers and wind tunnels, especially regarding the functionality of the rain gauge and collector, should be conducted and improvement made if deemed necessary.

Relevance to Climate Change: Investigating snowdrift and accumulation on and around buildings might not seem to be of urgency. Higher temperatures suggest a decreased frequency of snow and a higher likelihood for rain even in cold climates and traditionally snow-prone regions. To anticipate effective actions to mitigate impact of climate change on the built environment, different scenarios are modelled and the result can vary significantly, depending on the complexity of the investigated climate parameter. McCrystal et al. (2021) show results from the Coupled Model Intercomparison Project (CMIP6) indicating a transition from a snow-dominated to a more rain dominated precipitation in the Arctic. However, in spite of this general trend, some scenarios indicate a significant increase of snowfall by 2100 in winter and "most of the Arctic remains largely snow-dominated in winter and spring throughout the century". With respect to snow loading, a generally increased frequency of rain-on-snow (ROS) events should be taken into account leading to an increased weight of the snow on building roofs. Other studies (Strahlendorff et al., 2016; Jiping et al., 2012) indicate that warming in the Arctic leads to increases snowfall during boreal autumn and winter. In particular increased heavy snowfall in Europe during early winter and the northeastern and midwestern United States during winter. These results show that the effort on studying snow accumulation in the Arctic built environment will be of importance at least for the rest of the century. In a wider perspective, climate change quite likely leads to an increased snowfall in many northern countries. Even with some uncertainty regarding combination with wind speed and direction or ROS events, snow studies on buildings will play an important role for climate adaptation of cold climate built environment.

Acknowledgement

The authors would like to thank architect Peter Barfoed for allowing us using his private home for setting up the data acquisition computer of the weather station and for the support in surveying snow accumulation around the cube.

References

Brooks, A., Gamble, S., Dale, J., Bond, J., 2016. *Comparison of Physical Snow Accumulation Simulation Techniques*. Proc. of 8th International Conference on Wind Engineering, Nantes, France

Cappelen, J., Vraae Jørgensen, B., Vaarby Laursen, E., Sligting Stannius, L., Sjølin Thomsen, R., 2001. *The Observed Climate in Greenland, 1958-99 with Climatological Standard Normals, 1961-90*. Danish Meteorological Institute, Technical Report 00-18

Dai, A., 2008. *Temperature and pressure dependence on the rain-snow phase transition over land and ocean*. Geophysical Research Letters, Vol.35, doi:10.1029/2008GL033295

Davis, 2017. *User Manual for Integrated Sensor Suite – Vantage Pro2 Plus*. Davis Instruments, available online < https://www.davisinstruments.com/>, accessed March 2014

DS/EN 1991-1-4, 2007. *Eurocode 1: Actions on structures – Part 1-4: General actions – Wind actions*. European Standard (CEN), issued by Danish Standard 2007

DMI, 2021. *Vejrarkiv* (weather archive). Available online < https://www.dmi.dk/vejrarkiv/>, accessed on February 12, 2021

Fiebig, J., Koss, H.H., 2021. *Nuuk Cube Field Experiment – Part 2: Snow accumulation monitoring*. Prepared for publication in Journal for Cold Regions Science and Technology.

Flaga, A., Flaga, L., 2016. *Wind tunnel tests and analysis of snow load distribution on three different*
large size stadium roofs. Proc. of 8th International Conference on Wind Engineering, Nantes, France

Fulkes , J.R., 1935. *Rate of precipitation from adiabatic ascending air*. Monthly Weather Review, Vol.63, pp.291-294

Isyumov, N., Mikitiuk, M., 1977. *Climatology of snowfall and related meteorological variables with application to roof snow load specifications*. Canadian Journal of Civil Engineering, Vol.4

Kao, S.-C., Ganguly, A. R. , 2011. *Intensity, duration, and frequency of precipitation extremes under 21st century warming scenarios*. J. Geophys. Res., 116, D16119, doi:10.1029/2010JD015529.

Li, L., Pomeroy, J.W., 1997. *Estimates of Threshold Wind Speeds for Snow Transport Uning Meteorological Data*. Journal of Applied meteorology, Vol.36, 1997.

Liu, J., Curry, J. A., Wang, H., Song, M., & Horton, R. M. (2012). Impact of declining Arctic sea ice on winter snowfall. Proceedings of the National Academy of Sciences of the United States of America, 109(11), 4074–4079.

McCrystall, M. R., Stroeve, J., Serreze, M., Forbes, B. C., & Screen, J. A. (2021). New climate models reveal faster and larger increases in Arctic precipitation than previously projected. Nature Communications, 12(1), 6765. https://doi.org/10.1038/s41467-021-27031-y

Oke T.R., 1978. *Boundary Layer Climates*. Methuen & Co. Ltd

Schemenauer, R.S., Berry, M.O., Maxwell, J.B., 1981. *Snowfall Formation*. In „Handbook of Snow“, Gray, D.M., Male, D.H (Ed.), Part II – Snowfall and Snowcover. Pergamon Press

Snow, J.T., Harley, S.B, 1988. *Basic Meteorological Observations for Schools: Rainfall*. Bulletin American Meteorological Society, Vol.69, No.5, May 1988.

Snow, J.T., Harley, S.B, 1988. *Basic Meteorological Observations for Schools: Rainfall*. Bulletin American Meteorological Society, Vol.69, No.5, May 1988.

Strahlendorff, M., Duyck, S., Gille, J., Koivurova, T., Leonenko, A., von Schickfus, M., Stępień, A., & Thomas, J. (2016). "Climate Change in the Arctic". In *The Changing Arctic and the European Union*. Leiden, The Netherlands: Brill | Nijhoff.
doi: https://doi.org/10.1163/9789004303188_004

B Nuuk Cube Field Experiment – Part 2: Snow accumulation monitoring

Nuuk Cube Field Experiment – Part 2: Snow Accumulation Observations

Jennifer Fiebig, H. Holger H. Koss
Technical University of Denmark; Department of Civil Engineering, Section of Structures and Safety
jenfi@byg.dtu.dk; hko@byg.dtu.dk

Abstract: The built environment as well as individual building in arctic regions are exposed to extreme environmental conditions. Snow accumulation on and around buildings reduce the functionality of buildings and affect structural durability. For proper investigations of snow accumulation the applied simulation methods need to be validated. Even though similarity laws have been suggested in the past, only little concrete data on the weather conditions surrounding a snow event and resulting accumulation patterns are available from field measurements. For this reason a field study, the Nuuk Cube Experiment (NCE) was initiated to measure ground-near weather conditions during winter period in parallel to observation and documentation of snow accumulation on a nearby 1.2m cube. This paper focuses on the analysis of the observed snow accumulations throughout four winter seasons between 2017 and 2020. The analysis is based on direct observations, photographs and photometric scanning of the snow accumulation surrounding the cube. The study should shed some light on the question whether a continuous accumulation process affected by varying wind speeds and directions shows significant differences compared to the more typical uni-directional investigations of snow accumulations. Furthermore, does a continuous accumulation process result in a critical situation not covered by a uni-directional approach?

Keywords: Field study; Nuuk; Greenland; Precipitation; Snow accumulation; Cube; Full season effect

1 Introduction

1.1 Background

In Civil Engineering, studies of snowdrift and accumulation are usually conducted to obtain information regarding the resulting snow load on building roofs or to identify negative impacts on building or urban functionality due to significant snow accumulation around and in between buildings. In all cases, the method applied in a study has to reflect a process of snow transportation similar to nature. In wind tunnel testing, the fulfilment of this requirement is based on similarity laws yielding to scaling ratios for length, time, and mass and hereon derived quantities such as velocity, acceleration, or density. Since the physical description of snow in its properties and behaviour is characterised by a high variability, a universal or unambiguous formulation of snow transport and deposition processes is extremely challenging. The statement that "it is extremely difficult to fully simulate the behaviour of snow, and at the same time satisfy all similitude criteria

at a reduced scale" by Kwok et al. from 1992 still holds today. It is for this reason that investigation methods and studies are whenever possible compared to observation from full-scale. Table 1 gives a small overview on snow accumulation studies around buildings conducted in full-scale or simulations comparing their results to full-scale data. The table differentiates between three levels for sourcing validation data for snow accumulation studies: observations on real buildings in full-scale (1st Val.), studies in full-scale but on scaled or small buildings or objects sometimes combined with artificial wind (2nd Val.), and studies with artificial snow (e.g. snow canon) in a climatic wind tunnel (3rd Val.). In all cases, the snow consists of "real snow", i.e. ice crystals either of natural or artificial origin, which in turn allows including thermodynamic effects of the snow particles during transport, cohesion, accumulation and compacting under different environmental boundary conditions. This capability is missing when using substitutional material for the snow and constitutes the main difficulty for satisfying similitude criteria.

The test cases in Table 1 are a cube, a rectangular prismatic building (ground-mounted or elevated), and a composed geometry of rectangular shapes. The cube is a widely used generic benchmark, the rectangular designs – especially elevated – usually refer to observation stations in the Antarctic, and the composed design represent flat-roofed buildings in settlement or urban context in cold climate regions. Beside buildings, other structures and installations are investigated in field studies such as snow fences to protect settlements or roads from critical snow accumulation (Anno, 1985; Haehnel et al., 1993; Haehnel and Lever, 1997; Naaim-Bouvet et al, 2002).

Simulating snow accumulation on and around buildings experimentally at reduced scale relies on ensuring proper similarity to nature through fulfilment of scaling laws. To this end, Liu et al. (1993) focus in their study on describing the relevant physical properties of snow a Kwok et al. (1992) present a set of modelling parameters to be scaled. However, the inherent shortcomings of substitutional material to reflect real snow behavior requires an additional calibration of the respective test method to field study observations. For example, the model time duration of a snowdrift event was significantly adjusted in Kwok et al. (1992): theoretical required simulation times between 37 to 93 hours were reduced to 4 hours after matching sufficiently snowdrift observation from full-scale. Matha and Taylor (1990) advocate a two-step test procedure to reflect the influence from airborne snowflakes on the accumulation process.

It is evident that simulations at reduced scale rely on both, physical scaling laws and phenomenological calibration in almost equal measure. This leads to the necessity to collect as many phenomenological reference or validation data as possible. Any systematic documentation of snow accumulation observations will contribute to safeguard proper modelling. On this background, a

field experiment was initiated in 2017, where a 1.2m cube was installed in a relatively unobstructed area in the outskirts of the capital city of Greenland, Nuuk. Being an Arctic city with considerable snow precipitation (Cappelen et al., 2001), Nuuk is an ideal spot for field studies of snow accumulation on and around buildings and the monitoring campaign is in the following referred to as the "Nuuk Cube Experiment", or NCE. Through four winter seasons, the weather conditions were recorded continuously (Fiebig and Koss, 2023) and resulting snow accumulations were documented. In this paper, the observations of the snow accumulation are discussed as snapshots of a continuous process of

- snow deposition from precipitation,
- ground transportation by wind,
- accumulation in the flow field around the cube,
- and re-arrangement by changing wind directions and speed.

All studies reviewed in the literature survey focus on single wind direction per accumulation pattern. In this respect some of the central research aspects in this study are:

- Does a continuous accumulation process throughout an Arctic winter season lead to critical snow accumulations not reflected by single wind direction studies?
- Will a 1.2m cube completely be covered by snow at some point during an Arctic winter due to a continuous growth of snow layer for long exposure?
- Will the accumulation patterns maintain a classic "one wind direction" characteristic or a more random superposition of those?

Table 1. Selected studies on snow accumulation on and around buildings using real snow in the investigation as reference for validation of other simulations, or directly comparing to full-scale data. The term "real snow" refers to ice crystal particles either occurring naturally in field studies or created artificially in a climatic wind tunnel.

Snow accumulation studies specifically conducted in full-scale or including full-scale data for validation purpose.		wind direction φ	averaged wind speed U_{10} at 10m, U_H at roof, U_U uniform	single building	group arrangement	SNOW TYPE: natural		SNOW TYPE: arti-ficial	SNOW TYPE: substi-tute	SNOW TRANSPORT	
						field study	artificial field study	climatic wind tunnel study	wind tunnel study	snow fall	erosion
Building type/ geometry	Reference	# of steps [°]	# of steps [m/s]	S	G	FS 1st Val.	AF 2nd Val.	CWT 3rd Val.	WT	SF	ER
a) CUBE											
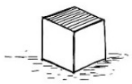	Liu et al. (2018)	4 φ = 0°- 45°	4 U_U = 1.5 - 4.5m/s	x	x		x			x	
	Beyers et al. (2004)	1* φ = 0°	1* U_{10} = 9.88m/s	x		x					x
	Oikawa and Tomabechi (2000)	7* φ ≈ -15°- 23°	7* U_H =1.7 - 5.2m/s	x		x					x
	Thiis (2003)	continuous φ ≈ ± 30°	continuous U_{10}= 0 - 18m/s		x	x				x	x
b) RECTANGULAR/ PRISMATIC											
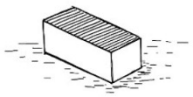	Thiis (2003)	continuous φ ≈ -45°- 15°	continuous U_{10} = 0 - 18m/s	x		x				x	x
	Kwok et al. (1992)	1 φ = 0°	1 U_{10} = 17m/s	x		x			1:50 1:100		x
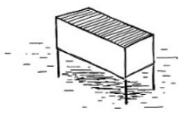	Mitsuhashi (1982)	1 φ = 90°	various U_{10} = 1.8 - 23m/s	x		x				x	x
	Kwok et al. (1992)	1 φ = 0°	1 U_{10} = 17m/s	x		x			1:50 1:100		x
	Beyers and Harms (2003)	1 φ = 0°	continuous U_{10} = 0 - 25m/s		x		1:25				x
c) COMBINED PRISMATIC RECTANGULAR											
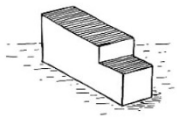	Matha et al. (1990)	1 φ = 0°	2* U_{10} = 4.25, 17m/s		x	x			1:50	x	x
d) SNOW FENCE											
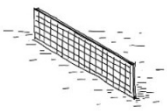	Anno (1985)	1 φ = 0°	U_{1m} = 9.84m/s	x		x			1:300	x	x
	Haehnel et al. (1993)	1 φ = 0°	$U_{\infty,m}$ = 3 – 6m/s	x					1:4 – 1:150		x
	Haehnel and Lever (1997)	1 φ = 0°	$U_{\infty,m}$ = 6m/s	x		x			1:12		x
	Naaim-Bouvet et al. (2002)	1 φ = 0°	U_H = 2 – 3m/s, 7.2 – 13.2m/s	x				x		x	x

* The study may focus on selective cases with specific directions and wind speeds but the validation data from full-scale show a higher variability.

$U_{\infty,m}$ – free stream velocity at model scale, U_{1m} – other specific reference height (here: 1m above terrain).

1.2 Observations in the Nuuk Cube Experiment (NCE)

Weather data on wind speed and direction, air temperature and humidity, barometric pressure, precipitation, sun radiation and UV index were measured over 27 months distributed over four winter seasons using a Vantage Pro2 Plus weather station by Davis Instruments located 3m from the cube. The snow accumulation on and around the cube was recorded through photometric scanning on 26 incidents (snow scan ID). Fig. 1 gives an overview of the data recording (Fiebig and Koss, 2023) and snow scans. For a number of practical reasons, the scanning could only be conducted at a limited number of occasions (months with yellow marked ID-number). Furthermore, visibility and contrast resolution of the taken photographs resulted into 16 usable out of 26 conducted scans (green marked scan ID-number). The 16 scans from which a numerical model of the scow accumulation could be obtained are grouped into five observation sequences (Obs1 to Obs5) according to the winter season they occur in (Table 2). Obs3 and Obs4 are treated as separate observation events since they are grouping around two periods of the same winter period but will also be compared to each other as consecutive events.

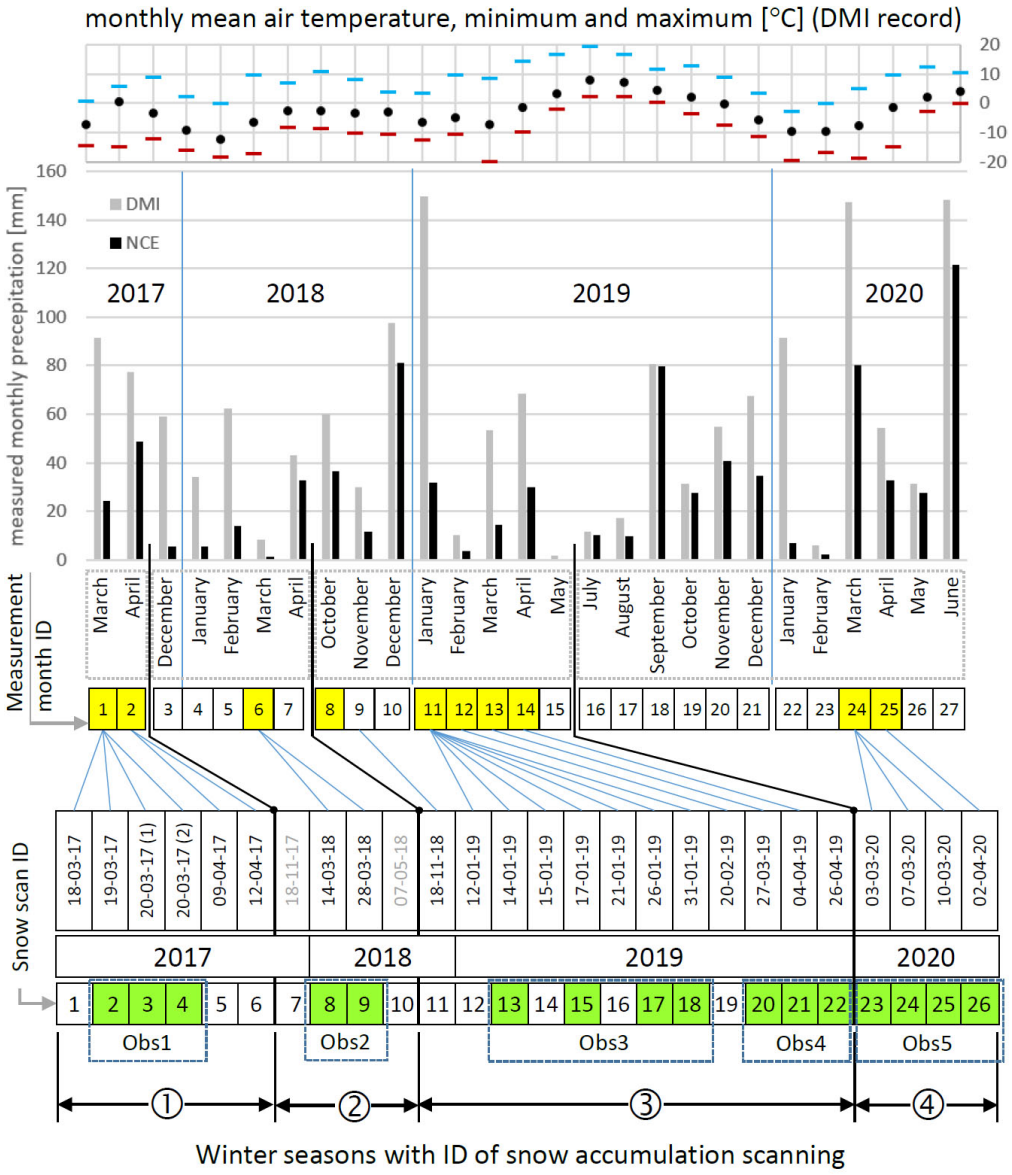

Fig. 1. Overview of the 27 months for weather data recording (measurement month ID) and snow accumulation scanning (snow scan ID). The scans were conducted in the months with yellow marked ID number. Only those scans marked with a green ID could be translated into a numerical model of the accumulation pattern.

Table 2. Observation periods for snow accumulations, corresponding scans and period measured in days the periods stretches over.

Observation period	Scan ID	Start date	End date	duration
Obs1	2, 3, 4	19-03-2017	20-03-2017	2 days
Obs2	8, 9	14-03-2018	28-03-2018	14 days
Obs3	13, 15, 17, 18	14-01-2019	31-01-2019	17 days
Obs4	20, 21, 22	27-03-2019	26-04-2019	31 days
Obs5	23, 24, 25, 26	03-03-2020	02-04-2020	33 days

1.3 Location of Cube and Weather Station

The location of the cube in the northern part of the developed area of Nuuk. The actual location was known for exhibiting significant snow cover during past winter seasons and being widely unaffected by the airflow around nearby buildings. Furthermore, the choice of the location was as well a compromise between a relatively open area and the possibility for indoor installation of the data recording equipment connected to the internet, short distance for wireless transmission from the weather station and for frequent observation and scanning of the snow accumulation. Further aspects of the data recording and validity of weather data are discussed in Fiebig and Koss (2023). The footprint of the cube is rotated 45 to north south direction to face the most frequent direction for snow events based on experience.

The wind sensor was located in close proximity and approximately at the same height as the top side (roof) of the cube. This position was specifically chosen to record the wind velocity directly relating to the wind field around the cube. In most field studies (Table 1), the measurement height for wind is 10m above terrain and all observations relate to this reference speed such as the threshold for ground transportation of snow. Wind velocities at other heights can be calculated with the logarithmic equation of the mean wind speed profile defined by shear velocity u^* as indication for terrain roughness. In case of the NCE, the ground-near location of the anemometer allows a more direct measurement of the wind speed driving the transport and accumulation process. Due to the uneven terrain surface at the cube location an extrapolation from a 10m reference position would require a more accurately calibrated mean wind speed profile.

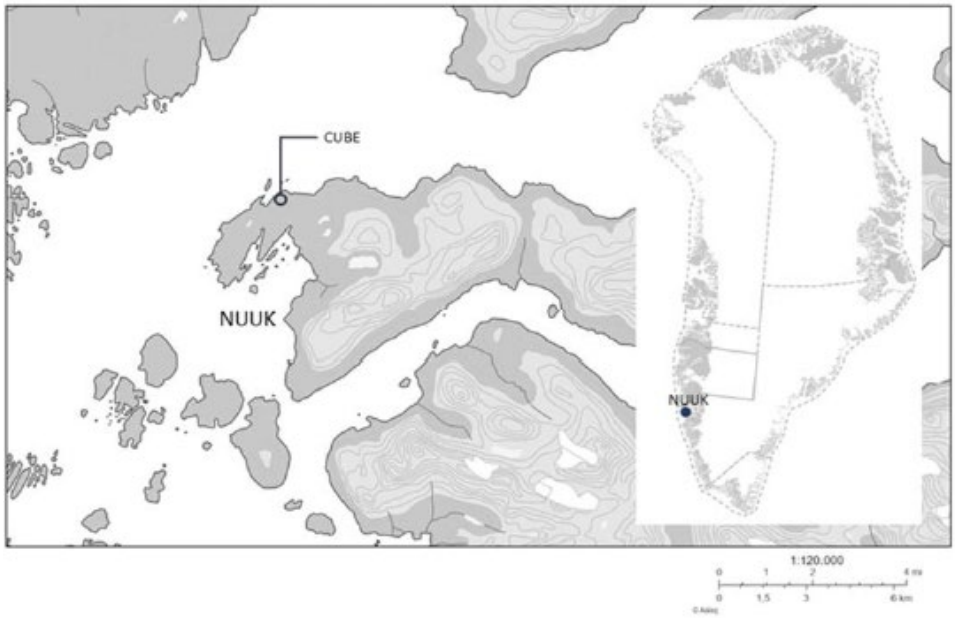

Fig. 2. Location of the cube in the northern part of Nuuk, Greenland, about 1500m west of Nuuk Airport and 350m south of the nearest shoreline (Asiaq, accessed on NunaGIS, October, 2022).

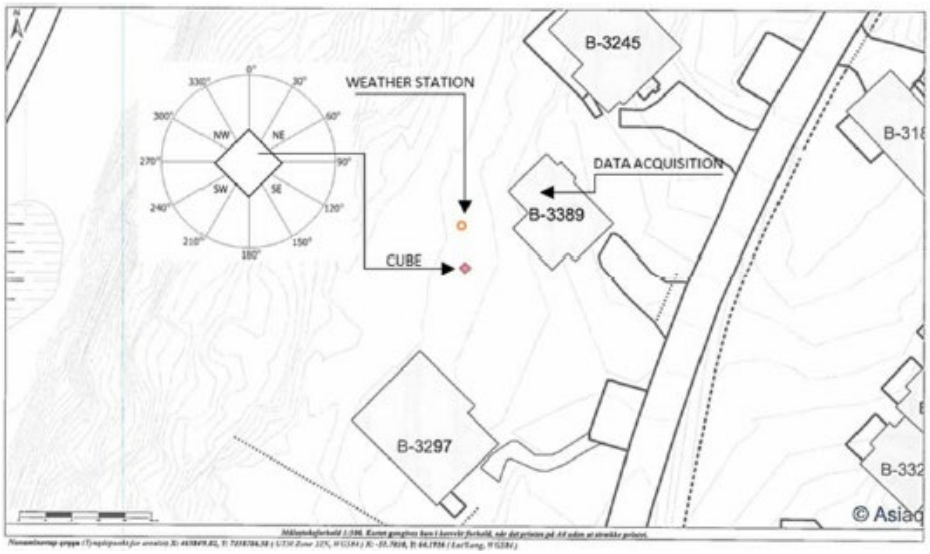

Fig. 3. The cube has been installed on an open stretch 13m west of the nearest building (observation base, housing of data acquisition computer). The surface topography is moderately uneven but still flat enough to allow representative snowdrift and accumulation. Geographic reference of cube position 64°11'37.3"N 51°42'121.2"W (64.1936, - 51.7030), elevation 36.7m above sea level (position and elevation provided by land registry office for Nuuk). Kommuneqarfik Sermersooq (Nuuk), approved plans from November 11, 2017.

The snow cover during winter season will affect the wind speed at anemometer height and the wind field around the cube at the same time. Hence, the influence on the driving force of snow transportation will be more accurately recorded compared to a reference wind speed at 10m above terrain surface. Fig. 4 shows the setup of the cube and weather station with and without snow cover.

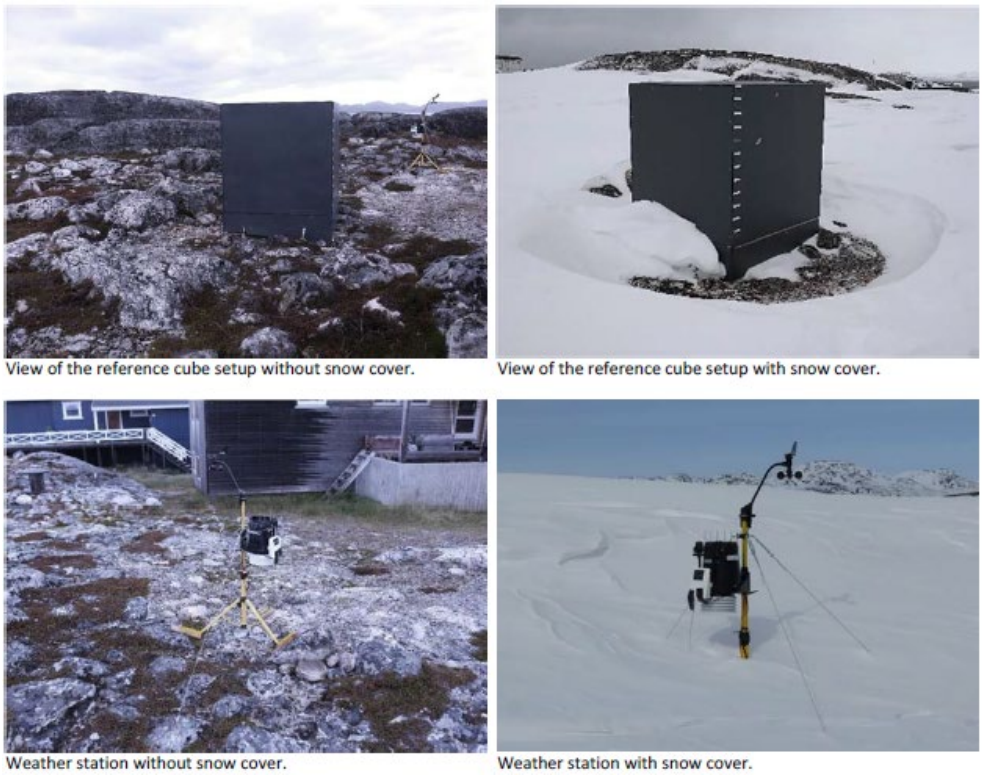

Fig. 4. Cube and nearby weather station with and without snow cover. The pictures to the left show the unevenness of the terrain requiring the cube to be mounted on a small platform for levelled and better anchoring. The pictures to the right show a typical winter situation with scour pattern in the snow around the cube and snow cover below the anemometer.

2 Observations of Snow Accumulations

2.1 Photometric Scanning

The snow accumulation pattern around the cube has been measured by photogrammetric processing of digital images which generated a 3D mesh. The digital images are processed using Agisoft Photoscan. According to Chiba and Thiis (Chiba and Thiis, 2016) it's necessary to have an overlap of 60% of each photograph, a large number of pixels (quality), and close distance. The accuracy is strongly affected by the weather conditions on-site. Depending on sunny or cloudy weather conditions, the mesh quality was increasing with light conditions. For some observations, the contrast of the snow surface and pattern was not strong enough in the digital images to generate a sufficient 3D mesh when it was cloudy. The photogrammetric process enables collecting millions of points over the surface of an object, which can be compiled into a point cloud. In order to optimize the processing time of the computer the generated mesh surface was reduced to 800.000 faces. This fastens the further processing with third-party software. The 3D spatial data is not in scale and has to be scaled in the software by setting a reference, which here has been the 10 cm marks at the Nuuk cube (see in Figure 2).

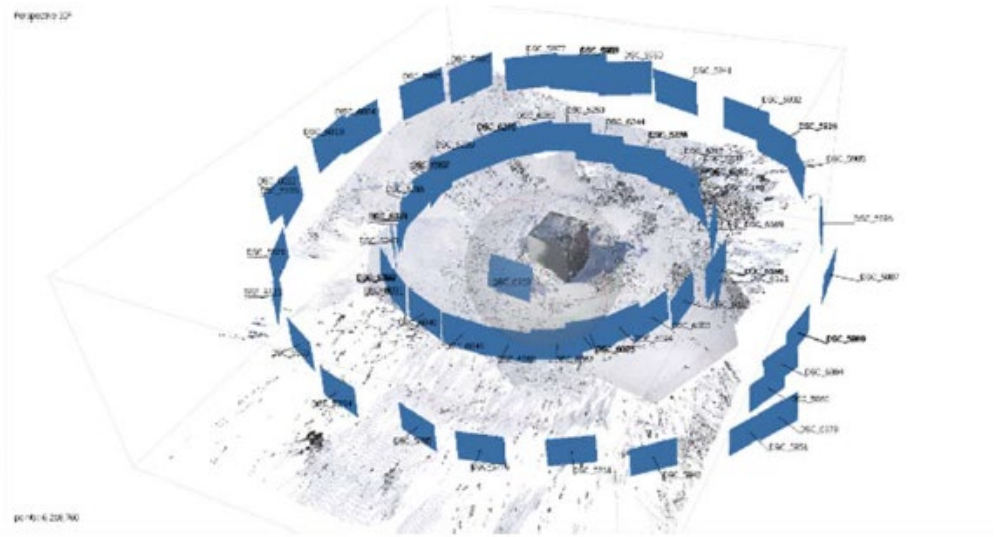

Fig. 5. Illustration of procedure for photometric measurement of snow accumulation around the cube, seen from southeast (SE). Pictures are taken along a perimeter at 3m and at 5m distance and transformed into a 3D spatial data (sequence of pictures taken on April 2, 2020, ID 26)

Actual photo of the snow accumulation around cube seen from SE (ID 26)

Rendering of digital model of snow accumulation seen from SE (ID 26)

Fig. 6. Comparison of the captured information through photometric scanning of snow accumulation with the actual snow in the left photo and the reconstruction to the right (ID 26).

Because the photogrammetry method can be performed with just a hand-held camera, a simplified setup was possible. This method gives more flexibility and easy access to the observed object. The advantage of using the photogrammetry method is no stationary configuration was needed to ensure a record of a variety of snow formations after a snow event. When a significant snow event occurred the owner of the house would inform about changes on the object cube. Even though the weather recordings are continuous throughout the winter season, the photo documentation of the snow accumulation has only been performed for individual days. During the period in between these days, accumulated snow at the cube might be altered due to drift, air temperature, and solar radiation. This alteration might be reconstructed to a certain degree by using the weather data but need to be considered speculative. Nevertheless, this configuration allowed more detailed documentation of the

snow accumulation shape and height than a stationary camera observation. Other than conventional methods, this method processed the accumulation shape and features in the most detailed way.

Additionally allows this method to compare snow accumulation with a 3D scan object of a wind tunnel model study. The advantage of the Nuuk-cube experiment is continuous access to the test site for observation, maintenance data recording, and internet uplink and with that a direct correlation between weather history and accumulation pattern development. The 3D generated mesh surface of the snow accumulations was compared to a reference mesh without any snow cover. In the surface comparison, the snow distribution and depth around the cube were measured and visualized as a color map. Then a surface deviation analysis was carried out in GOM Inspect Suite software which compares the differences between two surfaces. For the difference in height at the reference surface, we are comparing the Z coordinate to measure the snow depth. “In principle, the surface comparison calculates a deviation for each point of the used mesh in relation to the surface” (Schafmeister and Eberhardt, 2019). Table 2 gives an overview of the periods of continuous weather data recordings (NCE ID), the dates of snow accumulation photo documentation, and whether deviation analysis was carried out or not.

2.2 Wind Field around a floor-mounted Cube

A basic description of the flow field around a floor-mounted cube allows relating the observed snow accumulation pattern to past weather conditions, especially to wind speed and direction. For a cube two relative wind direction are of interest: wind approaching normal to one of its sides (incident angle $\varphi = 0°$) and a direction right on its corner ($\varphi = 45°$). Both cases create distinct flow patterns with zones highly exposed or sheltered from the airflow moving around the cube. The main flow features are illustrated in Fig. 7. The flow at 0° creates a strong vortex circulating in front of the cube and rotating towards the sides and is typically the driving mechanism for a wind scoop. This flow regime disappears for 45° but still high flow speeds can be expected near the edges of the cube.

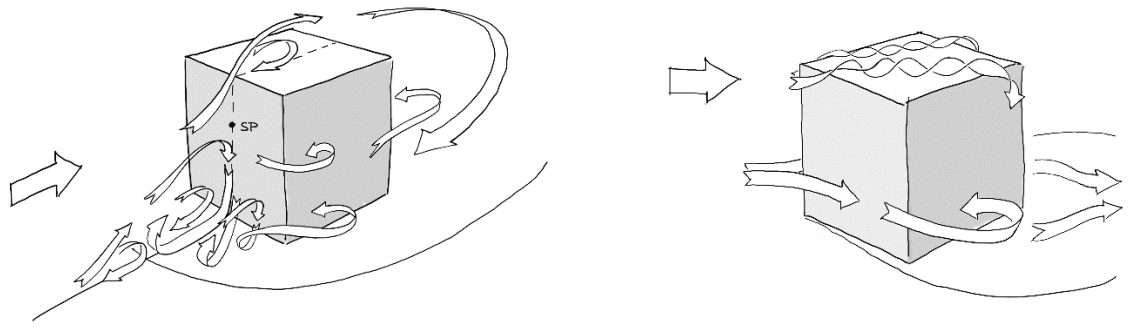

0° (south-easterly directions) 45° (northern directions)

Fig. 7. Anatomy of flow field structure around a floor-mounted cube for a wind direction normal to one of its sides. Drawing is based on flow visualization on a cube in the closed-circuit boundary-layer wind tunnel at DTU Construct.

2.3 Typical accumulation Pattern

Throughout the four winter seasons, the most frequently observed accumulation pattern is illustrated in Fig. 8. These patterns are because of their shape generally referred to as "kidney wind scoops" and consist of 'erosion' areas, usually located in zone of high local ground-near wind speed, and 'deposition' areas in zones sheltered from the wind flow around the cube. The pattern as such is defined by geometrical isopleths, which can be associated to the occurrence of the threshold airspeed for snow ground transportation or erosion ($U_{Th_{P1}}$, $U_{Th_{P2}}$, $U_{Th_{P3}}$) reaching down to different depths of the surrounding (otherwise undisturbed) snow layer dominated by the overall flow field as described in Fig. 7.

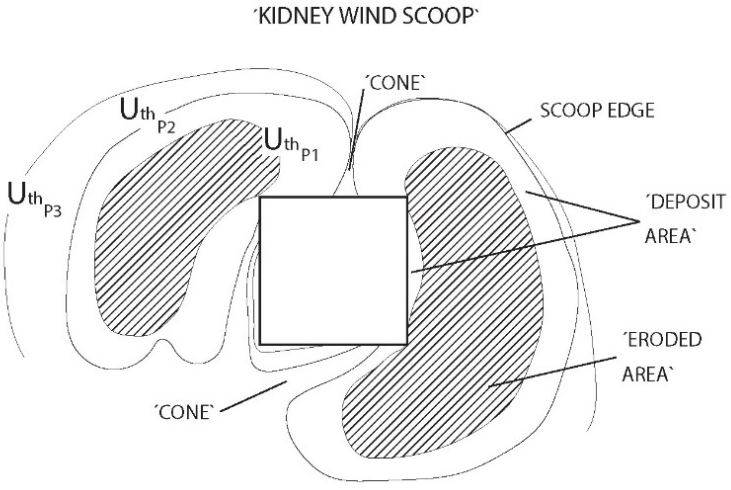

Fig. 8. Typical observation of snow accumulation patterns throughout the NCE Field Experiment. The typical feature are the areas with little or almost no snow accumulation in the zones exposed to high ground-near wind speeds. Accumulation appears in zones sheltered from the wind flow around the cube. The geometry of the pattern is described by isopleths.

A close relation of wind direction, resulting wind field and wind scoop geometry would suggests that the accumulation pattern responds (almost) immediately to the prevailing wind condition. Hence, such constant re-arrangement of snow deposition would indicate a low mechanical resistance towards the shear forces created by the wind flow on the snow surface. This would extent also to the inner structure of the snow layer since it could be 'dug out' by the wind. Even though the snow layer was not characterized throughout the observation months, it is unlikely to assume that periods of with air temperature significantly above 0°C or high sun radiation would not lead to some kind of solidification of the snow surface or inner stratification structure of hardened snow or ice.

In the following, the snow accumulation patterns in the five observation periods (Table 2) are discussed. The documentation and illustration may vary from case to case depending on the quality of the obtained image and data quality.

2.4 Observation Period 1 (Obs1)

The first measurement period is over a short observation period of only three days. The main weather data, i.e. wind speed and direction, precipitation, air temperature and relative humidity, as well as sun ration, surrounding the observations in this period are shown in Fig. 10. To relate the observed accumulation patterns to the past weather, the graph of the local wind speed includes a lower threshold wind speed of 3m/s for ground transportation of snow and a corresponding mean range for transportation between 6 and 8m/s measured at cube height at the nearby weather station (Fiebig and Koss, 2023).

The weather conditions in the first period show powdery snow conditions with cold air temperatures below -2 ~ -10 C°. The high humidity range up to 90% and the very cold temperatures let the snow be highly driftable. The low wind speed between ID2 and ID3 suggests no or very little snowdrift, whereas between ID3 and ID4 the wind speed reaches the average threshold for transportation and some effect can be expected. The time between these scans are only about four hours but some effect on the accumulation pattern could be observed. **Fig. 9** shows the morphology of the snow surface surrounding the cube of scan ID3 and ID4 together with corresponding photos of the snow cover in direct comparison. The overall characteristic of the accumulation pattern influenced by the flow field around the cube seem to remain but gets more pronounced due to the prevailing transportation process.

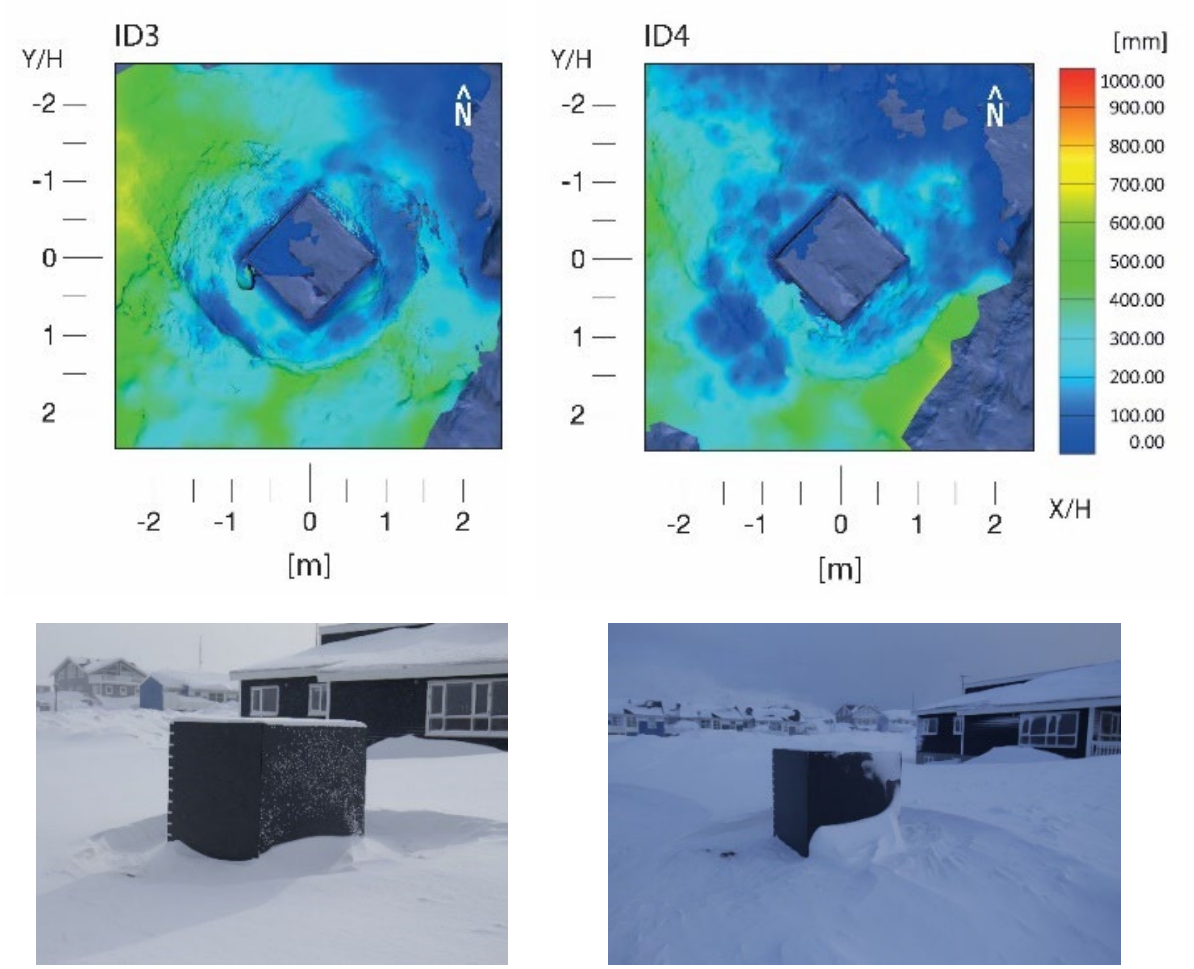

Fig. 9. Morphology of the snow surface surrounding the Nuuk Cube based on the numerical model from the photometric measurement ID3 and ID4 (upper row). Below, corresponding pictures of the snow cover and accumulation are shown.

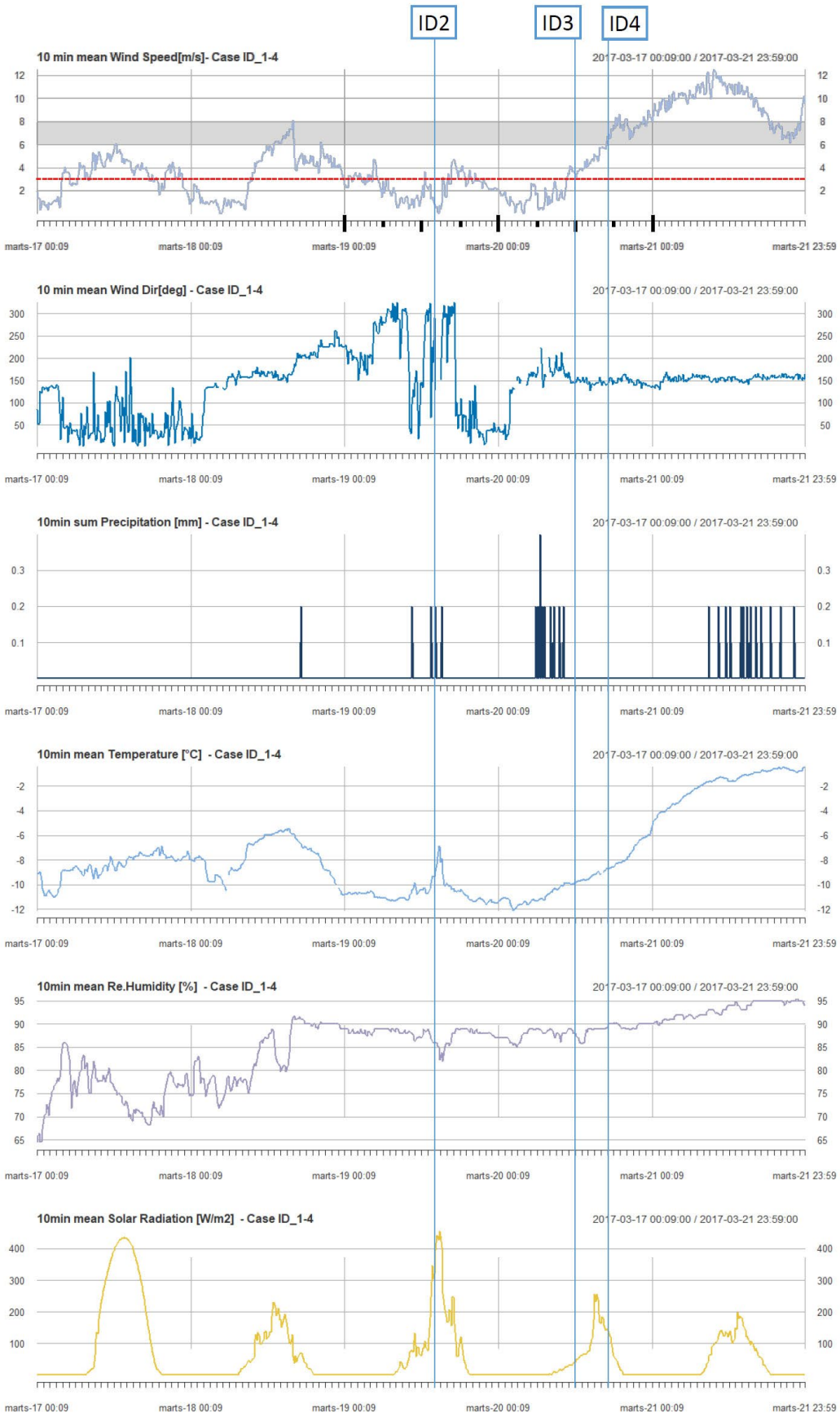

Fig. 10. Main weather data surrounding the observation period Obs1 including the scan ID 2, 3, and 4.

2.5 Observation Period 2 (Obs2)

In March 2018 was a low snowfall period. Within the measurement period, no fresh snowfall event occurred. This period is dominated by very unusual high temperatures with over + 5 C° at first and following with a rapidly falling temperature to – 10 C° (Fig. 12). Nevertheless, did the snow cover not melt fully, as shown in Fig. 11, hence his period was most likely a high sublimation (direct transition from solid to vapor) month and the snowpack temperatures were most likely colder than air temperatures.

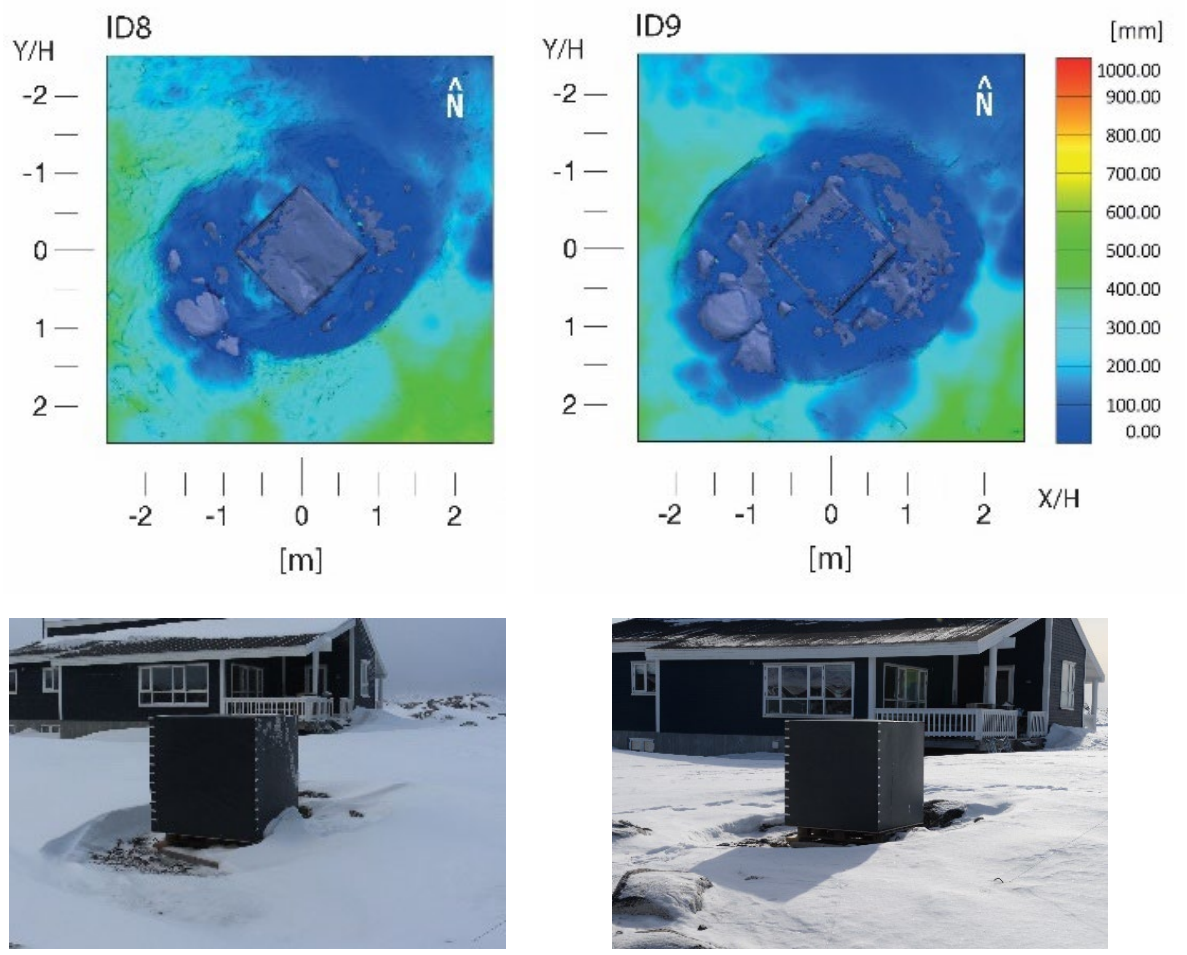

Fig. 11. Morphology of the snow surface surrounding the Nuuk Cube based on the numerical model from the photometric measurement ID8 and ID9 in the second observation period (upper row). Pictures of the corresponding snow cover and accumulation are shown below.

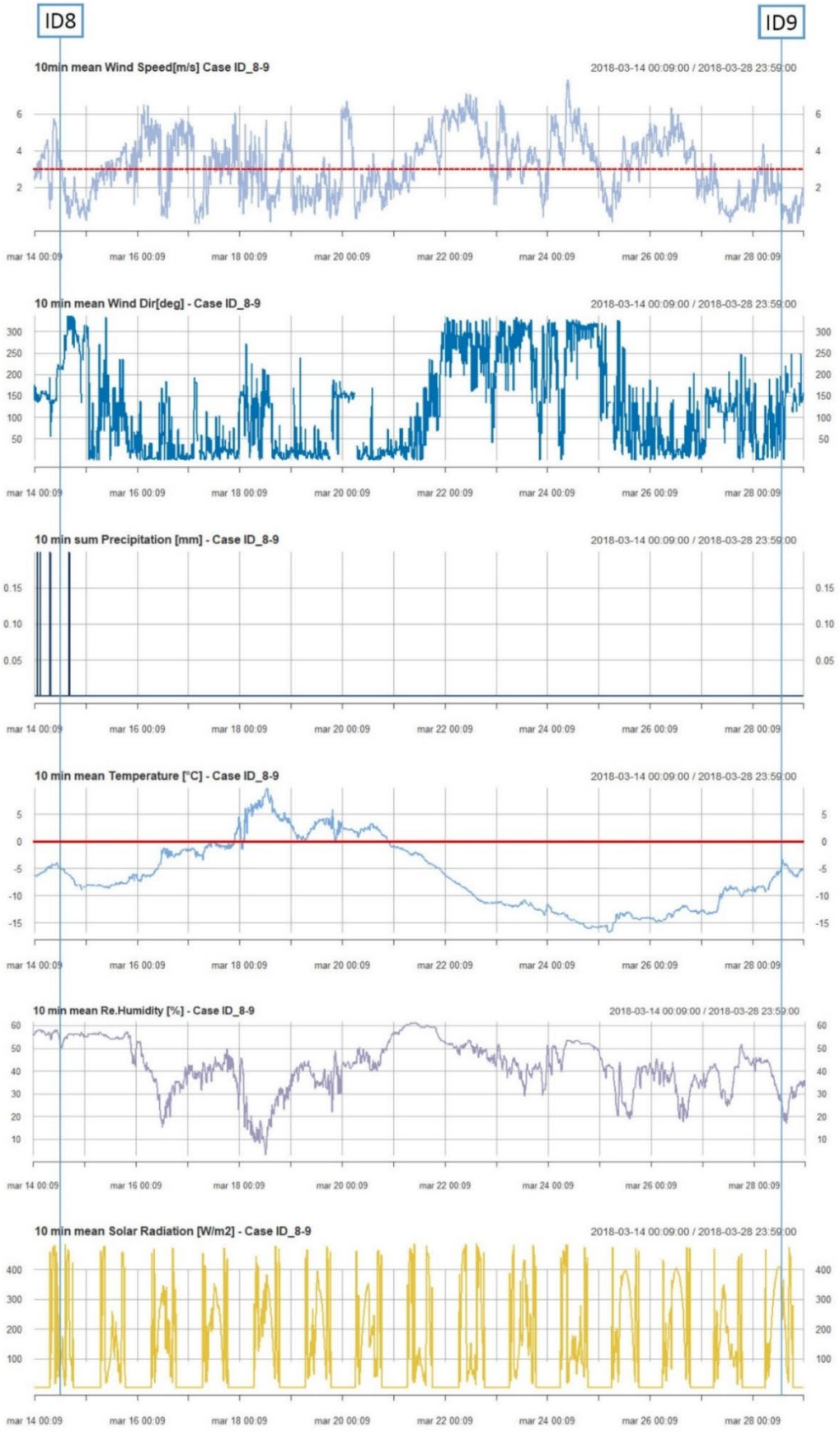

Fig. 12. Main weather data surrounding the observation period Obs2 including the scan ID 8 and 9.

2.6 Observation Period 3 (Obs3)

A multi-variant of climatic conditions periods of low and high snowfall amounts was observed for the 3rd observation period. The month started with a unidirectional wind event with strong winds from the Northeast and followed with a heavy snowfall event from the southeast in a multidirectional storm (Fig. 14). Hereafter smaller snow events occurred from southeast to south and on non-precipitation days northerly prevailing winds were recorded. “Snow-roller”, a meteorological rare phenomenon was observed within the recording period. In which cylindrical snowballs are formed by strong enough wind but not strong enough to drift the snow particles on the ground. They get blown along the surface and pick up further snow along the way. The records show a snowfall event with 2.6 (mm) precipitation and the most frequent wind direction from south-southeast with fluctuating wind directions with up to 45 degrees. A noticeable rapid increase in air temperature over the melting point and the high humidity dominated this event. The wind speed did occasionally exceed the threshold speed of 6m/s initiating wet heavy fresh snow to roll over the surface. Because of the temporary temperature increase, the snowpack surface went to solidification and remained its surface structure. Fig. 13 shows the snow surface scans at the beginning and end of this period (ID13 and ID18) demonstrating the largest difference between the observed accumulation patterns.

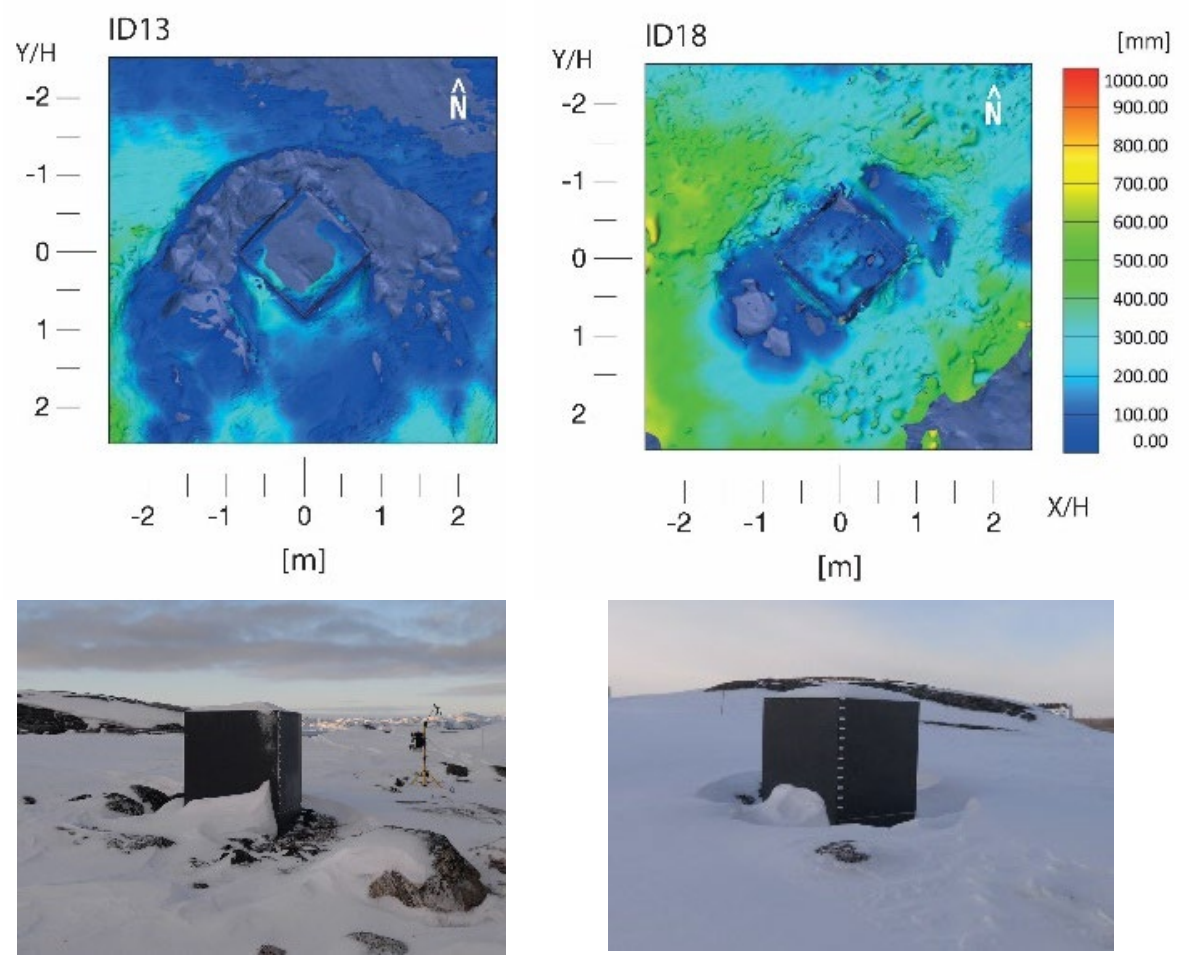

Fig. 13. Morphology of the snow surface surrounding the Nuuk Cube based on the numerical model from the photometric measurement ID13 and ID18 in the third observation period (upper row). Pictures of the corresponding snow cover and accumulation are shown below.

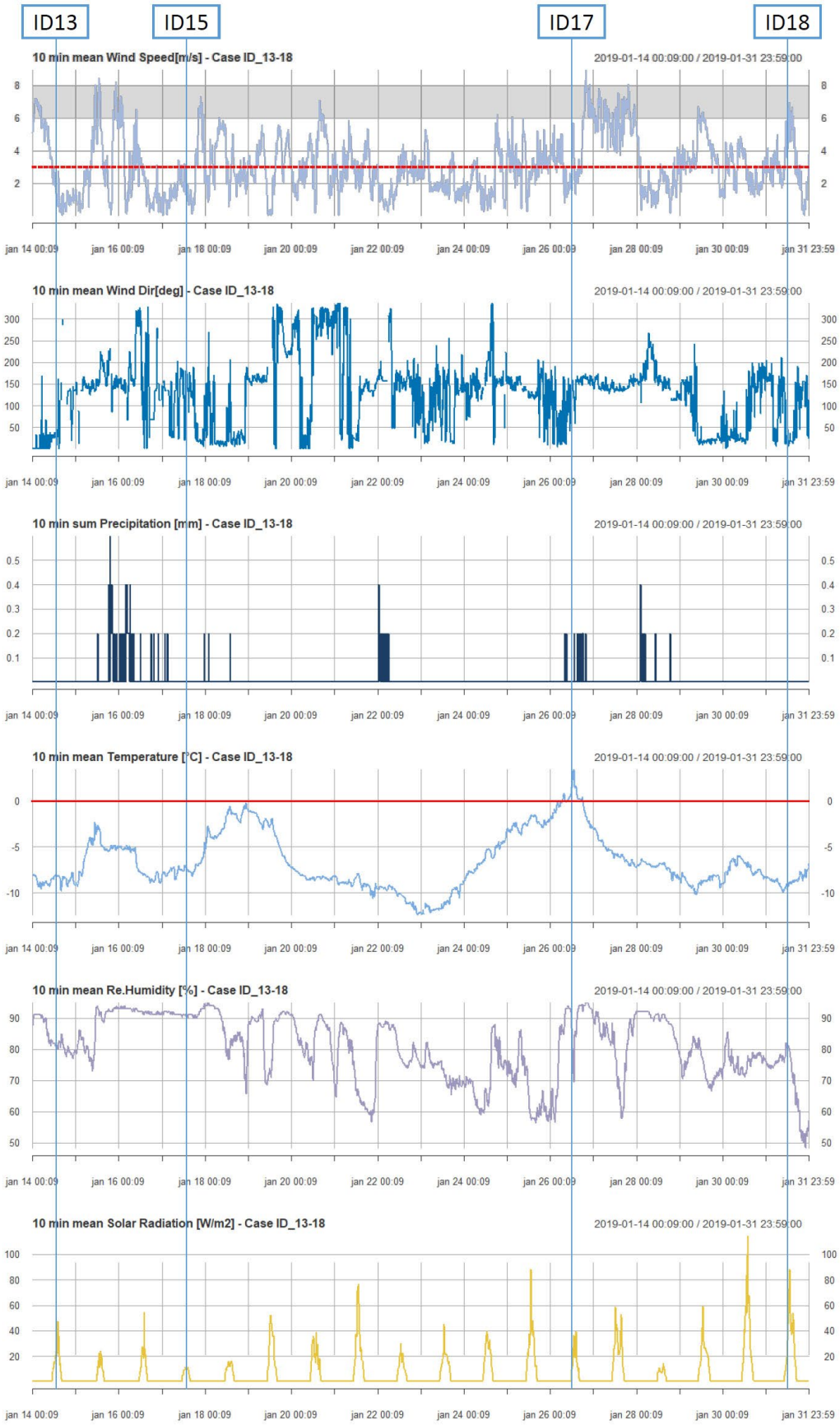

Fig. 14. Main weather data surrounding the observation period Obs3 including the scan ID 13, 15, 17, and 18.

2.7 Observation Period 4 (Obs4)

In observation period four the snow pattern remains approx. the same in shape and reduces gradually in height due to melting and sublimation processes of very high air temperatures > 5C° and low air humidity (Fig. 16). Heavy snowfall events occurred with temperatures over the melting point (> 0 C°). Blowing snowfall ranged from East to Southwest wind directions and fluctuates largely but due to the solidification of the snow cover surface, the snow pattern remained the same even with higher wind speeds > 10m/s. Very cold winds from the northeast prevailing at the beginning of the campaign created a thin hard snowpack surface. The accumulation cone at the windward wall of the cube was hard at the top layer and right underneath, shallow (Fig. 15). In the Arctic and sub-arctic regions, those properties are common to find, often the snow crystal classification is dominated by wind slab and depth hoar or fresh to fine-grained snow particles (Pomeroy and Brun, 1990). At the end of this campaign, a severe snowfall was recorded with up to 79.8 (mm) for over 3 days with strong winds from southeast and multiple directions on the second day of the snowfall. The snowfall event occurred at warm air temperatures, creating adhesive snowflakes accumulating at the south corner of the object cube. The very high humidity suppressed the melting or sublimation of snow. Fig. 15 shows the accumulation patterns of scan ID21 and ID22 (ID20 is very similar to ID22 and hence not shown here). Both are characterized by stronger winds from northern directions resulting in similar accumulation patters. The effect from high air temperature shown in ID22 through a more pronounced wind scoop around the cube.

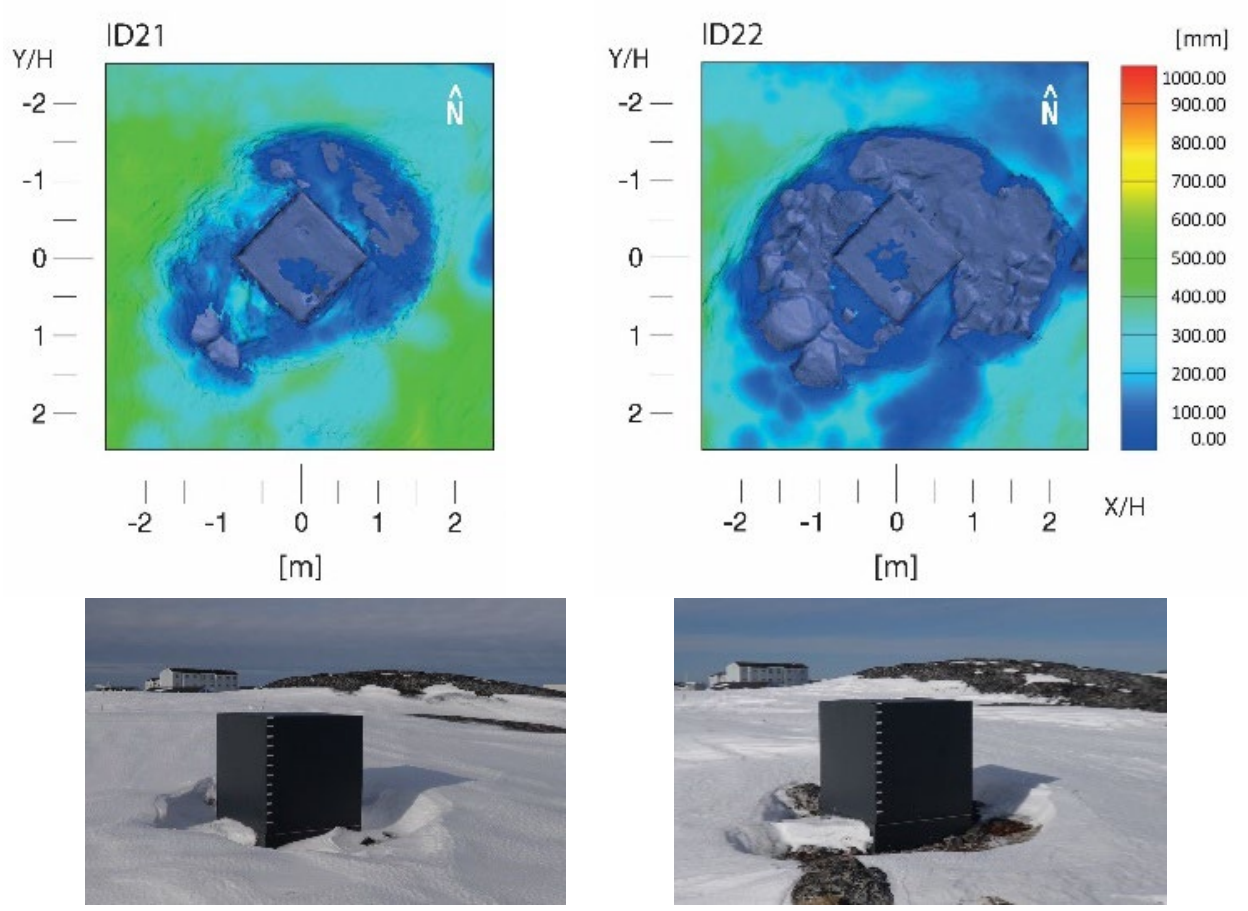

Fig. 15. Morphology of the snow surface surrounding the Nuuk Cube based on the numerical model from the photometric measurement ID21 and ID22 in the 4th observation period (upper row). Pictures of the corresponding snow cover and accumulation are shown below.

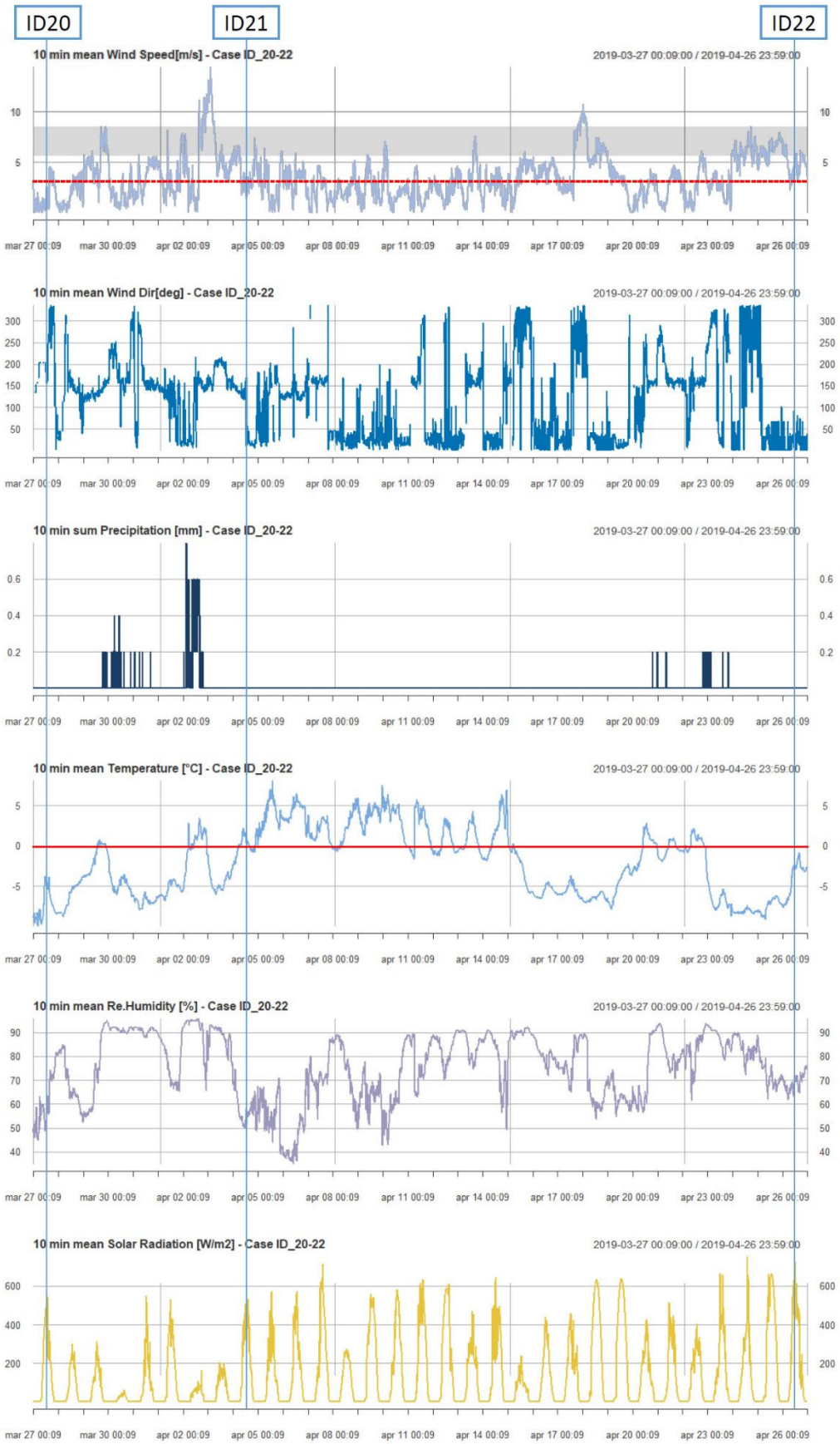

Fig. 16. Main weather data surrounding the observation period Obs4 including the scan ID 20, 21, and 22.

2.8 Observation Period 5 (Obs5)

Fig. 17 shows the accumulation patterns in the 5th observation period. Between all scan shifting winds between northern and southern direction dominate the accumulation process.

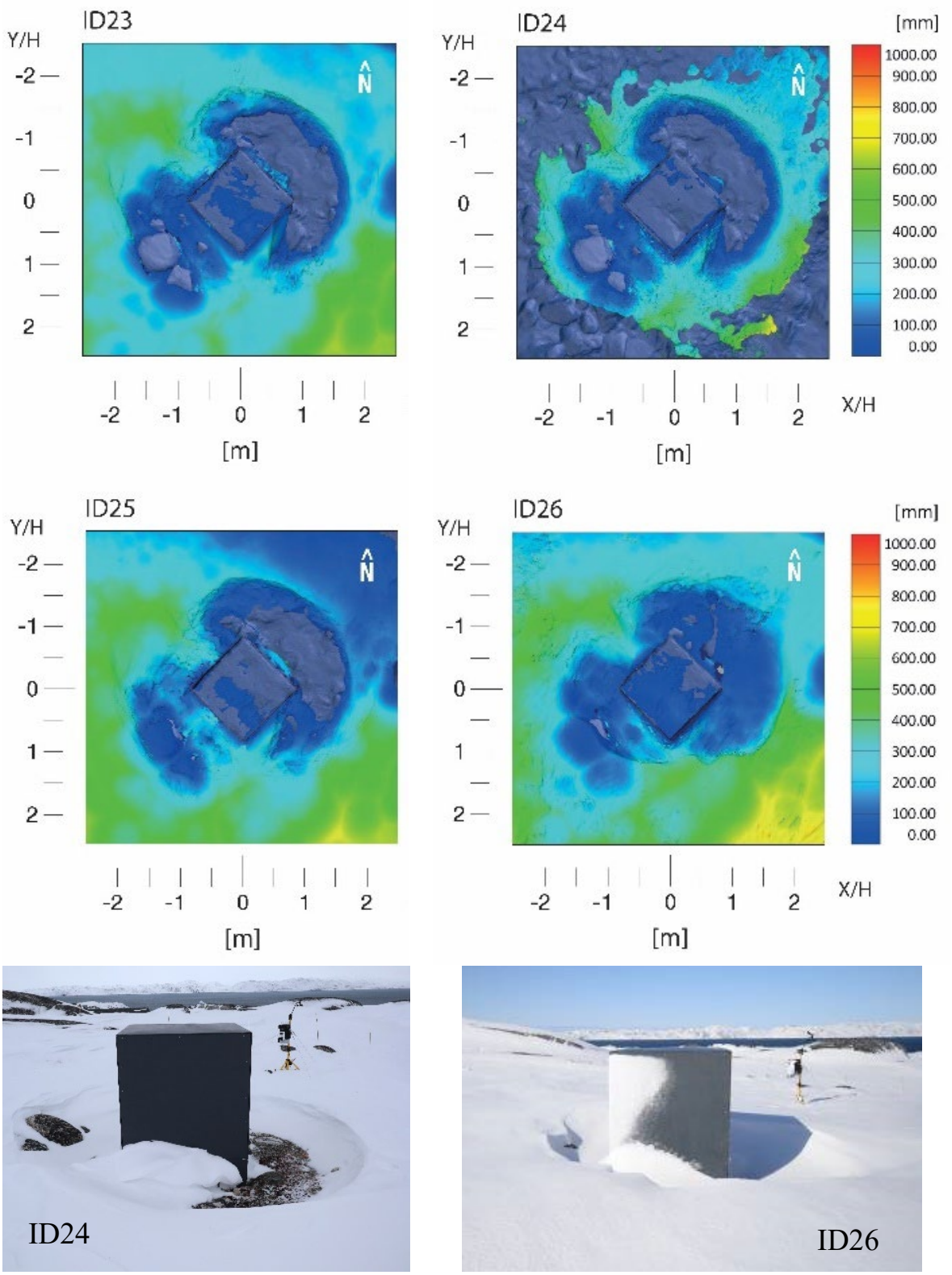

Fig. 17. Comparison of the snow surface morphology arround the Nuuk Cube based on the scans ID23 to ID26 in the 5th observation period. Pictures of the corresponding snow cover for ID24 and ID26 and accumulation are shown in the lower row. 1,1

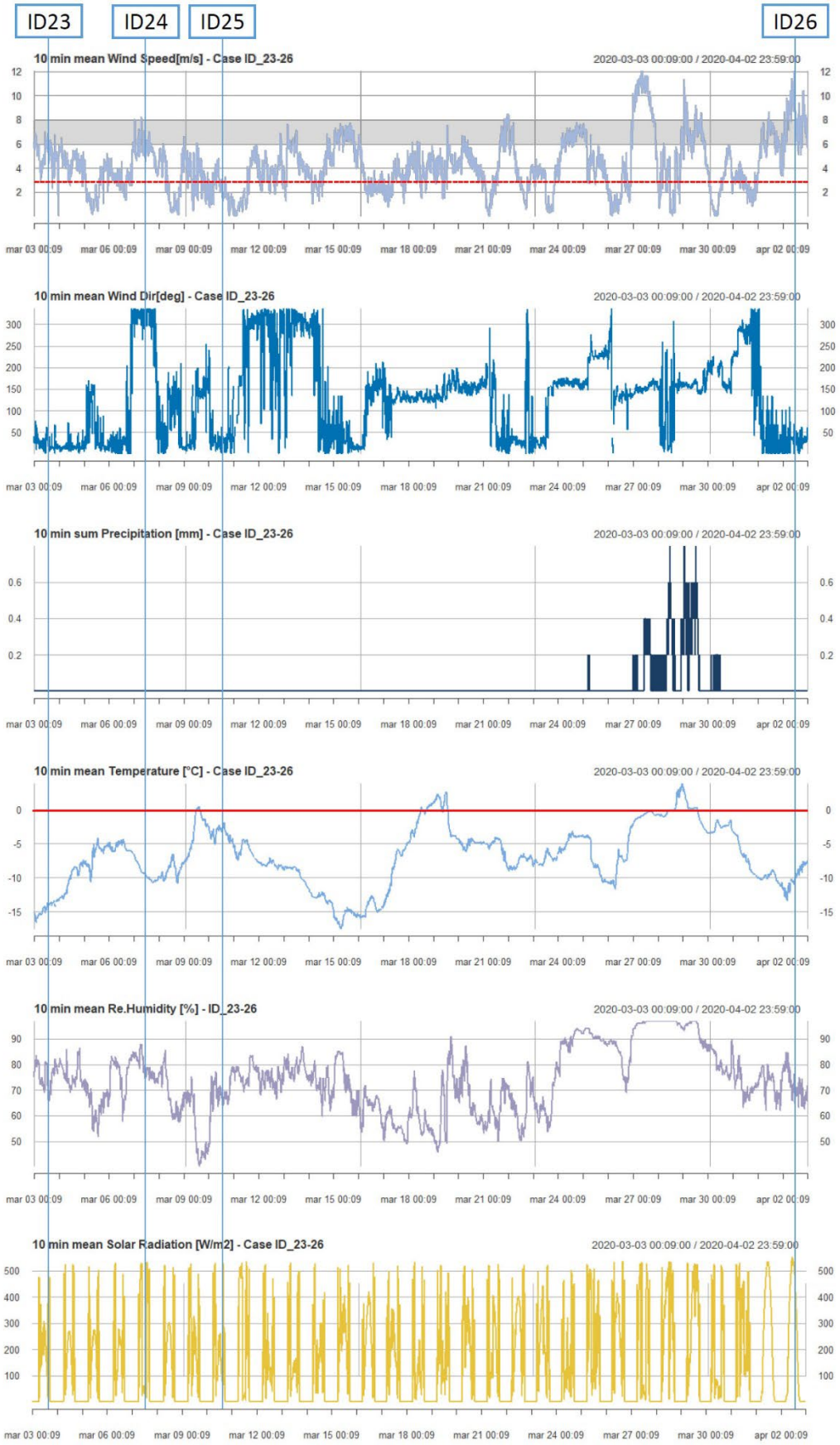

Fig. 18. Main weather data surrounding the observation period Obs5 including the scan ID 23, 24, 25, and 26.

The comparison of the accumulation patters from these four scans show a strong similarity (outer surface in scan ID24 is incomplete but similar snow covers as shown in the other scans can be assumed). However, the photos of ID24 and ID26 illustrate the influence from the shifting wind directions. ID24 shows accumulation in the lee zone (SE/SW sides of the cube) for northern wind directions with a clear scoop on the upwind side of the cube. 25 days later and with a recent significant snowfall under stronger winds from southern directions, the clear area on the northers side (previous upstream side) of the cube is now in the lee zone and slightly covered with snow. The scoop on the southern side of the cube is more pronounced but the accumulation directly at the base of the southern edge is still showing the accumulation seen in ID24. This is a typical example for superposition of single-direction accumulation patterns.

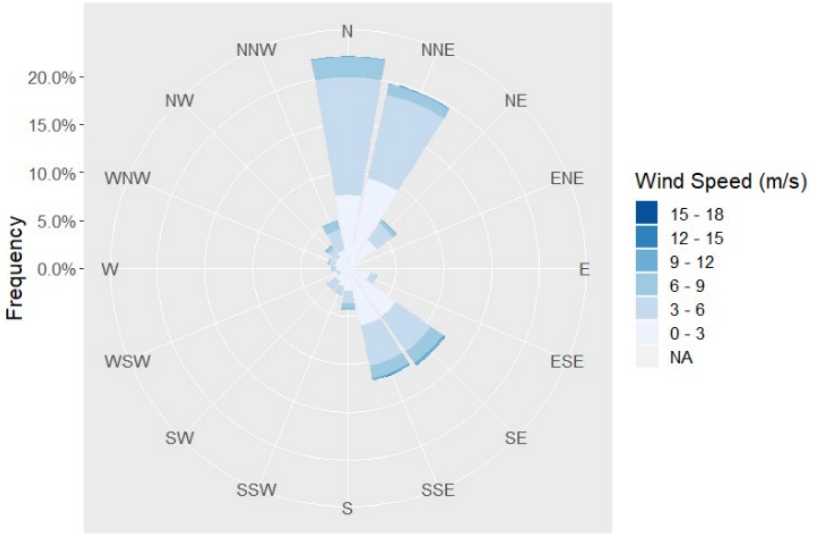

Fig. 19. Distribution of wind speeds and directions recorded in all observation periods.

In general it was observed throughout all winter seasons, that the influence of the flow field around the cube on the snow accumulation pattern in combination with changing wind directions and air temperatures, lead at the end to a wind scoop area extending one cube height H from the cube's walls. Even though the cube is mainly exposed to two wind directions (Fig. 19), the influence of the wake zone behind the cube as reported in the studies listed in Table 1 does not appear in the observation of the Nuuk Cube field study. All features with respect to snow coop and accumulation occur practically within 1H distance from the cube's wall (cube perimeter).

3 Summary and Conclusions

The snow pattern around a 1.2m cube was observed as the result of a continuous exposure to snowfall and ground transportation in four Arctic wind season. The accumulation was documented through photographs and photometric scanning providing data for a numerical 3D model of the snow surface at the time. The observations are grouped into five periods. Main aspect was to obtain knowledge on a continuous snow accumulation process in terms of resulting patterns and magnitude and as well on the effect of changing wind direction on the snow deposition and erosion. Following conclusions can be made:

- The cube was at no time during the observation period covered with snow or even significantly immersed even though the surrounding snow surface came up to about 30% of the cube's height.
- Furthermore, the snow accumulation does not grow to an extreme. In this sense, uni-directional study may be conservative but they do not reflect the superposition from different wind directions. Here, a clear scoop on all sides of the cube can appear as a result from changing wind directions. This suggests that deposition in the lee zone is a weaker process and can be suppressed or removed by the upstream flow field characterised by the stagnation pressure on the cube front side.
- The re-arrangement of ground snow and the accumulation of falling snow under the conditions of changing wind directions and velocities lead to an area around the cube where transport phenomena influenced by the presence of the cube appear within a distance of approximately 1H. The superposition of directional processes removes any effect of the wake flow on the accumulation process leaving the nearby flow field around the cube as the main or dominating driving mechanism for snow accumulation.
- Many accumulation patterns resemble uni-directional pattern even after changing or counter-directional wind directions. Hence, the re-arrangement of snow due to wind is erosion dominated. This applies to some degree as well to older snow layers exposed to plus temperatures and longer periods of intense sun radiation.

A particular observation was that at no time notable accumulation of snow appeared on the top (roof) of the cube. This matches as well observations on even larger flat-roof buildings in Greenland. This differs from observations in the Alpine region, where large amount of snow accumulates on

building roof. This may have something to do with the snow properties under precipitation. In the far future, influence from climate change As discussed in the analysis of the meteorological observations of the Nuuk Cube Experiment (Fiebig and Koss, 2023), a change in the precipitation characteristic of snow due to climate change can affect the observed accumulation in Greenland and in the Arctic in general. For example, an increased frequency of rain-on-snow (ROS) events might influence the accumulation pattern and the resulting weight of the snow at the same time both with consequences to the snow load to be considered.

Acknowledgement

The authors would like to thank architect Peter Barfoed for allowing us using his private home for setting up the data acquisition computer of the weather station and for the support in surveying snow accumulation around the cube.

References

Anno, Y., 1985. Modelling a snowdrift by means of activated clay particles. Ann. Glaciol. 6, 48–52.

Beyers, J.H.M., Harms, T.M., 2003. Outdoors modelling of snowdrift at SANAE IV Research Station, Antarctica. J. Wind Eng. Ind. Aerodyn. 91, 551–569. https://doi.org/10.1016/S0167-6105(02)00409-9

Beyers, J.H.M., Sundsbø, P.A., Harms, T.M., 2004. Numerical simulation of three-dimensional, transient snow drifting around a cube. J. Wind Eng. Ind. Aerodyn. 92, 725–747. https://doi.org/10.1016/j.jweia.2004.03.011

Chiba, T., Thiis, T., 2016. Accuracy of Snow Depth Measurements on Roofs measured with Photogrammetry. Proc. 8th Int. Conf. Snow Eng. 2, 337–341.

Fiebig, J., Koss, H.H., 2023. *Nuuk Cube Field Experiment – Part 1: Meteorological Observations*. Prepared for publication in Journal for Cold Regions Science and Technology.

Haehnel, R.B., Lever, J.H., 1997. Field measurements of snowdrift development rate, in: Proccedings of the Western Snow Conference 1997. pp. 1–7.

Haehnel, R.B., Wilkinson, J.H., Lever, J.H., 1993. Snowdrift Modeling in the CRREL Wind Tunnel, in: 61st Western Snow Conference. Quebec City, pp. 139–147.

K.C.S. Kwok, D.H. Kim, D. J. Smedley, H.F. Rohde, 1992. Snowdrift around buildings for antarctic environment. J. Wind Eng. Ind. Aerodyn. 41–44, 2797–2808. https://doi.org/10.1017/CBO9781107415324.004

Li, L., Pomeroy, J.W., 1997. Estimates of Threshold Wind Speeds for Snow Transport Using Meteorological Data. J. Appl. Meteorol. 36, 205–213. https://doi.org/10.1175/1520-0450(1997)036<0205:EOTWSF>2.0.CO;2

Liu, M., Zhang, Q., Fan, F., Shen, S., 2018. Experiments on natural snow distribution around simplified building models based on open air snow-wind combined experimental facility. J. Wind Eng. Ind. Aerodyn. 173, 1–13. https://doi.org/10.1016/j.jweia.2017.12.010

Matha, F.D.A., Anna, S., Taylor, D.A., 1990. SNOW DRIFTS ON FLAT ROOFS: WIND TUNNEL TESTS AND FIELD MEASUREMENTS. J. Wind Eng. Ind. Aerodyn. 34, 223–250.

Naaim-Bouvet, F., Naaim, M., Micheax, J.-L., 2002. Snow fences on slopes at high wind speed: physical modelling in the CSTB cold wind tunnel. Natural Hazards and Earth System Sciences, Vol.3/4, pp.137-145

N.Isyumov, M.Mikitiuk, 1997. Wind tunnel model studies of roof snow loads resulting from multiple snowstorms, in: Masanori Izumi, Tsutomu Nakamura, R.L.S. (Ed.), Snow Engineering: Recent Advances. Balkema, Rotterdam.

Oikawa, S., Tomabechi, T., 2000. Daily observation of snowdrifts around a model cube. Snow Eng. 2000 Recent Adv. Dev. 137–141. https://doi.org/10.1201/9780203739532

Pomeroy, J.W.W., Brun, E., 1990. Physical Properties of Snow. Snow Ecol. An Interdiscip. Exam. Snow-Covered Ecosyst. 97, 45–126.

Schafmeister, R., Eberhardt, P.R., 2019. KNOWLEDGE:Principles of the Surface deviationPrinciples of the Surface deviation.

Senese, A., Maugeri, M., Vuillermoz, E., Smiraglia, C., Diolaiuti, G., 2014. Using daily air temperature thresholds to evaluate snow melting occurrence and amount on Alpine glaciers by T-index models: The case study of the Forni Glacier (Italy). Cryosphere 8, 1921–1933. https://doi.org/10.5194/tc-8-1921-2014

Suzuya, J., Uematsut, Y., & Nozawa, T., 1993. Wind Effects on Snow Accumulation on a Flat Roof, in: Second International Conference on Snow Engineering. pp. 105–116.

Thiis, T.K., 2003. Large scale studies of development of snowdrifts around buildings. J. Wind Eng. Ind. Aerodyn. 91, 829–839. https://doi.org/10.1016/S0167-6105(02)00474-9

C Nuuk Cube Experiment – Wind Tunnel Experiment: Wind tunnel simulations of snow accumulation around buildings

Nuuk Cube Field Experiment – Part 3: Snow accumulation around Buildings

Jennifer Fiebig, H. Holger H. Koss
Technical University of Denmark; Department of Civil Engineering, Section of Structures and Safety
jenfi@byg.dtu.dk; hko@byg.dtu.dk

Abstract— The phenomenon of wind-driven snow is a significant challenge for the built environment in cold climate regions and approaches for its consideration in urban and building design varies considerably. For wind tunnel studies of snow precipitation, drift and accumulation the question of similarity hinges on three main aspects: flow field similarity relating to the proper modelling of the atmospheric boundary layer and the airflow around and between objects, the motion of the substitutional material particles while airborne, and the adhesive behaviour of the particles to the surfaces of terrain and buildings models as well as to each other. For modelling the wind flow and airborne particle motion standard similarity rules in wind tunnel testing can be applied. Modelling the adhesive behaviour, however, is limited due to inadequate reflection of thermodynamic effects and transformation of snowflakes in nature. This deficiency is usually compensated by approximating the appearance of snow accumulation in nature through the right choice of substitutional material in the scaled experiment. Consequently, simulations using simplified particle models for snowdrift and accumulation studies rely substantially on a phenomenological similarity to observations in full-scale. This applies equally for both, experimental and numerical simulations. This paper examines the involved similarity considerations with particular focus on the phenomenological aspect. For this purpose, a 1.2m cube was installed in Nuuk, Greenland, to gather data and observations of snow accumulation during three consecutive arctic winters Nuuk Cube Field Experiment. Based on the comparison of experimental results to the field study, a developed simulation approach for snow accumulation in wind tunnel testing allows identifying critical building design situations on reduced scale models.

KEYWORDS: Snow, wind, snowdrift, snow accumulation, wind tunnel testing, arctic environments, scaling similarity, field experiment.

1. Introduction

In cold regions, wind-driven snow particles lead to complex snow accumulation on and around buildings. Unevenly distributed snow formations frequently damage the supporting structure, reduce structural durability and affect indoor climate due to melting water, and consequently restrict the functionality of buildings. Wind tunnel testing is a proven method for simulating the airflow interaction of building structures and provides a suitable platform for investigating snow transportation and deposition to identify critical situations at the building design. In nature, snow transport can appear in the form of creep, saltation or suspension. In the creep layer, particles stay in contact with the ground and might just move within the layer. Saltation appears in a layer 0.10 m

to 1 m above the ground and suspension (aka. turbulent diffusion) from 10 m to 100 m (Figure 1). In the creep layer, particles stay in contact with the ground and might just move within the layer. First particle motion along the surface appears when wind speed exceeds a critical threshold value. Drifting begins when the surface shear stress exceeds the threshold value and particle starts hopping over the surface. Field data from literature estimated threshold wind speeds for snow transport for dry snow at 4 to 11 m/s and wet snow at 7 to 14 m/s (Li and Pomeroy, 1997). This depends on the size, shape, and density of the particle and its adhesion ability. In practice, wind tunnel tests with substitute materials are used to simulate snow accumulation. Similarity measures describe how true to nature the behaviour is, e.g. the simulation at a reduced scale. In recent years, much research has been done on similarity parameters such as geometry ratio, wind profile, particle motion and duration. However, testing with snow substitute materials does not allow full similarity due to the intrinsic difference to real snow (Anno, 1984; Kim et al., 1991; Kind, 1986; Naaim-Bouvet, 1995; Naaim-Bouvet and Naaim, 1998), especially regarding effects related to thermodynamic behavior. The similarity requirements contradict each other and compromises are inevitable. Dominant aspects of similarity are often chosen according to their relevance (Delpech et al., 1998; Kind, 1986, 1976). To obtain similarity of the snow mechanism similarity parameters in combination with full-scale observations are necessary when testing at a reduced scale. Mitsuhashi (Mitsuhashi, 1982) provides full-scale observations that have been used by others (Anno and Tomabechi, 1985; Kim et al., 1991) to control their wind tunnel study. Since the lack of sufficiently documented snowdrift and accumulation cases in full-scale is an issue for ensuring proper scaling, an observation campaign on a 1.2m cube located in Nuuk, Greenland was started in 2017. The study emphasizes on the correlation of the observed snow accumulation on and around the cube with directly on-site measured weather data such as wind speed and direction, air temperature, relative humidity, solar radiation, and precipitation. The collected data gives an insight into the process of snow accumulation around a generic object throughout an arctic winter. The obtained data serves to evaluate the empirical similarity of the experimental simulation used for snow studies in arctic developed and urbanized areas.

In wind tunnel studies snowdrift is frequently simulated through erosion and accumulation of a pre-applied uniform layer of substitute material. It is furthermore assumed that the effect of airborne snow is covered by particles entering the suspension layer during the erosion transport process. This, as a good approximation for snow transport in stronger wind events, may be insufficient for snow events in combination with low or moderate wind speed. This paper presents an experimental

method to simulate the phenomenon of a snowdrift in a boundary-layer wind tunnel at a reduced scale with a heavy emphasis on the phenomenological similarity to a comprehensive full-scale observation in Nuuk, Greenland. For practical application in snow accumulation studies, a design test case was developed in a previous study (Fiebig, 2023) to identify critical situations for building design and arctic city planning. Field tests of an object cube in Nuuk city in Greenland − the Nuuk Cube field experiment (Fiebig & Koss, 2023a, 2023b) revealed information regarding arctic winter weather conditions to suggest a test case scenario that allows investigating snow accumulation around buildings. Results of a series of wind tunnel tests carried out to test snow accumulation in different typical urban building pattern, are presented.

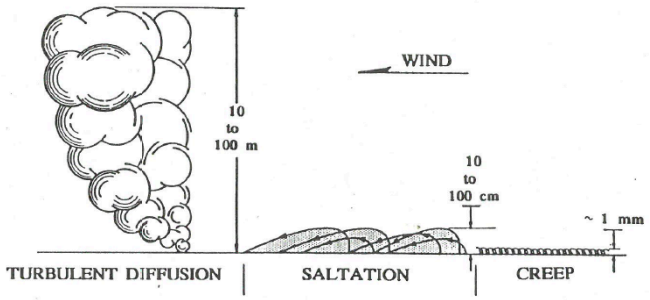

Figure 1 Drawing of three modes of transport for blown snow from (Mellor, 1965)

2. Wind tunnel simulation

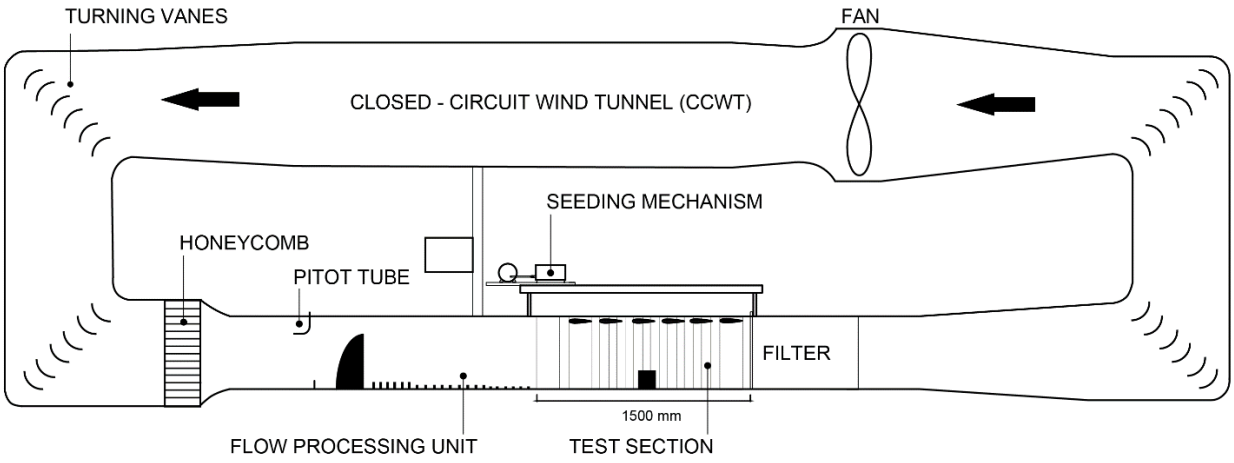

Figure 2 Closed-circuit wind tunnel (CCWT) with a retrofitted configuration for snowdrift simulations

Figure 2 shows the overall layout of the closed-circuit boundary layer wind tunnel at DTU Civil Engineering with the integrated experimental setup for snow studies. The open test section of the closed-circuit boundary-layer wind tunnel at DTU Civil Engineering is at walls and ceiling equipped with spaced wing profiles to be blockage tolerant (Kong and Parkinson, 1997) and with a digital-controlled seeding mechanism. For the generation of the turbulent boundary-layer a combination of Counihan random turbulence generators, wall barrier, and roughness fields have been installed in the flow-processing unit (FPU). Since at times very low airspeeds are applied, the flow velocity is controlled with a standard Pitot tube at the FPU entrance and a low-speed hot-wire probe (LSHW) at the entrance to the test section. To study the role of ground moving and airborne snow on accumulation characteristics, the seeding mechanism allows the controlled and repeatable release of substitute material into the test section (Figure 8). The test section has a cross-flow dimension of 0.48 x 0.48m and a length of 1.5m with blockage-tolerant walls. The wind tunnel air velocity is controlled at a reference height of 150 mm with a low-speed hot-wire anemometer (LSHW) upstream of particle release shown in Figure 4.

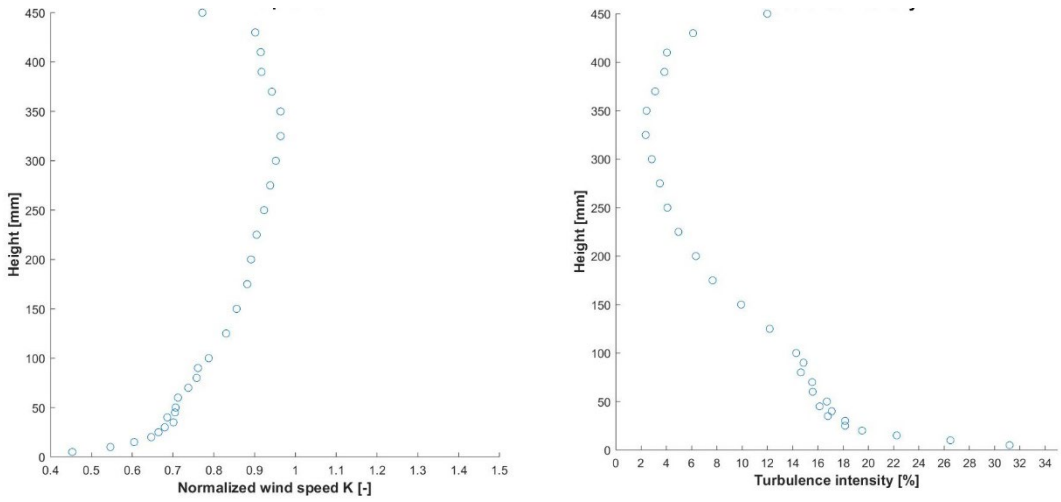

Figure 3 Measured mean wind speed profile and turbulence intensity in the Closed-circuit wind tunnel (CCWT).

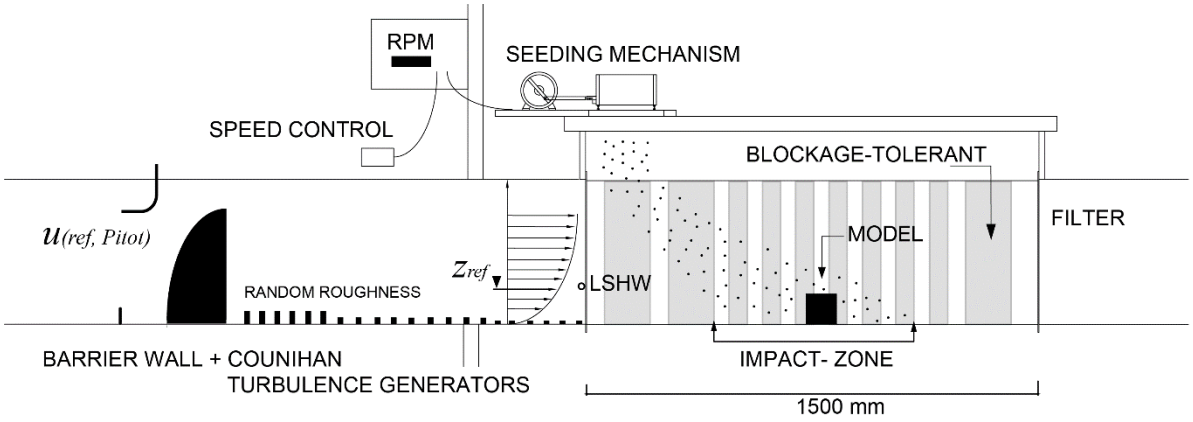

Figure 4 Wind tunnel test section with barrier wall 5 cm height and Counihan turbulence generators 6 cm width. Half-open test section (blockage-tolerant).

Model snow particle selection

The choice of the material used at the test facility of the boundary-layer wind tunnel at DTU was selected in accordance with its ability to perform a wind tunnel procedure that can simulate low speed dry snowfall events as well as wet high wind speed events in form of erosion, as identified in the Nuuk Cube Field Experiment (NCFE) (Fiebig & Koss, 2023a). As a consequence, Natron seemed to be a promising material to replicate the snowdrift phenomenon observed for the low-Arctic region. Natron showed high ability for erosion with a threshold speed at $U_{Th,Pitot}$ = 5,3 m/s (Fiebig, 2023) and a good angle of repose. Saw dust had similar good properties, but since the particle size was too large and the density too low, it could not show strong adhesion when applied (Fiebig, 2023).

Applying the similitude requirements from the specification tests of different substitute materials in earlier studies (Fiebig, 2023), the following assumption are made for the Nuuk Cube model simulation:

To determine the theoretical similarity parameters the prototype snow (nature snow) and model properties (substitute materials) for the snowdrift simulation are defined in Table 1. The max. daily mean wind velocity measured from the weather station in the NCFE in winter is $\overline{U}_{(1,4)}$= 7,3 [m/s]. In winter periods (October to April) the mean average pressure level was 1002.1 mb and the min. average temperature was - 6.6°C. Therefore is ρ_{a_P} = 1,31 [kg/m3]. At the time of the model experiment, the density was at ρ_{a_m} = 1,22 [kg/m3]. The threshold friction velocity is calculated with $U_t^* = A\sqrt{gD_p\,\rho_p/\rho_a}$ (Kind, 1990). Here A is an empirical constant of 0,11 (for sand 0,22, it might

vary for other spherical or granular materials) (Kind, 1990). $U^*_{t\,p} = 0{,}15$ refers in literature to a uncompacted dry snow (Kind, 1976). It should, however, be noted that this value differs depending on the climatic conditions of the full-scale observation. In this experiment, we chose an arctic heavy snow particle measured in Greenland (ρ_p = 600 [kg/m3]) to be more appropriate to the site-specific climate region. The similarity parameters for the model was calculated and the results are compared with the prototype snow in Table 2. The biggest mismatch of prototype and model is the similitude requirement of the conventional geometric Froude number. The densimetric particle Froude number has a smaller mismatch of 2,6. In literature, the time scale has been adapted from Anno (Anno, 1984) to a dimensionless time comparing prototype to model snowdrift growth rates. In this study, the Time scale was adapted to the deposit process (growth of cone at equilibrium) and therefore an empirical parameter. The length scale for the 1:20 Nuuk Cube model was $L_m = 6$ cm (cube 1,2 m in full-scale) for the model cube. After 30 minutes the particles which had aggregated on the windward wall started to elapse. In Anno's experiments, the snow 'cone' reached similar height whether with a duration of 50 min or 38 min (Anno and Tomabechi, 1985).

Table 1 Prototype and model properties for snowdrift simulation

Parameter Properties	Prototype value	Model value
Particle diameter D_p [µm]	500 - 3000	127
Air density ρ_a [kg/m³]	1,31	1,22
Particle density ρ_p [kg/m³]	440 - 600	2240
Surface friction velocity u_*[m/s]	0,48	0,28
Threshold friction velocity U_t^*[m/s]	0,17	0,17
Threshold velocity U_{Th} [m/s]	4 -11(dry snow) or 7 - 14(wet snow)	5,3
Fall velocity U_f [m/s]	0,3 - 2,0	0,44
Max daily mean wind velocity $\overline{U}_{(Z)}$[m/s]	7,3	4,63*

*mean Wind velocity at model cube height on terrain Z_{ref}

Table 2 Similarity parameters with Natron

Eqn. No.	Theoretical similarity parameters	Prototype value	Model value
1	θ	45 - 90°	39°
2	$\frac{D}{L}$	5 x 10^{-4}	1,27 x 10^{-4}
3	$\frac{u_*}{U_t^*}$	2,82	1,65
4	$\frac{U_f}{U}$	4,1 x 10^{-2}	10,4 10^{-2}
5	$\frac{U^2}{D\ g}\ \frac{\rho_p}{(\rho_p - \rho_a)}$	1,09 x 10^4	1,72 x 10^4
6	$\frac{U^2}{L_h\ g}$	4,53	21,88
7	$\frac{\rho_p}{\rho_a}$	458	1878
8	$\frac{T_\mathrm{p}}{T_m}$		T_m ~ 30 min

Note: L_h = dimension of Nuuk Cube with 1,2m

Nuuk Cube test case

In most test procedures particles are applied as a uniform layer over the test model before increasing wind speed assuming snow accumulates uniformly around buildings or roof structures. But observations in nature negate this theory. Due to wind direction and building shape, we have areas where particles are not transported behind e.g. a roof structure. Simply because the architecture did not allow interference air motion. Based on the findings in literature and observation in full-scale the method of this research is performed as snowfall and snowdrift configuration for the modeling procedure (Fiebig & Koss, 2023a, 2023b). Modelling snow with substitution material implies inevitably a simplification of the physical process regarding thermodynamics, wind-driven transportation, and compacting. As a consequence, the ambition of the simulation does not aim at establishing a full physical similarity but rather a phenomenological similarity to observations in nature. For the evaluation of the experimental simulation, a test of the model cube was carried out for validation to nature. To validate the model studies, snowdrift conditions have been monitored during three winter periods in Nuuk, Greenland. The monitoring shall indicate a suitable test

program and match with snow accumulation shapes close to full-scale observations. Afterward, the wind tunnel tests can be readjusted to calibrate the procedure.

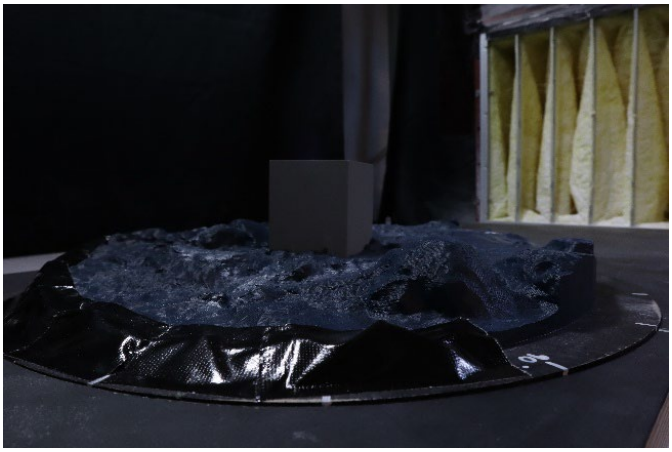

Figure 5 Nuuk Cube test model in 1:20 with 3D printed surface terrain measured with Photogrammetry

Figure 6 Nuuk cube field experiment on terrain without snow cover.

In the present study, a 1:20 scale model of the observation cube in Nuuk was 3D printed (see Figure 5), and a 3D printed terrain surface with 45 cm radius was placed on the cross dimensions of the test section. The model should be able to reflect sufficiently the air motion around the object. According to Anno (Anno, 1984) the terrain surface properties (rough or smooth material) should be the same as in nature. Therefore, a 3D terrain of the rough ground properties in Greenland (see in Figure 6) was built for the cube model.

Experimental Test procedure

Each "snowdrift event" in the wind tunnel simulation is defined as a two-step approach. First, a snowfall is accompanied by an inflow velocity speed of $U_{ref,LSHW}$= 1,5 m/s at the model height (reference height of 150 mm at low-speed hot-wire anemometer (LSHW) after the flow-processing unit (FPU). Second, a snowdrift with a velocity up to 6,6 m/s is performed without snowfall. In the first step are particles fed slowly through the seeding mechanism with a seeding rate of approximately 500 RPM while the low speed velocity is applied. This continued for 30 min, until particles have aggregated as maximum peak cone accumulation height at the windward model cube wall. In Anno's experiments, the snow 'cone' reached similar height whether with a duration of 50 min or 38 min (Anno and Tomabechi, 1985). The duration of the test was therefore determined empirically. The test condition at the day of test performance are documented in Table 3.

Table 3 Test conditions and parameters of snowdrift performance:

Atm.Pressure:	1024	[kPa]
Rel. Humidity RH :	42	[%]
Duration of ejection of particles T_m:	30	[min]
Velocity speed $U_{ref,LSHW}$:	1,5	[m/s]
RPM seeding mechanism :	500	[-]
SSM:	Natron	[-]

Table 4 Velocity Steps for Erosion Test and Speed-up Factors each for one minute:

			U_{Th}	
Velocity step:	1	2	3	4
Speed-up Factor β:	2.00	1.33	1.00	0.80
Velocity Ratio Ω:	0.50	0.75	1.00	1.25
$U_{ref,LSHW}$ *:	**2.6**	**3.9**	**5.3**	**6.6**

*Note: Z_{ref}= 15 cm, Height of Hot-Wire above WT floor

During the second step, without snowfall, the velocity was slowly increased in speed ratios up to $U_{ref,LSHW}$ = 6,6 m/s. The threshold speed U_{Th} for Natron in Table 4 was used to determine the velocity ratios obtained in a specification test in earlier studies (Fiebig, 2023). The first velocity step starts at 2,6 m/s and lasts for about one minute to obtain the first isopleth U_{Th} around the Nuuk Cube model. The test continuous here for each step with another minute. Unlike experimental wind comfort tests with substitute material in erosion mechanism, the wind tunnel velocity speed was stopped after the fourth velocity steps. Here, the desired geometrical shapes through erosion obtained show a similar accumulation as observed in the Nuuk Cube field experiment. The accumulation

dimensions on and around the model cube were measured with a 3D structured light scanner. First, the model was scanned without model snow, and then a second time after the test was performed with model snow. The surfaces were then compared in an analysing software (GOM inspect) which produces a three-dimensional representation of the height deviations. In this way, the accumulation model shapes can be compared to full-scale accumulation shapes. The setup and results of the monitoring study are described in (Fiebig & Koss, 2023a, 2023b).

Event configuration

The event configuration results from the observation data of the Nuuk Cube Experiment in Greenland. In Nuuk winter season, the predominant wind direction is from northerly directions, but unstable and rough weather is from the southeast to southwest, which is called “nigersuaq” (Cappelen John(ed), 2013) in Greenlandic. At site, the two prevailing wind directions are identified from North-Northeast and from South-Southeast. The configuration in the wind tunnel experiment is therefore a snowdrift performance from North and Southeast for the first test ID V1 and for the second test ID V2 from North-Northeast to South-Southeast.

3. Experimental generic buildings

The developed simulation approach in previous work (Fiebig, 2023) can be used to identify critical situations for a building design (e.g. ice formation or load on roof structures). The choice of using experimental wind tunnel testing, instead of numerical simulations, were based on the fast availability of the experimental technique and the fact that despite the limited similarity to real snow (e.g. no thermodynamic similarity), the method offers validation data for numerical simulations not only despite but rather because of their partial similarity. In addition, for urban scale testing, this simulation approach can also work for much smaller scale and increase the number and size of models tested compared to numerical simulations. The meteorological observation and snow accumulation monitoring of the Nuuk Cube field experiment (Fiebig & Koss, 2023a, 2023b) allowed a simplified wind tunnel simulation to investigate preliminary generic urban layouts. For the first analysis, different generic building arrangements are tested to explore the behavior of snow accumulation within building arrangements in smaller model scale testing. The “windbreak” principle from Ralph Erskine has been used in literature to propose a possible layout for an Arctic city (Erskine and Collymore, 1994). An adaptive approach of Erskine’s theory was proposed by

Kuismanen, K. (Kuismanen, 2008), which was a study case (CASE Rajakylä Oulu) for Oulu city (Figure 7). The urban pattern was tested at a small scale without a boundary-layer wind tunnel facility. Another similar urban layout to Ralph Erskine was based on a theoretical approach from Leo R. Zrudlo (Zrudlo, 1982), but this layout was not chosen for the generic study. For the generic study, simplified layouts seemed more appropriate to start with and link them later to typical urban typologies used in urban planning.

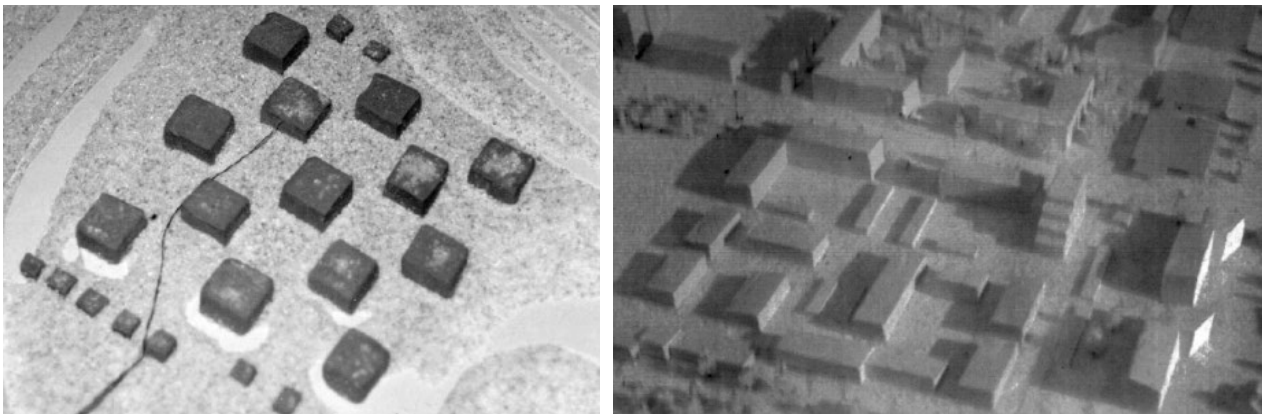

Figure 7 Arctic building arrangements by Kuismanen 2008 for study case of CASE Rajakylä Oulu city.

All suggested layouts for the study are listed in Figure 8. A generic layout proposal of the city of Oulu, Finland, and the city of Norilsk in Russia was tested as an example of existing urban structures in cold regions (1, 2). Those represent generic urban forms that are commonly used in architecture. Typical urban patterns like enclosures generate universal comfort in city planning (3) and are therefore also included in the test program. Open enclosures are considered in the test program as a variation to reduce the accumulation issue in closed courtyards (4). The generic example of a maximum density with rectangular volumes varying in height stepwise towards the center was tested as an extreme case to slow the wind speed to a maximum (6). A typical building block design in Nuuk from the ’60s as a shifted grid to reduce circulation was suggested as a test case, instead of a building block along the prevailing wind direction that can accelerate wind velocities between buildings.

1

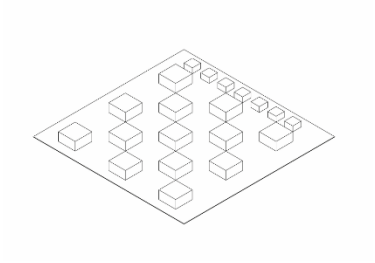

Soft Windbreak principle

FAR = 0.38

2

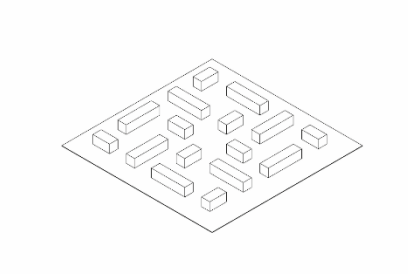

Oulu and Norilsk City

FAR = 0.31

3

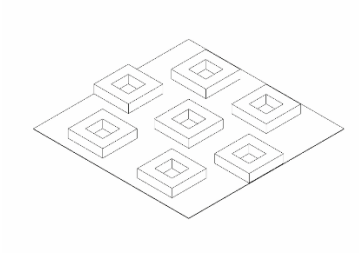

Enclosures

FAR = 0.52

4

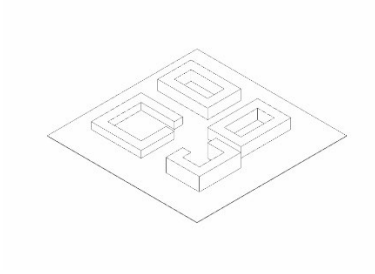

Open Enclosures

FAR = 0.38

5

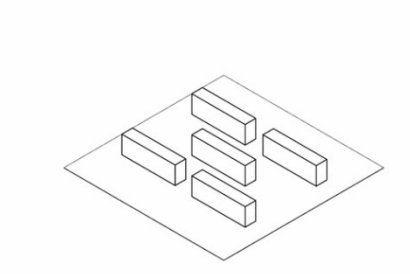

Nuuk Block

FAR = 0.23

6

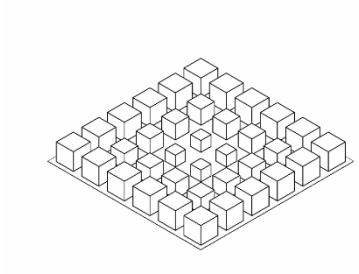

Windshield

FAR = 0.75

Figure 8 Typical Urban generic pattern compared to their density. The model floor in the wind tunnel test section was a 45 x 45 cm test area. The density is measured as an abstract density parameter "Floor area Ratio", FAR.

The generic urban layouts presented are expressed as an abstract density parameter and stand for "Floor area Ratio" (FAR) which is used to measure and describe the density of a city block or district. The model floor in the wind tunnel test section has an area of 45 x 45 cm. For practical purposes, the fictive site conditions are based on that square and have 2,5 x 2,5 cm grid lines. The buildings are placed within those grid ratios.

4. Results Nuuk Cube Experiment

Figure 9 shows the model test sequence after a snowfall and erosion test procedure. The analysis of the measured cumulative snow depth in mm of the model snow for two performed tests is shown in Figure 10.

The first test, ID V1, was performed with snowfall and erosion from both, Southeast and North direction (Figure 9, 10). This procedure was once more repeated (a multi-storm event like in nature) to study the accumulative quantity of snowdrifts. The second test, ID V2, was performed with snowfall and erosion from the Southeast and North-northeast and was not repeated. In test version V1 the maximum cone accumulation growth at the southeast wall has elapsed due to vortex-induced forces at the model cube and showed a phenomenon also observed in full-scale (shown in Figure 12).

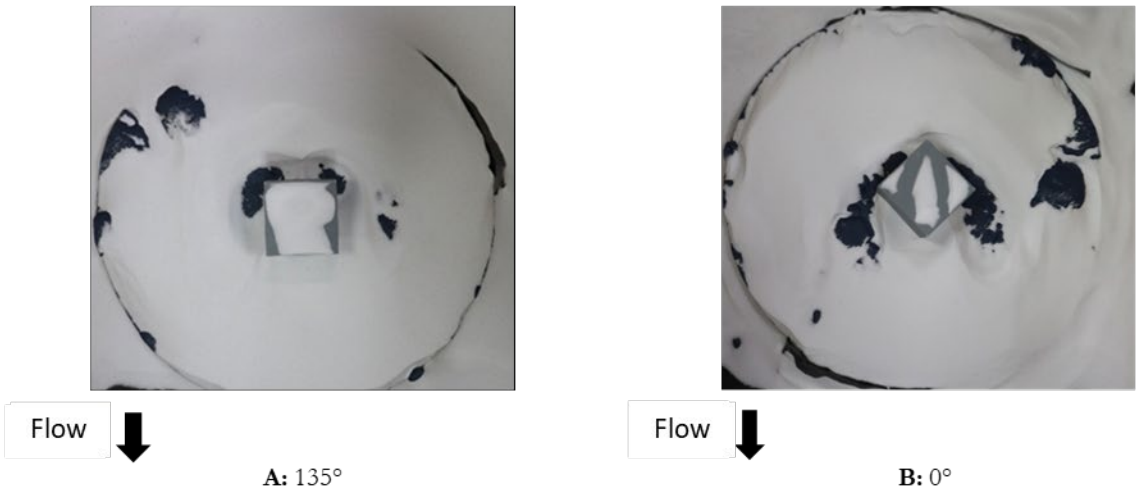

Figure 9 A photograph of the model Nuuk cube in scale 1:20 during test performance. A: First snowfall and erosion test: Snow accumulation with flow direction from Southeast 135° B: Second snowfall and erosion test: Snow accumulation after flow direction from North 0°.

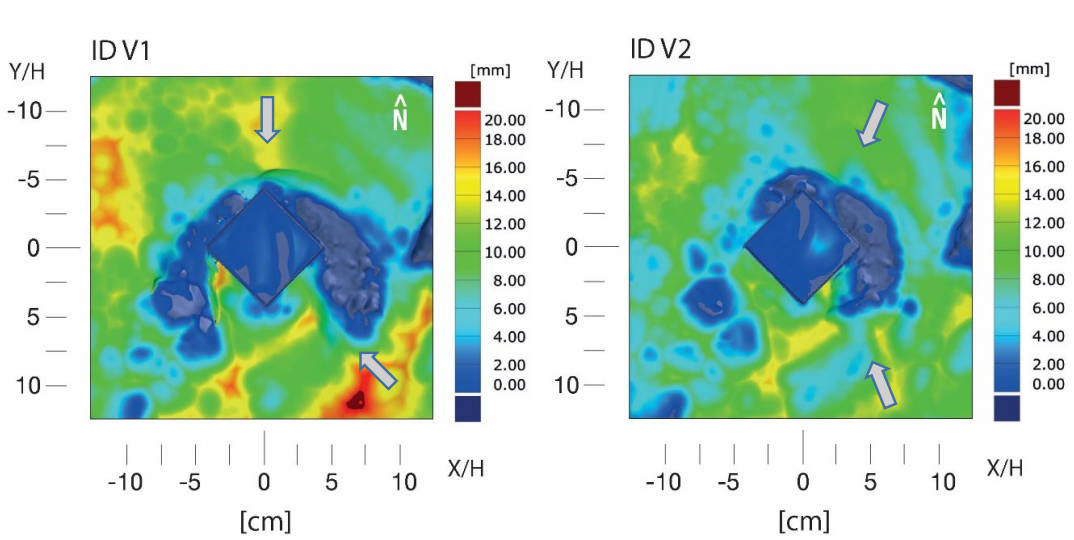

Figure 10 Result of model snow accumulation patterns around the 1:20 model cube. ID V1: (SE and N); ID V2:(SSE and NNE)

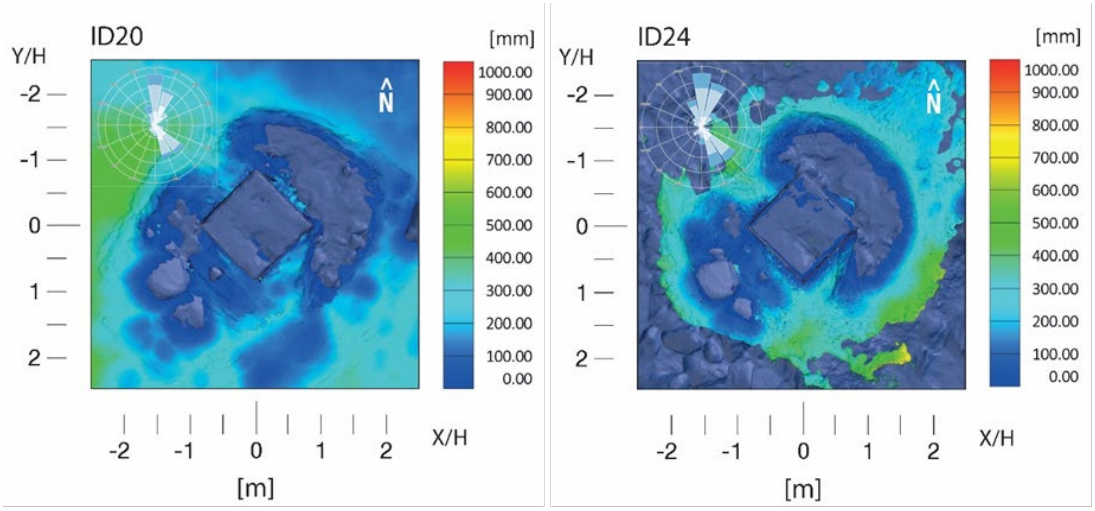

Figure 11 Measured snow accumulation height from full-scale monitoring. ID 20: 27-03-2019; ID 24: 07-03-2020.

A **B**

Figure 12 A: Nuuk cube (ID 24) 07/03/20; B: Model cube test ID V1

Strong erosion areas are observed closely surrounding the model and prototype cube leaving a cone-shaped accumulation at the northwest and south-southwest to south-southeast cube wall (Figure 12). Larger deposit areas around the test model are further out from the cube at the windward and leeward sides with 14 to 18 mm height, results are shown in Figure 10. In full-scale, the cone was deposited higher at the northwest wall compared to the model. In the wind tunnel experiment it was observed that the model cube has deposited a cone at the northwest wall, like in full-scale, but due to the high threshold velocity step more particles have been eroded than in nature. This can be adjusted by choosing lower wind velocity speed ratios from Table 4.

5. Results of generic urban buildings

An overview of the snowdrift tests at the test section of the closed-circuit boundary layer wind tunnel for different typical urban building patterns after the test performance is shown in Figure 13. The upstream wind tunnel flow direction is indicated with an arrow at the top left. The generic urban layouts are presented in the following order: (1) Soft Windbreak principle, (2) Oulu and Norilsk, (3) Oulu and Norilsk (45°), (4) Enclosures, (5) Open Enclosures, (6) Nuuk Block, (7) Dense windshield.

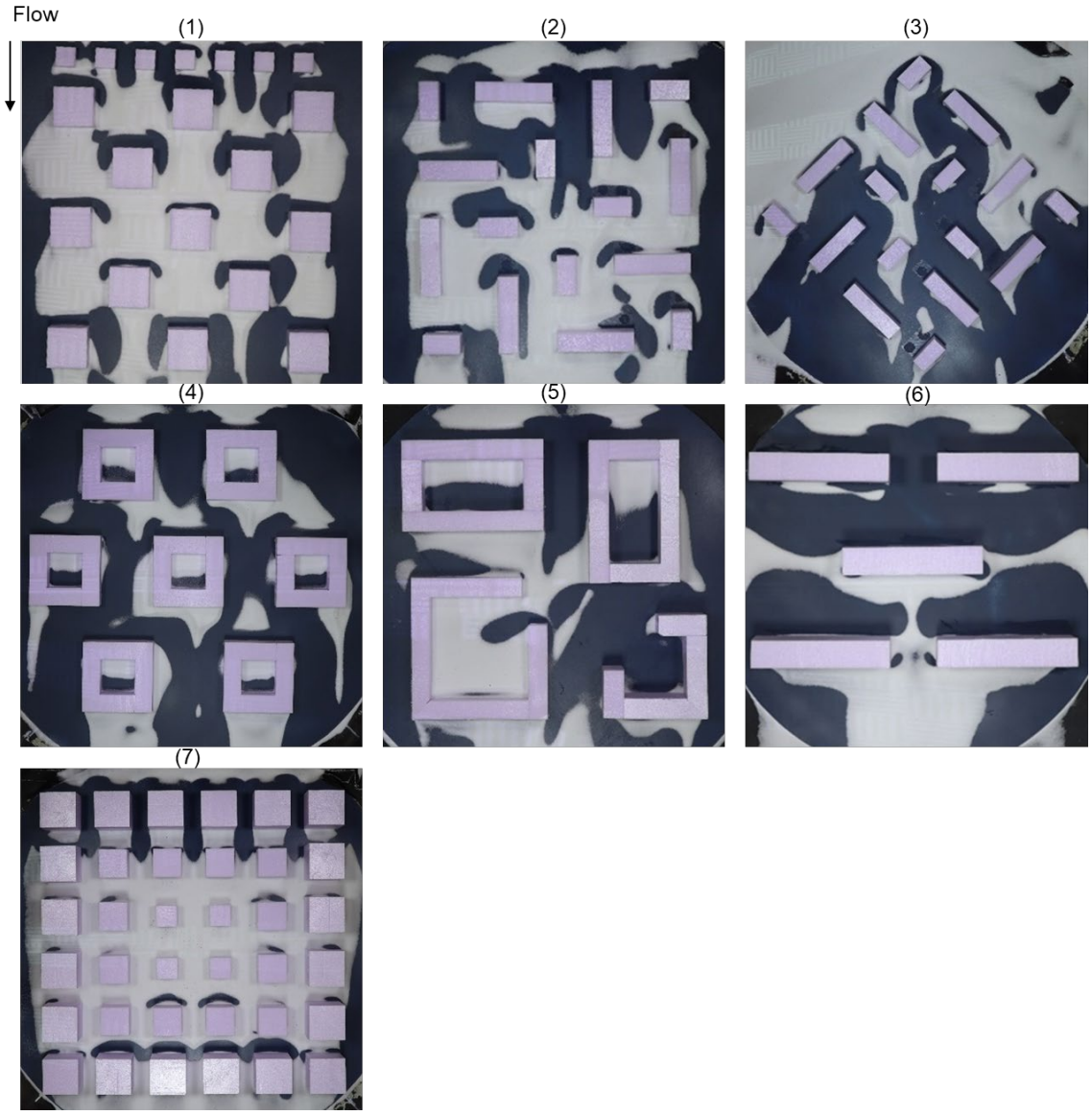

Figure 13 Photographs of snowdrift tests in the test section of the closed-circuit boundary layer wind tunnel for different typical urban building pattern. The wind tunnel flow direction is indicated with an arrow at the top. (1) Soft Windbreak principle, (2) Oulu and Norilsk, (3) Oulu and Norilsk (45°), (4) Enclosures, (5) Open Enclosures, (6) Nuuk Block, (7) Dense windshield.

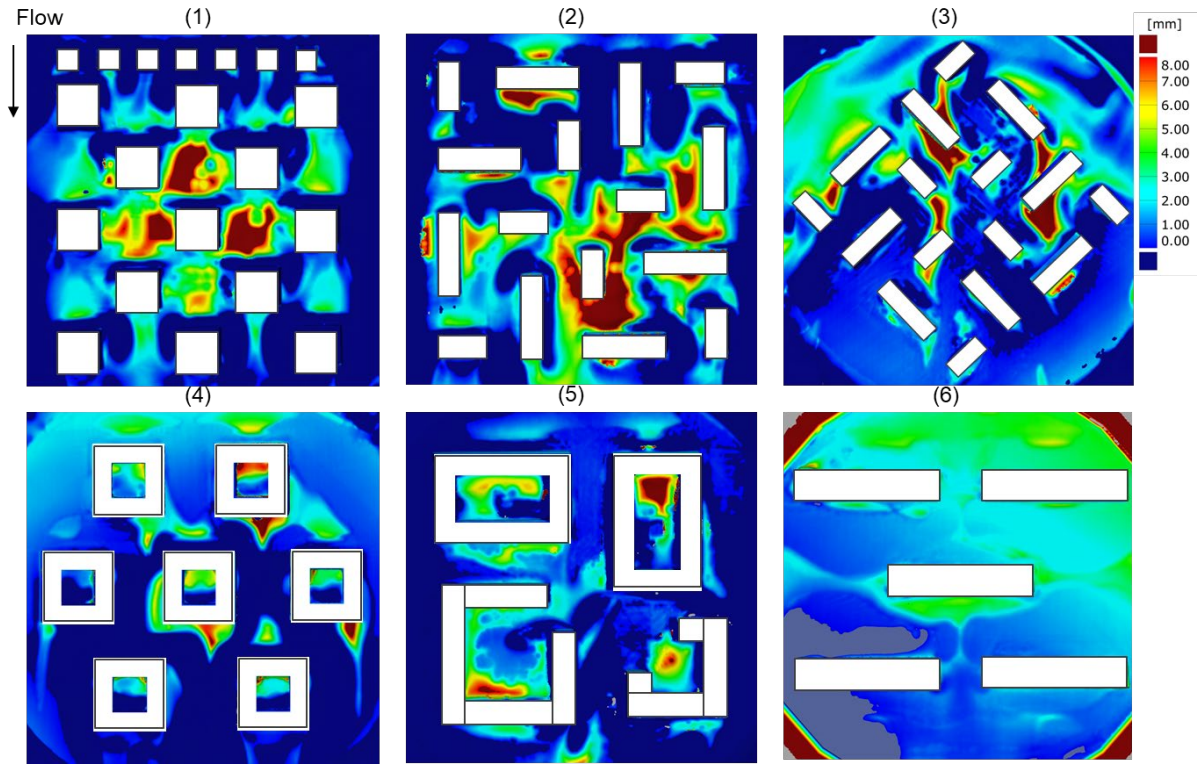

Figure 14 (1) Soft Windbreak principle, (2) Oulu and Norilsk, (3) Oulu and Norilsk (45°), (4) Enclosures, (5) Open Enclosures, (6) Nuuk Block.

The results show the erosion pattern, which identifies zones exposed to local strong winds and those that are well protected (Figure 13). The drift pattern can identify results for the prevailing wind direction regarding the possible ground-level dispersion of snow accumulation with a group of buildings that are typically observed in nature. In case of the (1) Soft Windbreak principle by Kuismanen 2008 were no significant snow deposition leeward the first row of small object cubes (2,5 x 2,5 cm). However, the snow depth in the second row of the larger cube elements (5 x 5 cm) was comparatively large (see Figure 14). For the Oulu and Norilsk city block design larger snow accumulations occurred with a flow direction orthogonal/ parallel to the building objects. With a shift of 45° flow direction more particles are errored and smaller deposits accumulate in the leeward zones, which is also in accordance with the experiments by Kwok et al. (1993). They also showed larger accumulation with a 90° orientation to the flow direction and a decrease in accumulation when turned to 0° and 45°. This seems to still occur in a group of buildings. Similar for the Nuuk Block design, here the lower density ratio allows more wind flow between the buildings and therefore creates less shelter. Also the (4) City Enclosures, do show reasonable snow formations and agree with flow pattern, with larger opening ratio more interference with the flow recirculating behind the building. The model scan result of the (7) Dense windshield the scanning was not successful. The

model buildings are to close and created shade so the structured 3D light scanner could not detect the area between the buildings. But in the photograph in Figure 13 only a small amount of particles eroded within the building configuration. It is not clear how large the accumulation depth occur around the buildings, but it could be observed that the velocity was reduced significantly when using a high density ratio of FAR= 0.75.

6. Discussion

In this paper the author established a set-up and empirical similitude considerations for simulations investigating the interaction of ground-level accumulation and around a group of buildings. The accumulation behavior of the different substitute materials under the airflow conditions in the wind tunnel tests was compared to the results from the field experiment to establish proper scaling rules. The simulation results of the Nuuk Cube object agree with full-scale observations, validating the snowdrift simulation. Modelling the adhesive behaviour, however, is limited due to inadequate reflection of thermodynamic effects and transformation of snowflakes in nature. This deficiency is usually compensated by approximating the appearance of snow accumulation in nature through the right choice of substitutional material in the scaled experiment. Consequently, simulations using simplified particle models for snowdrift and accumulation studies rely substantially on a phenomenological similarity to observations in full-scale. This applies equally for both, experimental and numerical simulations. This paper examines the involved similarity considerations with particular focus on the phenomenological aspect.

It is important to know which phenomenon of snow accumulation should be reflected in the tests. As a first conclusion, some substitute materials are more advantageous for simulating specific accumulation phenomena than other. Consequently, the choice of material shall rather be based on the expected dominating accumulation phenomenon than on a one-material-fits-all-purpose approach (Fiebig, 2023). The observations in Figure 11 and Figure 12 show clearly the same simulation pattern and also the approximate snow accumulation height in model and full-scale was observed in Figure 10 and Figure 11 with a slightly larger accumulation at the Northwest side of the Nuuk Cube. But the cone formation at the South corner of the Nuuk cube was measured in average with 300 mm, when scaling the model height of 14 mm to full-scale we could predict a snow accumulation height of 280 mm. This is an exceptionally good agreement considering the large variability of snow properties in nature and the discrepancies to model particles. Further studies should be planned to test variations to relate density and height with snow accumulation behaviour.

The full-scale observations could not observe accumulation on the cube roof top as observed in the model test. But assumptions are made regarding the possible effect of surface heat due to solar radiation on the dark painted roof. More details of the Nuuk Cube Field study in Fiebig & Koss, 2023b. Therefore are any interpretations of snow distribution on the model cube speculative. The scanning method also has great weaknesses in determining accurate snow quantities. Only the distribution characteristics and dispersion can be determined more accurately when models are tested in small scales and multiple buildings, as shading does not allow measurements when the scanner has no light source. In the case of the single object of the Nuuk Cube in model scale of 1:20 we found good agreement with the measure snow depth. It is recommended to study further instruments to obtain accurate measuring results.

7. Conclusion

The wind-tunnel experiments reproduced accurately the features observed in full-scale measurements, by its characteristically features such as the modelling of the eroded area and deposit area. This illustrates, that the material used to simulate snowdrift in wind tunnel studies should be chosen on the ability to reflect observed characteristics of snow depositing in nature for the low-arctic region, rather than based on strict similarity laws. This method, if not numerical, imposes marginal conditions. 'Strict' similarity in snowdrift modelling are approximations. Here the significance of the relevance of snowdrift similitude parameters occurs, as other researchers discussed before (Kim et al., 1991; Smedley et al., 1993). The choice of one material and its constant properties is approximate to the large variety of full-scale snow particles. Discrepancies occurred with 'strict' similarities e.g. geometric scale of particle diameter, conventional densimetrical particle Froude number and conventional geometric Froude number, gravity and fluid force, particle inertia and fluid inertia forces. For geometrical similarity of snowdrift patterns, wind tunnel simulations provide good results. Observed differences depend largely on the perspective. From an engineering point of view, those differences in drift patterns are not significant. On the other hand for theoretical consideration to establish similarity it is of importance. Despite the large discrepancies between the theoretical similarity laws, the similarity is obtained with the snowdrift pattern geometry around an object. The most applicable empirical similitude requirements to achieve good agreement with the snowdrift pattern at the model are:

1. The angle of repose θ of the substitutional material shall approximate the angle of real snow as close as possible. This force also determines the particle growth duration.
2. We use therefore the empirical time scale based on an 'equilibrium' state of the snow cone growth. For different substitutes and a range of model length scales, one should use the specification procedure to identify the time scale: $T_m = \theta_{max}$.
3. Particle ejection process $\frac{u_*}{U_t^*}$, based on the threshold of particle movement observed in the wind tunnel determines the velocity scaling. The author proposes Anno's (Anno, 1984) expression of the ratio of friction speed $\frac{u_{*\mathrm{p}}}{u_{*m}} = \frac{U_{t\mathrm{p}}^*}{U_{tm}^*}$.
4. The geometrical similitude is the most important consideration and the snowdrift pattern is a combination of erosion and deposition depending on the friction speed ratio. If the friction speed $u_{*\mathrm{p}}$ is larger than $U_{t\mathrm{p}}^*$ erosion occurs, particles deposit when $u_{*\mathrm{p}}$ is equal to $U_{t\mathrm{p}}^*$ (Anno, 1984).

The development of the documented experimental setup is suitable for a study of snow deposition and accumulation not only on the ground-area saltation but also on roof structures in the suspension layer. Furthermore, the documentation of the used material and the parametric possibility allows benchmark, with numerical methods of snowdrift simulation, to collect a wide range of data.

Acknowledgements

Financial support for the research project is partly provided by Laust Løgstrup, Director of Qeqqata Kommunia in Greenland, and fonds from the Technical University of Denmark DTU. Special gratitude is owed to Peter Barfoed at Nuuk Architects (Tegnestuen Nuuk) for his support for the field study.

References

Anno, Y., 1984. REQUIREMENTS FOR MODELING OF A SNOWDRIFT. Cold Regions Science and Technology 8, 241–252.

Anno, Y., Tomabechi, T., 1985. DEVELOPMENT OF A SNOWDRIFT WIND TUNNEL. Cold Regions Science and Technology 10, 153–161.

Cappelen John(ed), 2013. Technical Report 13-04 Greenland - DMI Historical Climate Data Collection -with Danish Abstracts. Copenhagen.

Delpech, P., Palier, P., Gandemer, J., 1998. Snowdrifting simulation around Antarctic buildings. Journal of Wind Engineering and Industrial Aerodynamics 74–76, 567–576. https://doi.org/10.1016/S0167-6105(98)00051-8

Erskine, R., Collymore, P., 1994. The Architecture of Ralph Erskine.

Kim, D.H., Kwok, K.C.S., Rohde, H.F., 1991. Similitude Requirements of Snowdrift Modelling for Antarctic Environment. Sydney.

Kind, R.J., 1990. Mechanics of Aeolian Transport of Snow and Sand. Journal of Wind Engineering and Industrial Aerodynamics 36, 855–866.

Kind, R.J., 1986. Snowdrifting: A review of modelling methods. Cold Regions Science and Technology 12, 217–228. https://doi.org/10.1016/0165-232X(86)90036-4

Kind, R.J., 1976. A critical examination of the requirements for model simulation of wind-induced erosion/deposition phenomena such as snow drifting. Atmospheric Environment (1967) 10, 219–227. https://doi.org/10.1016/0004-6981(76)90094-9

Kong, L., Parkinson, G. V., 1997. A 3-D tolerant wind tunnel for general wind engineering tests. Journal of Wind Engineering and Industrial Aerodynamics 69–71, 975–985. https://doi.org/10.1016/S0167-6105(97)00221-3

Kuismanen, K., 2008. Climate-conscious architecture—design and wind testing method for climates in change. University of Oulu, Finland.

Li, L., Pomeroy, J.W., 1997. Estimates of Threshold Wind Speeds for Snow Transport Using Meteorological Data. Journal of Applied Meteorology 36, 205–213. https://doi.org/10.1175/1520-0450(1997)036<0205:EOTWSF>2.0.CO;2

Mellor, M., 1965. Blowing Snow, Cold Regions Science and Engineering, Part III, Section A3c.

Mitsuhashi, H., 1982. Measurements of snowdrifts and wind profiles around the huts of Showa Station in Antarctica. Antarctic Record.

Naaim-Bouvet, F., 1995. Comparison of Requirements for Modeling Snowdrift. Surveys in Geophysics 16, 711–727.

Naaim-Bouvet, F., Naaim, M., 1998. Snowdrift modelling in a wind-tunnel: vertical and horizontal variation of the snow flux. Annals of Glaciology 26, 212–216.

Smedley, D.J., Kwok, K.C.S., Kim, D.H., 1993. Snowdrifting simulation around Davis Station workshop, Antarctica. Journal of Wind Engineering and Industrial Aerodynamics 50, 153–162. https://doi.org/10.1016/0167-6105(93)90070-5

Zrudlo, L.R., 1982. A MODEL FOR AN INTEGRATED DESIGN APPROACH TO SETTLEMENT PLANDING IN THE ARCTIC.